Influence of Operational Characterization Methods on DOM Physicochemical Properties and Reactivity with Aqueous Chlorine

Christopher J. Tadanier

Dissertation submitted to the Faculty of the Virginia Polytechnic Institute and State University in partial fulfillment of the requirements for the degree of

Doctor of Philosophy

in

Civil Engineering

William R. Knocke, Co-chair

Duane F. Berry, Co-chair

James P. Wightman

Andrea M. Dietrich

John C. Little

Marc A. Edwards

12 June 1998

Blacksburg, Virginia

Influence of Operational Characterization Methods on DOM Physicochemical Properties and Reactivity with Aqueous Chlorine

Christopher J. Tadanier

(ABSTRACT)

The physicochemical properties and chemical reactivity of dissolved organic matter (DOM) are of tremendous practical significance in both natural and engineered aquatic and terrestrial systems. DOM is frequently extracted, fractionated, and concentrated from environmental samples using a variety of operationally defined physical and chemical processes in order to facilitate study of specific physicochemical properties and aspects of its chemical reactivity. This study was conducted to systematically examine the influence of operationally defined physical and chemical characterization methods on observed DOM physicochemical properties and reactivity with aqueous chlorine. The effects of chemical separation were evaluated by applying an existing resin adsorption based procedure which simultaneously extracts and fractionates DOM and inorganic constituents into hydrophobic and hydrophilic acid, base, and neutral dissolved material matrix (DMM) fractions. Physical separation based on DOM apparent molecular weight (AMW) was also evaluated using batch ultrafiltration (UF) data in conjunction with a suitable membrane permeation model. Linear independence of membrane solute transport was theoretically described using non-equilibrium thermodynamics and experimentally demonstrated for AMICON® YC/YM series UF membranes. Mass balances on DMM fraction constituents in untreated and previously coagulated natural waters indicated that quantitative recovery (100 ± 2%) of DOM constituents was achieved, while recovery of inorganic constituents such as iron and aluminum was substantially incomplete (30%-74%). Comparison of whole-water DOM properties with those mathematically reconstituted from DMM fractions demonstrated a marked shift in DOM properties toward lower AMW. Evidence of pH induced partial hydrolysis of protein, polysaccharide, and ester DOM components was also observed. Decreased specific Cl_2 demand (mmol ΔCl_2/ mmol DOM) and specific trihalomethane formation (mmol THM/mmol DOM) following chemical fractionation were attributed to increased molar DOM concentration and decreased DOM association with colloidal iron oxide surfaces. Collectively, the results of this research indicate that operational characterization methods result in alteration of DOM physicochemical properties and reactivity with aqueous chlorine, and caution is therefore advisable when interpreting the results of studies conducted using chemically extracted or fractionated DOM.

Acknowledgments

I wish to thank each of my committee members for their gracious participation. Special appreciation is extended to my principle advisors Dr. William R. Knocke and Dr. Duane F. Berry for their insightful comments during the course of this work, and their tireless efforts during the review process. I would also like to thank Senior Analytical Chemist Marilyn Grender and Laboratory Manager/Safety Director Julie Petruska for generously sharing their expertise during the method development phase of this work. The assistance of fellow graduate student John Siczka in performing DOM chemical fractionations is greatly appreciated. Gratitude is due to the Charles E. Via Doctoral Fellowship Program and the Virginia Water Resources Research Council for financial support. Finally, and most importantly, I thank my wife Beth and son Elliott for their ceaseless love and support during this long and arduous process.

Copyright Information

Table of Contents

Table of Tables

Table of Figures

Chapter 1

Recovery of Dissolved Material Matrix Components Following Resin Exchange Based Fractionation of DOM in Natural Waters

Abstract

The organic and inorganic components of natural waters are intimately interrelated and constitute a dissolved material matrix (DMM). The objectives of this study were to systematically investigate the recovery of both organic and inorganic components in chemically fractionated natural waters, to evaluate possible redistribution of these components among isolated DMM chemical fractions, and to examine interactions between DMM physicochemical properties and coagulation behavior of chemically fractionated waters. Untreated and previously coagulated natural waters were fractionated into hydrophobic and hydrophilic acid, base, and neutral DMM fractions using a resin exchange based protocol. Mass balances on non-volatile dissolved organic carbon (NPDOC), UV_{254} absorbing material, iron, and aluminum were used to evaluate DMM component recovery. Quantitative (98%-102%) was achieved for dissolved organic matter (DOM); whereas, iron and aluminum recovery was substantially incomplete (30%-74%). Aluminum recovery was higher than iron recovery in all waters, and recovery of both metals increased following coagulation. Incomplete metals recovery was attributed to imperfect elution from cation exchange resin. DMM component distribution among chemical fractions was altered by coagulation; with DOM preferentially removed in the hydrophobic acid fraction, and substantial incorporation of residual aluminum coagulant in basic DMM fractions. Chemical fractionation of natural waters by resin exchange may result in alteration of DMM physicochemical properties or reactivity due to incomplete recovery and redistribution of iron and aluminum.

Introduction

Dissolved organic matter (DOM) is ubiquitous in both natural and engineered aquatic and terrestrial environments, and is intimately involved in a myriad of physical, biological and geochemical processes. The fate and transport of environmental pollutants is strongly influenced by pollutant-DOM interactions including complexation of trace metals (*1*) and sorption of organic pesticides and hydrocarbons (*2*). The solubility of both organic and inorganic pollutants is frequently increased due to pollutant-DOM interaction (*3-5*), and the bioavailabilty of both nutrients and pollutants may be significantly decreased in the presence of DOM (*6*). Dissolved organic matter may also serve a number of central functions in the carbon and energy budgets of aquatic and terrestrial ecosystems (*7*) such as providing a carbon or energy source for microbial metabolism (*8-12*), acting as a growth promoter for phytoplankton and algae (*13,14*), and enhancing or regulating a wide variety of plant physiological processes (*15-17*). The presence of DOM can dramatically affect the operation and performance of engineered water and wastewater treatment systems. Dissolved organic matter has been observed to influence coagulation and subsequent solid-liquid separation processes (*18*), exert a significant oxidant demand (*19*), and has received considerable attention as the source organic precursor molecules involved in formation of halogenated disinfection by-products during drinking water treatment (*20,21*).

Comparatively large quantities of material, on the order of several hundred mg or more, are typically required to study the chemical characterization, biogeochemical reactivity, or treatability of DOM in a laboratory setting. Due to the relatively low concentration of DOM in most natural waters (< 10 mg/L) (*22-25*), hundreds or thousands of liters of water are required to provide the material necessary for meaningful characterization of aquatic DOM. Storage of such large volumes of unprocessed water may be operationally impractical, and it may be difficult to prevent microbial or abiotic alteration of DOM in dilute natural water samples during the long periods which may be necessary to conduct detailed experimental reactivity or treatability studies. Repeated sampling of smaller sample volumes is also not practical, as the character of DOM in any given water source may change dramatically over time due to cyclic or random climactic and geomorphological variations. Moreover, many analytical techniques involved in DOM chemical characterization and reactivity analyses require DOM concnetrations which are one to several orders of magnitude greater than those characteristic of natural waters. For these reasons, it is generally necessary to extract and concentrate the DOM from a natural water of interest to facilitate analysis.

In addition to concentrating DOM components the ideal extraction method would have the following characteristics: 1) complete recovery of all DOM constituents regardless of physicochemical properties, 2) physiochemical properties of DOM unaltered by extraction, 3) DOM-inorganic constituent interactions unaltered by extraction, 4) extracted DOM free of chemical impurities or contaminants, 5) extracted DOM in a form that is not susceptible to physical, chemical, or biological alteration during storage, and 6) DOM extraction unaffected by source water composition. Realistically, no analytical procedure simultaneously satisfies all the DOM extraction criteria outlined above. Instead, the ultimate choice of an extraction method, and extent to which inorganic constituents are removed from DOM concentrates by additional desalting procedures, must be based on which extraction criteria are most important to the analysis at hand. Chemical characterization of DOM generally requires a low ash isolate, as inorganic constituents often interfere with spectroscopic techniques used to evaluate elemental and functional group content. Conversely, reactivity and treatability studies may be strongly affected by removal of inorganic constituents such as transition metals ($Fe^{2+/3+}$ and $Mn^{2+/4+}$) and group IIA and IIIA metals (Ca^{2+}, Mg^{2+}, and Al^{3+}), which may influence the physicochemical character of DOM through sorption and complexation interactions.

A variety of analytical methods have been developed which utilize various physical and chemical separation driving forces to affect DOM extraction from natural waters. Preparative DOM extraction methods include low temperature vacuum distillation (*26*), lyophilization (*27-29*), freeze concentration (*30-34*), coprecipitation with inorganic salts (*35,36*), ultrafiltration (*37*), reverse osmosis (*28,38-40*), solvent extraction (*41*), and sorption on various solid surfaces such as alumina (*42-44*), carbon (*45*), and a variety of ionic and non-ionic polymeric organic resins (*46-51*). However, none of these extraction methods is entirely satisfactory due to incomplete recovery of DOM or impracticality of use for processing the large volumes of water required to obtain even modest amounts of extracted material. A thorough review of the relative merits of each of these extraction methods is beyond the scope of the current discussion; however, several excellent reviews are present in the literature (*52-54*).

Since no single method is entirely satisfactory for extraction of DOM from natural waters, several analytical procedures are often combined into a coherent extraction protocol. For example, an extraction protocol which utilizes sequential hydrophobic and ion exchange resin sorption steps has been developed which simultaneously extracts and concentrates DOM into hydrophobic acid, base, and neutral and hydrophilic acid, base, and neutral fractions (*55*-*57*). Aside from any loss of DOM constituents due to irreversible sorption on exchange resins or other system components, all DOM constituents are segregated into one of six chemically discrete fractions based on hydrophobic and acid-base characteristics. This protocol was selected for the current work based on its theoretical recovery of all DOM constituents in a water sample, ability to process large sample volumes, and simultaneous concentration and chemical fractionation of DOM. Hereafter, this analytical method will be referred to as the *Dissolved Material Matrix (DMM) Fractionation Protocol*.

Extraction and fractionation schemes similar to the DMM Fractionation Protocol have not been widely utilized to chemically characterize DOM, principally due to the laborious nature of these methods. Variations of the procedure outlined by Leenheer have been utilized to extract and chemically fractionate DOM from natural waters (*52*,*56*-*63*), and DOM previously extracted from soil samples (*64*-*68*). However, the recovery efficiency of extracted DOM has frequently either not been measured or not reported. Also, those studies in which DOM recovery efficiency has been determined have generally resulted in substantially incomplete recovery of DOM. Furthermore, the recovery and possible redistribution of inorganic constituents among extracted DMM fractions has not been addressed. Clearly, the recovery of both organic and inorganic DMM constituents must be largely complete if the results of characterization, reactivity, or treatability studies using chemically fractionated DOM are to be meaningfully interpreted in relation to the environment from which the DOM was extracted. Therefore, the objectives of this study were 1) to systematically investigate the fractionation and recovery of DOM, iron, and aluminum from untreated and previously coagulated natural waters using the DMM Fractionation Protocol, 2) to evaluate the possible redistribution of these organic and inorganic components following application of the DMM Fractionation Protocol, and 3) to use the DMM Fractionation Protocol as a tool for evaluating the interaction between DOM physicochemical properties and coagulation behavior of natural waters.

Materials and Methods

DOM Separation in the DMM Fractionation Protocol

The DMM Fractionation Protocol is based on sequential application of frontal adsorption and ion exchange chromatographic separation steps, in which chemically discrete DOM fractions are individually removed from a water sample by selective sorption onto and elution from one of three polymeric resin sorbents. Selectivity of DOM-resin interaction results from differences in resin material hydrophobicity and pH dependence of both DOM solute and resin surface ionizable functional group protonation. Application of the DMM Fractionation Protocol results in separation and concentration of DOM in a water sample into hydrophobic acid, base, and neutral; as well as, hydrophilic acid, base, and neutral fractions. However, it must be recognized that although the primary objective of the DMM Fractionation Protocol is to extract and fractionate DOM, inorganic constituents are also segregated and concentrated into the six chemically discrete fractions produced by this procedure. Furthermore, the isolation of organic and inorganic DMM constituents may occur somewhat independently of one another. The six chemically discrete fractions recovered are therefore termed DMM fractions. The various steps in the DMM Fractionation Protocol are shown schematically in Figure 1.1, and are discussed individually in the paragraphs which follow.

Hydrophobic DOM is isolated by hydrophobic interaction with non-ionic methyl-methacrylate XAD-8 resin. The desired volume of sample water is first passed through a column of XAD-8 resin at neutral pH to isolate hydrophobic base (HPO-B) and hydrophobic neutral (HPO-N) DOM. These organic fractions are selectively removed from the sample at neutral pH since HPO-N DOM molecules have a characteristically low density of ionizable functional groups and HPO-B DOM molecules are generally deprotonated under neutral to slightly alkaline pH conditions. The HPO-B DMM fraction is recovered from the XAD-8 column by elution with dilute HCl (pH 1-2), which reduces the affinity of the non-ionic resin for the now protonated, and hence positively charged, basic DOM molecules. Selective isolation of hydrophobic acid DOM (HPO-A) is achieved by acidifying the sample to pH 2 (which protonates acidic functional groups) and passing the sample through the XAD-8 column a second time. The HPO-A DMM fraction is recovered by elution of the XAD-8 resin column with dilute NaOH (pH 12-13), which releases the now deprotonated, and hence negatively charged, sorbed HPO-A DOM molecules. The HPO-N DMM fraction is not subject to elution by pH dependent charge manipulation, but may be recovered by soxhlet extraction of the XAD-8 resin in methanol. The sample now contains only hydrophilic DOM and some portion of the original inorganic constituents.

Hydrophilic DOM remaining in the acidified sample (pH 2) is isolated by two sequential ion exchange steps, again using pH dependent manipulation of solute charge to produce selectivity of separation. Hydrophilic base (HPI-B) DOM is isolated by passing the acidified sample through a column of hydrogen saturated MSC-1 strong cation exchange resin. Positively charged hydrophilic base DOM molecules and hydrated inorganic cations are removed from solution by exchange with resin bound protons. The HPI-B DMM fraction is recovered from the MSC-1 resin by elution with NaOH, which promotes release of bound DMM constituents by simultaneously deprotonating basic DOM molecules and thermodynamically saturating the resin with sodium ions. Hydrophilic acid (HPI-A) DOM is isolated by passing the acidified sample through a column of Duolite A-7 weak anion exchange resin which is in the free base form. Protonated (neutrally charged) HPI-A DOM molecules and hydrogen saturated (pH 2) hydrated anions are retained by the unprotonated secondary amine resin functional groups. The HPI-A DMM fraction is recovered by returning the Duolite A-7 resin to its free base form using NaOH as eluant. Following the cation exchange step, the sample contains only hydrophilic neutral (HPI-N) DOM molecules in largely de-ionized water. Since removal of solutes during the resin exchange steps of the DMM Fractionation Protocol does not appreciably reduce sample volume, the remaining HPI-N DMM fraction is concentrated by low temperature rotary vacuum distillation.

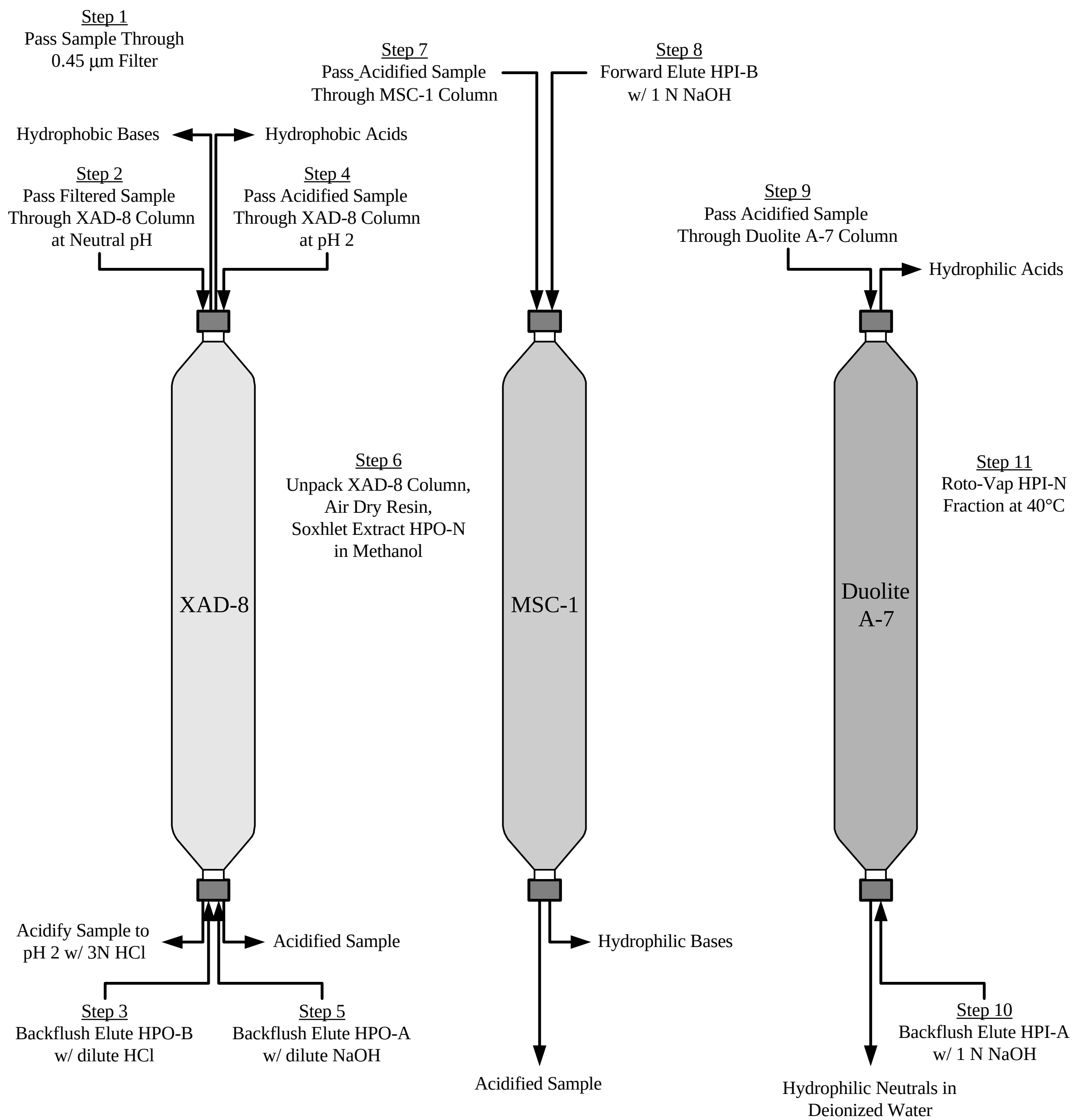

Figure 1.1: Schematic representation of the Dissolved Material Matrix Fractionation Protocol.

Pilot-Scale DMM Extraction Procedure

A pilot-scale fractionation apparatus consisting of three borosilicate glass columns with equal resin bed volumes V_B of 300 mL each was constructed. Sample volumes were selected based on consideration of the XAD-8 resin column capacity factor k', which describes solute retention at column breakthrough ($C = 0.5 \cdot C_0$). The value of k' for an organic solute is defined as,

$$k' = \frac{\text{Mass of solute sorbed on XAD-8 resin}}{\text{Mass of solute dissolved in column pore water}}, \qquad (1)$$

and is related to breakthrough (elution) volume V_E and the column void volume V_0 by,

$$V_E = V_0(1 + k'). \qquad (2)$$

V_0 for the pilot-scale XAD-8 column was determined to be $0.64 \cdot V_B$, as measured by the gravity drainable volume from the water filled column. Values of V_0 between $0.60 \cdot V_B$ and $0.65 \cdot V_B$ have been previously reported for XAD-8 resin columns (*29,56*). The hydrophobic-hydrophilic breakpoint for solute separation, or elution volume at which an organic solute is 50 % eluted and 50 % retained $V_{0.5r}$, is equal to $2 \cdot V_E$ for a symmetrical column breakthrough curve. Substitution into Eq. 2 yields,

$$V_{0.5r} = 2 \cdot V_0(1 + k'_{0.5r}), \qquad (3)$$

where $V_{0.5r}$ and $k'_{0.5r}$ are the applied (elution) sample volume and capacity factor at the solute hydrophobic-hydrophilic breakpoint, respectively.

The distribution of $k'_{0.5r}$ values for DOM in natural waters has been observed to be bimodal, with hydrophilic molecules exhibiting $k'_{0.5r}$ values of < 10 and hydrophobic molecules exhibiting $k'_{0.5r}$ values > 40 at column breakthrough (*25*). Therefore, $k'_{0.5r}$ values between 10 and 40 were used in this study to operationally define the hydrophobic-hydrophilic break-point for XAD-8 fractionation of DOM. A $k'_{0.5r}$ value of 30 was selected for pilot-scale fractionation of untreated and previously coagulated Lake Drummond waters, which by Eq. 3 specified a sample volume of 12 L. A $k'_{0.5r}$ value of 15 was selected for pilot-scale fractionation of untreated and previously coagulated Chickahominy River waters, resulting in a sample volume of 6 L. The same resin bed volume and column geometry was used for all fractionations so that similar hydraulic conditions were maintained: for a given column geometry decreasing resin bed volume decreases bed height, which can result in undesirable flow conditions such as channeling and excessive resin bed bypass.

The pilot-scale columns were filled with each resin in slurry form, then rinsed with HCl, NaOH, and ultra-pure water to remove any residual contaminants. Sample waters were applied to the columns by gravity from a 2 L borosilicate glass reservoir at 10 BV/h. The effluent NPDOC concentration of each column was monitored periodically during sample application to ensure premature breakthrough had not occurred. The void volume of each column was flushed with ultra-pure water or dilute HCl as appropriate following sample application, and the flushing solution combined with the processed sample prior to the subsequent extraction step. DMM fractions were recovered from the resins as shown schematically in Figure 1.1, with concentrations and volumes of flushing solutions and eluents as described in Appendix B.

Resin Preparation

Macroporous polymeric resins require significant preparation prior to use in the DMM Fractionation Protocol, as they contain significant quantities of both organic and inorganic impurities which would otherwise contaminate isolated DMM fractions. Unpolymerized resin monomers, dispersion agents, and resin fines are among the organic contaminants commonly present in macroporous resins as received from the manufacturer (*69*). Macroporous resins are frequently stored and shipped in a salt imbibed form in which the beads are saturated with NaCl and Na_2CO_3 to inhibit microbial growth (*70*).

Numerous resin preparation procedures have been utilized for macroporous resin cleanup, but most are variations of the following general scheme: immerse in water at an alkaline pH for 24 hr or more to completely wet the resin and solublize salts, rinse several times with ultra-pure water to remove salts, counter-flow floatation in ultra-pure water to remove resin fines, and soxhlet extraction in one or more organic solvents to remove organic contaminants. XAD-8 resin was soxhlet extracted sequentially in methanol, acetonitrile, and methylene chloride, while MSC-1 and Duolite A-7 resins were soxhlet extracted in methanol and acetone, respectively. Although the resin cleanup process is quite laborious and lengthy, requiring up to several months to prepare even modest quantities of resin, adequately cleaned resin is critical to successful application of the DMM fractionation procedure. Specific details of the resin preparation scheme used in this study are given in Appendix A.

Adequacy of the resin preparation scheme was verified by GC-MS analysis of contaminant concentrations in the extraction solvents as a function of extraction time. Each of the extraction solvents was periodically sampled during soxhlet extraction and the relative concentration of each extracted resin contaminant monitored by comparison of successive peak areas. The GC-MS analyses were performed on a Hewlett-Packard 5890 Series II gas chromatagraph coupled to a Hewlett-Packard 5970 mass selective detector. The GC injection port temperature was held at 220°C and the transfer line at 280°C. A DB-5ms narrowbore capillary fused silica column (30 m × 0.25 mm i.d. × 0.25 μm film thickness: J&W Scientific, Folsom, CA) was used to provide analyte separation. The GC oven temperature program consisted of an initial temperature of 35°C held for 9 min., an increase from 35°C to 40°C at 1°C/min. with a final hold time of 3 min., and an increase from 40°C to 150°C at 15°C/min with a final hold time of 1 min. Mass spectrometer detection parameters included a 4 min. solvent delay and a mass detection range of 45 amu to 425 amu. A sample volume of 3 μL with splitless injection was used for all analyses.

Sample Collection, Preparation, and Storage

The natural waters used in this study were collected as surface samples from Lake Drummond near Suffolk, Virginia and from the Chickahominy River near Providence Forge, Virginia. Both of these waters are highly colored, a characteristic often associated with substantial input of allochthonous DOM. The geomorphology of the landscape surrounding these water sources is consistent with allochthonous DOM input, as Lake Drummond acts as a drainage basin for the Great Dismal Swamp and the Chickahominy River watershed contains predominantly marginal wetlands and low lying forest. Samples were transported to the laboratory where they were immediately (within 24 hr) processed to produce stock solutions for use in all further experiments. Raw waters were pre-filtered through 0.45 μm membrane filter cartridges to remove large particulate matter and detritus. The DOM content of Lake Drummond water was approximately 45 mg/L following filtration, and dilution was therefore required to produce a stock solution suitable for application of the DMM Fractionation Protocol (*25*). The Lake Drummond sample was diluted with ultra-pure water to achieve a DOM concentration of approximately 10 mg/L C. The DOM content of filtered Chickahominy River water was approximately 7.5 mg/L; therefore, no dilution was required. The pH values of the filtered samples were adjusted to 6.3 with Na_2CO_3, and the ionic strengths adjusted to 0.0025 with NaCl. Stock solutions were stored in 20 L aliquots at 4°C in the dark.

Additional processing of the stock solutions was required to support study of the impact of coagulation on the distribution and recovery of DMM constituents. In order to permit direct comparison of untreated and coagulated water DMM constituent distributions, 12 L of stock Lake Drummond solution and 6 L of stock Chickahominy River solution were coagulated. Each stock solution was coagulated in 500 mL aliquots using a Phipps & Bird six paddle jar testing apparatus. Coagulation was conducted at pH 5.5 with a coagulant dose of 50 mg/L alum ($Al_2(SO_4)_3 \cdot 14.3H_2O$), conditions which were determined to constitute an enhanced coagulation scheme for the Lake Drummond stock solution. For the purpose of comparing treatment effectiveness, the same conditions were used for coagulation of both waters. A rapid mix period of 2 min at 100 RPM was used followed by a 30 min tapered flocculation period consisting of 10 min each at 40, 30, and 20 RPM consecutively. Coagulated stock solutions were allowed to settle for 1 hr and the supernatants decanted and filtered through 1 μm membrane filters. Coagulated stock solutions were stored at 4°C in the dark until application of the DMM fractionation procedure.

Analytical Methods

Non-purgable dissolved organic carbon (NPDOC) content was measured by thermal combustion with infrared detection of CO_2 using a Shimadzu TOC-5000 Total Carbon Analyzer operated in the non-purgable organic carbon mode. A high sensitivity tungstun impregnated glass wool thermal combustion catalyst was used throughout this study to improve the accuracy and precision of NPDOC measurements at low carbon concentrations (≤ 10 mg/L). With the high sensitivity catalyst installed, the coefficient of variation for replicate NPDOC measurements was routinely less than 1 %, even at carbon levels as low as 0.5 mg/L. The use of high sensitivity catalyst was deemed appropriate since the determination of changes in DMM constituent distribution resulting from coagulation sometimes required taking the difference between two NPDOC measurements of similar magnitude. Performance of the carbon analyzer was monitored by including two QA/QC standards with each batch of ten samples analyzed. All standards and samples were acidified to pH 2 with 3 N HCl and sparged with TOC grade air for 2 min. prior to analysis, in order to remove trace volatile compounds and inorganic carbon (CO_2).

Absorbance of ultraviolet light at 254 nm was measured in accordance with Method 5910 of *Standard Methods for the Examination of Water and Wastewater* (*71*). A Beckman DU-600 spectrophotometer operated in the fixed wavelength mode, and equipped with an optical quality quartz glass cuvette with a 1 cm light path length, was used for all absorbance measurements. Ultra-pure water was used as the UV absorbance blank. A pH value of 2 was used for all UV_{254} measurements performed in this study. This pH was selected for measurement of UV_{254} absorbance in order to minimize interference due to reflection of incident UV light by colloidal material – principally colloidal metal oxides (*71*). Previous characterization of the apparent size distribution of iron in Lake Drummond source water demonstrated that it contained significant quantities of colloidal mineral-phase iron (*72*), and due to the similarity of the Chickahominy River water source, significant quantities of colloidal iron were also anticipated to be present in this water.

Flame atomic adsorption spectroscopy was used to quantify iron and aluminum. All metal analyses were performed using a Perkin-Elmer Zeeman 5100 PC instrument operated in the graphite furnace mode. Two point calibration curves were prepared for iron (0 and 40 μg/L) and aluminum (0 and 20 μg/L) before each batch of samples analyzed. Samples, which had been previously acidified to pH 2 with 3 N HCl, were serially diluted as necessary with 0.5% (v/v) HNO_3 to obtain metal concentrations within the instrumental analysis range. The limit of detection for all metals analyzed in this study was 1 μg/L.

Results

Distribution and Recovery of Dissolved Material Matrix Components

The DMM Fractionation Protocol was applied to four working solutions, 12 L each of untreated and coagulated Lake Drummond stock solutions and 6 L each of untreated and coagulated Chickahominy River stock solutions, in order to assess the distribution and recovery of DMM components. The distributions of several specific DMM components including NPDOC, UV_{254} absorbing material, iron, and aluminum were measured. Mass balances were subsequently performed on these DMM components by comparing component values measured for each whole (unfractionated) working solution with cumulative values recovered in corresponding DMM fractions. Ideally, the recovery efficiency for each DMM component would be 100 percent, indicating that DMM constituents were not irreversibly sorbed onto fractionation system components and organic contaminants were not released from resin materials during fractionation.

Non-purgable Dissolved Organic Carbon

The distribution of NPDOC among DMM fractions isolated from untreated and coagulated Lake Drummond and Chickahominy River working solutions, as well as NPDOC recovery, are graphically represented in Figure 1.2. The NPDOC recoveries of Lake Drummond untreated and coagulated working solutions were 96.0 and 101 percent, respectively. Similarly, the NPDOC recoveries of Chickahominy River untreated and coagulated working solutions were 101 and 99.9 percent, respectively. No evidence of contamination by organic resin material was detected, as determined by GC-MS analysis of the extracted DMM fractions under the same chromatographic conditions used to evaluate the adequacy of initial resin preparation.

Although the sites from which the natural water samples were collected for this study are located 106 km apart on non-interconnected waterways, the samples were collected at different times of the year, and XAD-8 k' values differed for DMM extraction from the two source waters, the distribution of NPDOC among the DMM fractions extracted from comparable Lake Drummond and Chickahominy River working solutions was quite similar. In both untreated waters the HPO-A DMM fraction dominated the NPDOC distribution, accounting for 72.7 and 65.8 percent of NPDOC in Lake Drummond and Chickahominy River working solutions, respectively. The HPI-N DMM fraction contained the next largest amount of NPDOC in both untreated waters, comprising 10.9 and 14.0 percent of NPDOC. Each of the remaining four DMM fractions contributed less than 10 percent of the total NPDOC in both untreated working solutions. The basic DMM fractions isolated from both untreated working solutions were particularly small, representing between 1.64 and 3.62 percent of total NPDOC.

Previously coagulated Lake Drummond and Chickahominy River working solutions also displayed similar NPDOC segregation patterns, with HPO-A and HPI-N DMM fractions still dominating the NPDOC distributions. Although coagulation generally reduced the amount of NPDOC in the DMM fractions extracted from both waters, the Lake Drummond HPO-N, HPI-A, and HPI-B DMM fractions showed modest increases in NPDOC. Due to their relatively small magnitudes in the NPDOC distribution of the untreated Lake Drummond working solution, redistribution of DOM into HPO-N, HPI-A and HPI-B DMM fractions following coagulation represented NPDOC increases of 21.8 to 101 percent. As seen in Figure 1.2, the HPO-A DMM fractions of both waters were preferentially removed by coagulation.

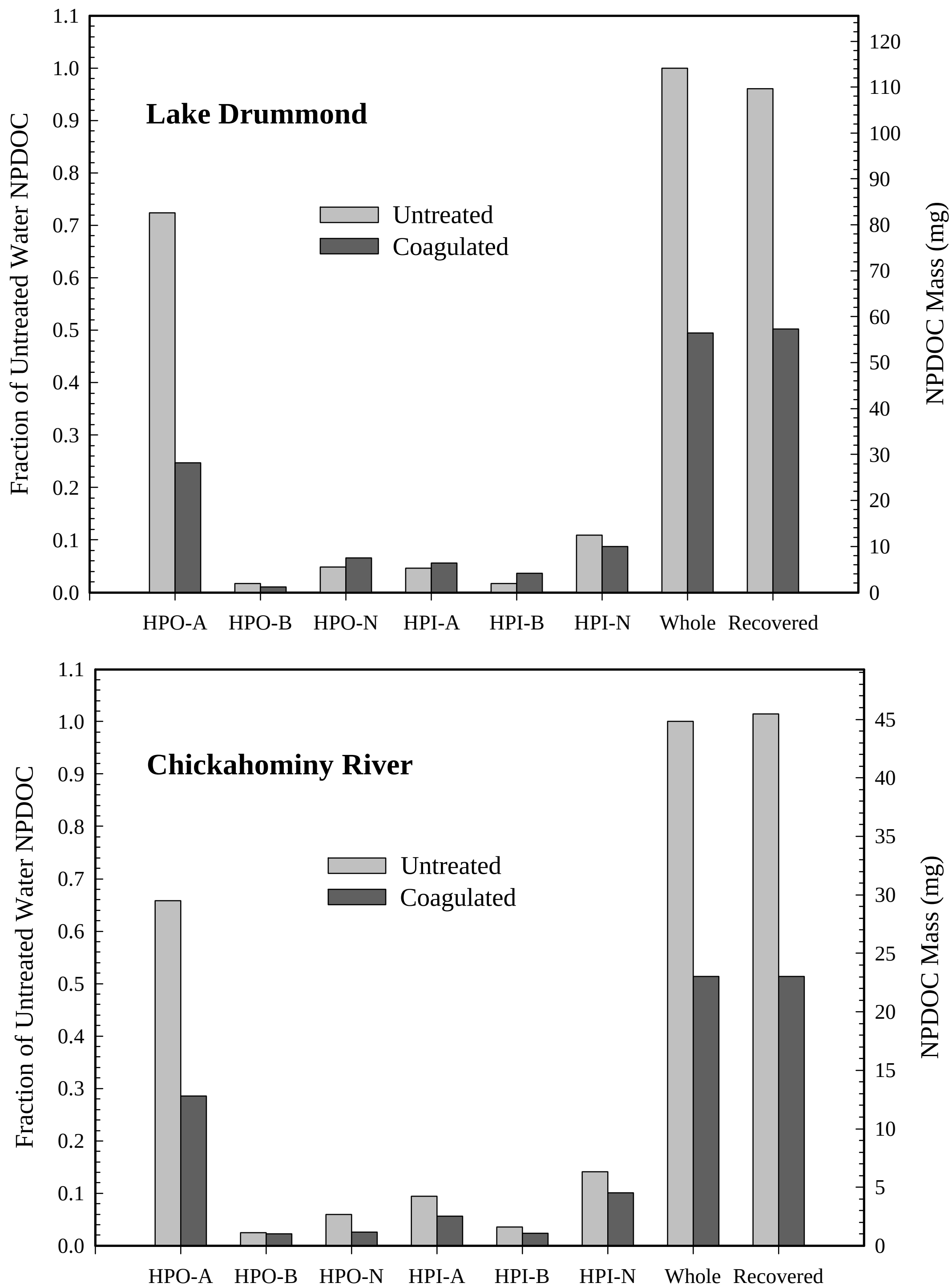

Figure 1.2: Distribution and recovery of NPDOC in DMM fractions isolated from untreated and coagulated working solutions.

UV_{254} Absorbing Material

A mass balance parameter termed the Effective Mass of UV_{254} Absorbing Material ($EMUV_{254}$) was defined based on the Lambert-Beer Law,

$$A = a \cdot c \cdot b\,, \qquad (4)$$

where *A* is absorbance, *a* specific absorptivity (L/mg·cm), *c* concentration (mg/L), and *b* light path length (cm). Substituting $c = m/V$ into Eq. 4 and rearranging yields the computational expression for $EMUV_{254}$,

$$EMUV_{254} = a \cdot m = \frac{A \cdot V}{b}\,. \qquad (5)$$

$EMUV_{254}$ was used as a surrogate mass balance parameter since determination of *a* for the complex mixture of interacting UV_{254} absorbing components present in natural waters is not required.

The distribution of $EMUV_{254}$ among DMM fractions isolated from untreated and coagulated Lake Drummond and Chickahominy River working solutions, as well as $EMUV_{254}$ recovery, are illustrated graphically in Figure 1.3. The $EMUV_{254}$ recoveries from untreated and coagulated Lake Drummond working solutions were 96.8 and 101 percent, respectively. Recoveries of $EMUV_{254}$ from untreated and coagulated Chickahominy River working solutions were 102 and 99.4 percent, respectively.

The HPO-A DMM fraction contained the vast majority of $EMUV_{254}$ in both untreated working solutions, accounting for 82.6 and 76.3 percent of the total $EMUV_{254}$ in these waters, respectively. Each of the remaining five DMM fractions recovered from these waters contained less than 7 percent of $EMUV_{254}$ in the unfractionated whole water. As with the untreated working solutions, the HPO-A DMM fractions of previously coagulated working solutions contained the majority of $EMUV_{254}$; albeit, with diminished relative magnitudes. Although coagulation altered the distribution of $EMUV_{254}$ among substituent DMM fractions for both Lake Drummond and Chickahominy River waters, examination of Figure 1.3 indicates that the absolute amount of $EMUV_{254}$ in each DMM substituent group generally decreased following coagulation. The HPO-B and HPI-B fractions recovered from Lake Drummond water were notable exceptions to this trend, containing more $EMUV_{254}$ after coagulation.

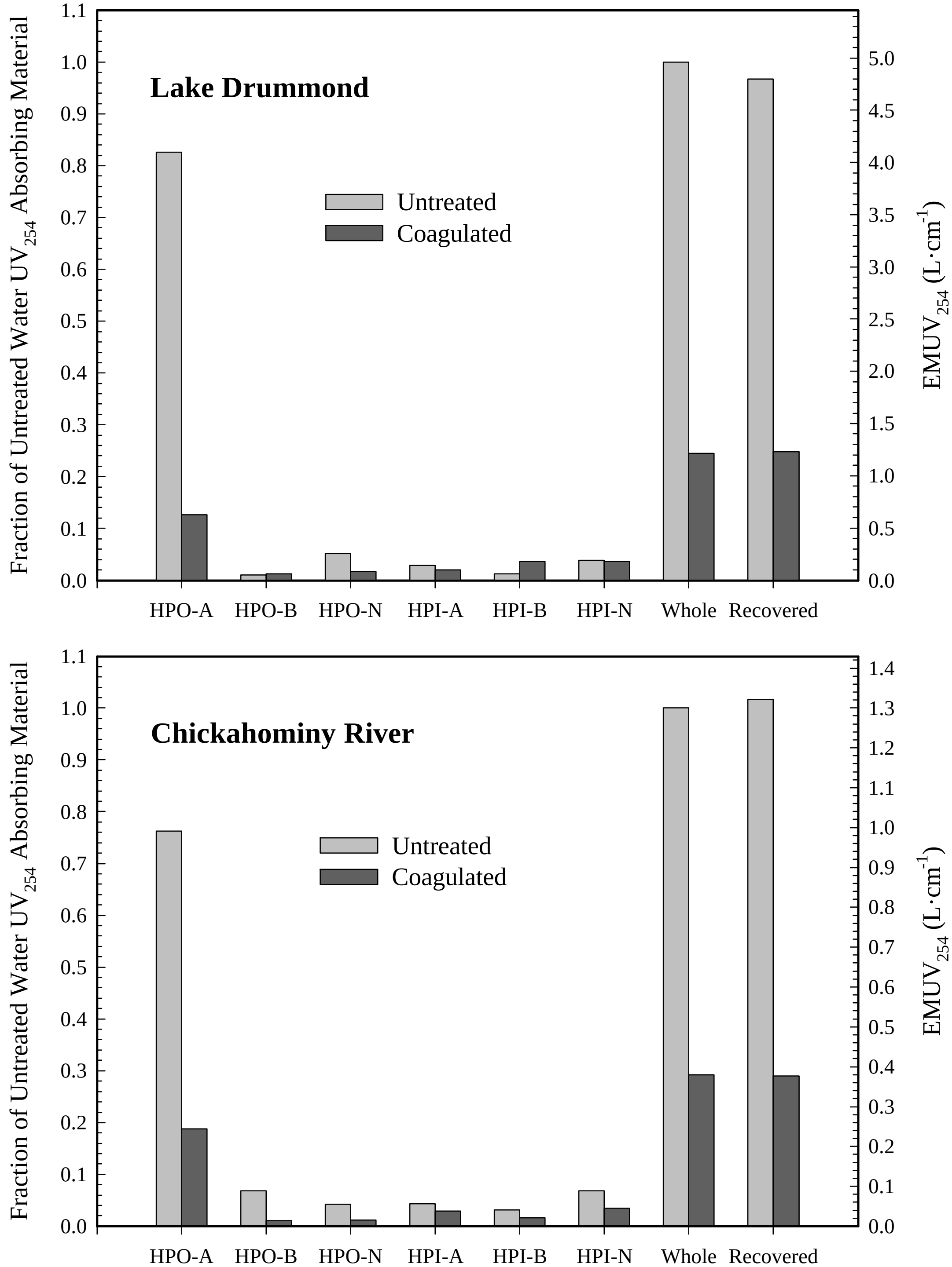

Figure 1.3: Distribution and recovery of UV_{254} absorbing material in DMM fractions isolated from untreated and coagulated working solutions.

Iron

In contrast to the cumulative recoveries of NPDOC and $EMUV_{254}$ from DMM fractions, the recovery of iron from waters subjected to the DMM Fractionation Protocol was substantially incomplete. The iron distributions and recoveries from fractionated untreated and coagulated Lake Drummond and Chickahominy River working solutions are shown in Figure 1.4. The cumulative iron recoveries from the DMM fractions of untreated Lake Drummond and Chickahominy River working solutions accounted for only 38.6 and 30.2 percent of the total iron present in these waters, respectively. Iron recovery from previously coagulated working solutions was somewhat higher than from corresponding untreated waters: 52.2 and 45.7 percent of the iron in untreated Lake Drummond and Chickahominy River working solutions was recovered in the DMM fractions of the respective coagulated working solutions.

There was considerable variation in the amount of iron present in DMM fractions isolated from Lake Drummond and Chickahominy River working solutions. In both untreated working solutions the HPO-A DMM fraction contained the largest component of recovered iron, representing 88.1 and 80.6 percent of the iron accounted for by the respective fractionations. Of the remaining five DMM fractions isolated from untreated Lake Drummond and Chickahominy River working solutions, only the HPO-B DMM fractions contained a sizable component (> 5 percent) of recovered iron. Collectively, the hydrophobic DMM fractions contained 96.9 and 96.1 percent of the iron recovered from the untreated waters.

Coagulation dramatically reduced the mass of iron in both untreated water working solutions and all of their DMM fractions, with reductions between 29 and 100 percent. Previously coagulated Lake Drummond and Chickahominy River working solutions also displayed markedly different iron segregation patterns compared with corresponding untreated working solutions; preferential removal of iron from HPO-A DMM fractions was observed.

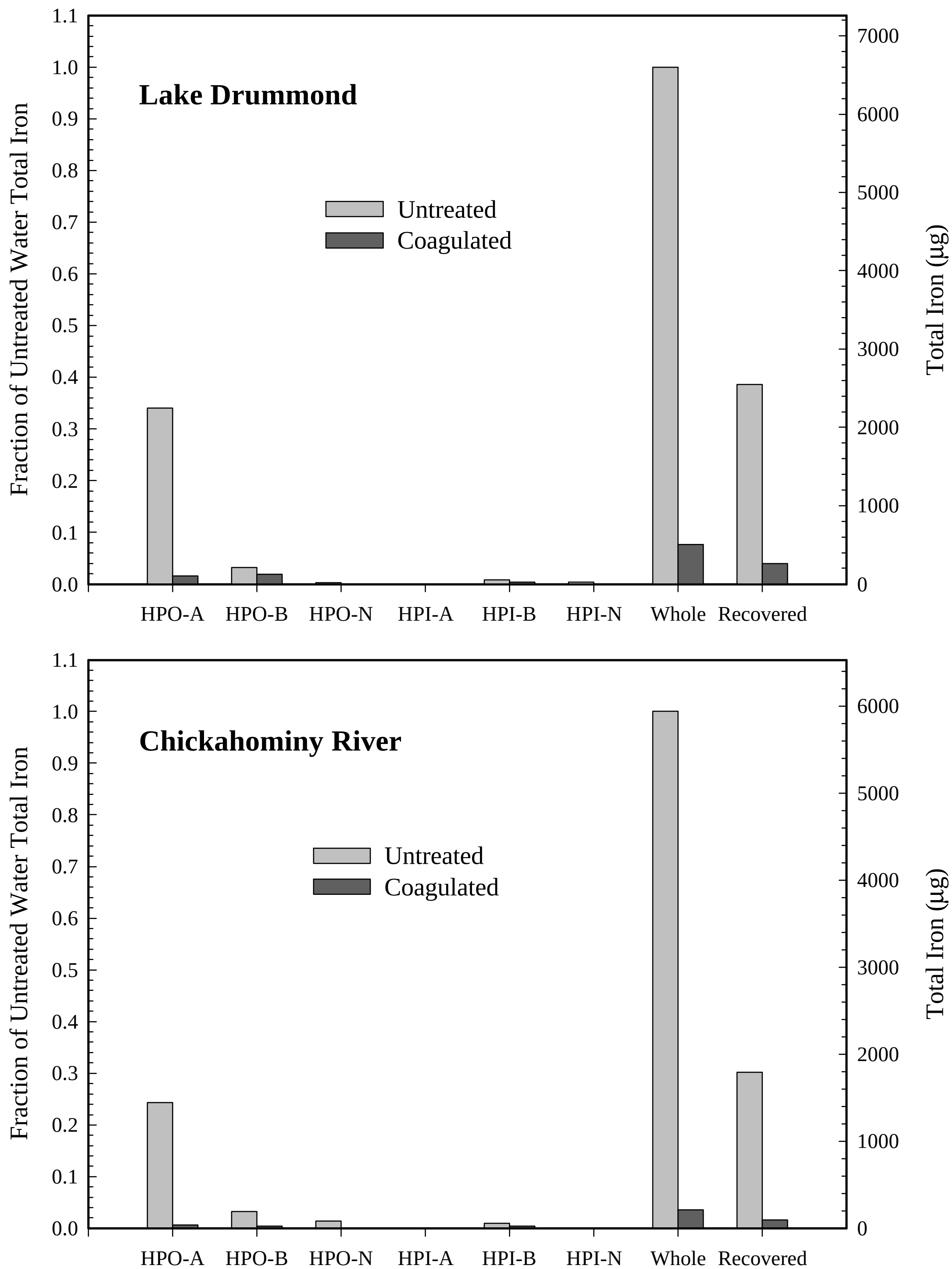

Figure 1.4: Distribution and recovery of iron in DMM fractions isolated from untreated and coagulated working solutions.

Aluminum

The cumulative recovery of aluminum in DMM fractions extracted from untreated and coagulated working solutions was also incomplete, although somewhat higher than the recovery of iron. The aluminum distributions and aluminum recoveries of untreated and coagulated Lake Drummond and Chickahominy River working solutions are illustrated in Figure 1.5. Examination of Figure 1.5 indicates that the cumulative recoveries of aluminum from Lake Drummond and Chickahominy River water DMM fractions accounted for only 52.8 and 59.2 percent of the aluminum present in the respective untreated working solutions. The recovery of aluminum was somewhat higher for coagulated working solutions, with 64.6 and 73.9 percent of the aluminum present in the coagulated Lake Drummond and Chickahominy River working solutions included in their respective DMM fractions.

As with the other DMM constituent properties previously examined, the distribution of aluminum among the DMM fractions of both untreated working solutions was nonuniform. For both untreated working solutions greater than 96 percent of the aluminum recovered was contained in the HPO-A, HPO-B, and HPI-B DMM fractions collectively; although, the distribution of aluminum among these fractions was different for the two raw waters. The relatively small mass of aluminum recovered in the remaining three DMM fractions was similarly distributed for both untreated waters, with approximately 2.5 percent, 1.2 percent, and 0.1 percent found in the HPI-N, HPO-N, and HPI-A fractions, respectively.

Following coagulation the mass of aluminum recovered in individual DMM fractions generally decreased, with the notable exception of the HPO-B and HPI-B fractions of Lake Drummond water and the HPO-B fraction of Chickahominy River water. The mass of aluminum in the basic Lake Drummond DMM fractions increased by approximately 4.8 times as a result of coagulation, while the mass of aluminum in the Chickahominy River HPO-B fraction increased only marginally. The increased aluminum content of coagulated Lake Drummond basic DMM fractions was clearly residual in nature, since whole water aluminum and recovered DMM fraction aluminum values of the coagulated water were 2.5 to 3 times higher than those of the untreated water.

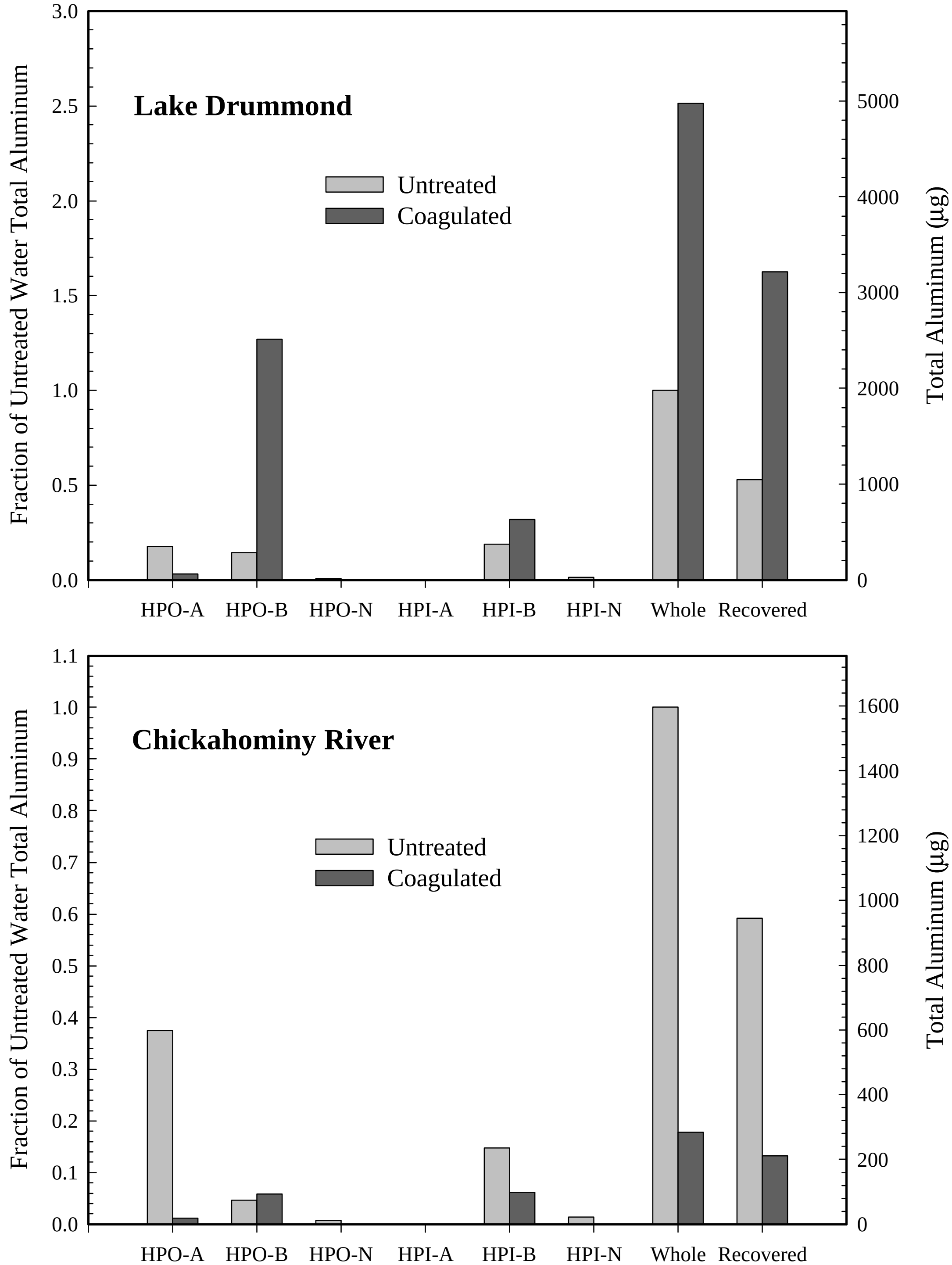

Figure 1.5: Distribution and recovery of aluminum in DMM fractions isolated from untreated and coagulated working solutions.

Discussion

Recovery of DMM Components

Previously reported experience with resin based DOM fractionation schemes similar to the DMM Fractionation Protocol implemented in this study resulted in DOM recoveries ranging from 64 to 154 percent (*56*-*58*,*62*). The recovery of DOM from untreated and coagulated waters fractionated here, as measured by NPDOC and UV_{254} absorbing material, indicates that the DMM Fractionation Protocol is capable of quantitative DOM extraction, with minimal loss of organic material due to irreversible sorption on fractionation system components. It is also evident that measurable contamination of extracted DMM fractions by organic resin material can be avoided if suitable care is taken during resin preparation. Quantitative recovery of organic material in the DMM fractions isolated in this study was observed for sample volumes as small as 6 L.

Unlike the recovery of organic material from DMM fractions, which was virtually complete for all working solutions, the recovery of iron and aluminum was markedly incomplete. Possible mechanisms which could explain the loss of iron and aluminum from a natural water sample during application of the DMM Fractionation Protocol include mechanical sieving of mineral phase colloids by the resin columns and irreversible adsorption of soluble metal ions on one or more of the exchange resins or glassware. A previous pH adjustment-ultrafiltration study with the same untreated Lake Drummond working solution used in this work has shown that DOM-metal complexes in this water were not disrupted over the range of pH values used in the DMM Fractionation Protocol, while DOM-mineral phase colloids were rapidly solublized at acidic pH values (*73*). Therefore, mechanical sieving alone does not adequately explain the observed loss of iron and aluminum during DMM fractionation, and irreversible sorption of soluble metal ions must be at least partially involved. The significantly increased recovery of iron and aluminum observed for both coagulated working solutions suggests that much of the unrecovered metal fractions were colloidal in nature, as the removal of colloidal mineral phase metal oxides by coagulation would increase the proportion of iron and aluminum present as largely recoverable DOM-metal complexes.

The observation that recovery of iron and aluminum was substantially less than 100 percent, while the simultaneous recovery of organic DMM constituents was always nearly 100 percent, led to the postulate that unrecovered fractions of iron and aluminum were not in the form of DOM-metal complexes – but rather consisted of mineral phase colloids. Given that mineral phase metal oxide colloids present in the untreated Lake Drummond working solution were solublized by the acidic pH maintained following the first sample pass through the XAD-8 resin, the most likely location for strong sorption of soluble metal ions was thought to be the MSC-1 cation exchange resin. Due to their high valancy and small hydrated ionic radius, soluble iron and aluminum ions are tightly bound by cation exchange resins, and incomplete exchange of these species during elution of the HPI-B DMM fraction from MSC-1 resin is therefore possible. In order to further elucidate the mechanism of incomplete metal recovery by the DMM Fractionation Protocol, a partial fractionation scheme was designed which specifically evaluated the elution of soluble iron from cationic MSC-1 resin.

A 35 L aliquot of pre-filtered (0.45 μm) but undiluted Lake Drummond water (~45 mg/L NPDOC, pH 6.3) was passed through a 1.65 L XAD-8 resin column at 10 BV/h to simulate removal of colloidal mineral phase material by mechanical sieving during the first XAD-8 resin pass of the DMM Fractionation Protocol. The sample was then acidified to pH 2 with 3 N HCl and applied to a 1.65 L MSC-1 resin column at 10 BV/h. The MSC-1 column was eluted with 1 N NaOH as per the DMM Fractionation Protocol, and the iron content of the recovered eluent and processed sample measured. The MSC-1 column was then eluted with 4 BV of 2 N HCl and the eluent analyzed for iron. The distribution and recovery of iron by the partial fractionation scheme outlined above is listed in the two left-hand columns of Table 1.1.

Table 1.1: Elution efficiency of iron From MSC-1 cation exchange resin.

Partial Fractionation Scheme		*DMM Fractionation Protocol*	
Fractionation Step	% Total Iron	DMM Fraction(s)	% Total Iron
XAD-8 Sieving/Sorption	1.63	HPO-B + HPO-N	3.39
Processed Sample	28.1	HPO-A + HPI-A + HPI-N	34.5
1 N NaOH MSC-1 Eluent	1.55	HPI-B	0.74
2 N NaOH MSC-1 Eluent	67.4	Unrecovered Iron	61.4
Total Recovery	98.7	Total Recovery	100

The partial fractionation scheme and DMM Fractionation Protocol do not produce individually comparable material fractions. However, the distribution of iron produced by the partial fractionation scheme was generally consistent with that produced by the DMM Fractionation Protocol based on expected segregation behavior of DMM fractions. Material retained by XAD-8 sieving/sorption would roughly correspond to the HPO-B and HPO-N DMM fractions, material remaining in the processed sample would include the HPO-A, HPI-A, and HPI-N DMM fractions, material in the 1 N NaOH MSC-1 eluent would represent the HPI-B DMM fraction, and material in the 2 N NaOH MSC-1 eluent would consist of unrecovered cations. With the foregoing segregation of DMM fractions in mind, the iron distributions generated by the two extractions were similar (Table 1.1).

Although the recovery of aluminum from MSC-1 cation exchange resin was not measured for the partial DMM fractionation described above, it is reasonable to assume that somewhat similar behavior would have been observed. The significant portion of recovered aluminum present in the HPI-B DMM fractions of the untreated waters may have been the result of partial elution, since strong cation exchange resins have a comparatively lower affinity for aluminum than iron in dilute HCl solutions (*74*). The relatively large percentage of residual aluminum isolated in the HPO-B fraction of the coagulated Lake Drummond water may be explained by the combined effects of mechanical sieving and mineral-phase colloid dissolution. Since the DOM-aluminum species present in the settled and filtered coagulated water were freshly precipitated, and therefore not highly crystalline in nature (amorphous), the dissolution kinetics of these species were expected to be faster than for well-aged iron colloids naturally present in the untreated working solution. Colloidal aluminum species retained during the first sample pass through the XAD-8 resin may have been dissolved to a greater extent during the pH 2 elution of the HPO-B DMM fraction than similarly retained colloidal iron species. Thus, the observed differences in the distribution of iron and aluminum among the DMM fractions of coagulated Lake Drummond water may be due to different dissolution rates for these species at low pH (≤ 2).

Distribution of DMM Components

The distribution of organic material among DMM fractions isolated from the raw working solutions used in this study was broadly similar to the DOM distributions typical of surface waters. DOM isolated from both water sources was predominantly hydrophobic in character, with the hydrophobic DMM fractions comprising 65 percent or more of the total DOM in each sample matrix. Moreover, the acidic DMM fractions contained approximately 75 percent of the DOM isolated from both untreated working solutions, which is consistent with previous reports of XAD-8 resin based characterization of DOM in surface waters (*56-58,60-62,75*). Considerable variation in the relative apportionment of acidic DOM between hydrophobic and hydrophilic fractions has been observed in various DOM fractionation studies, with hydrophilic values generally ranging from 5 to 25 % of total sample DOM. The very small proportion of DOM isolated in the basic DMM fractions and small to moderate amounts of DOM in the hydrophobic and hydrophilic neutral DMM fractions; respectively, is characteristic of typical DOM distributions observed for surface waters.

The variation in acidic DOM distribution between hydrophobic and hydrophilic fractions depends not only on physicochemical differences of DOM between water sources, but also on the XAD-8 k' used for fractionation. As the selected k' value increases, the applied sample volume ($V_{0.5r}$) increases proportionally (Eq. 3), resulting in an increased DOM loading onto the XAD-8 resin. Due to the finite number of sorption sites (capacity) in any XAD-8 resin column, increased DOM loading results in increased hydrophobicity of sorbed material. Competition between DOM molecules of varying hydrophobicity for available sorption sites results in selective removal of more hydrophobic DOM from solution, which effectively shifts less hydrophobic DOM into hydrophilic DMM fractions as DOM loading ($V_{0.5r}$) increases. Comparison of DOM distributions resulting from pilot-scale (this work) and preparative-scale (*76*) fractionation of similarly prepared

Lake Drummond untreated working solutions given in Table 1.2 demonstrates the expected shift of DOM from hydrophobic to hydrophilic DMM fractions when k' is increased from 30 to 88.

Table 1.2: Effect of XAD-8 k' on the distribution of recovered DOM (%) among DMM fractions.

DMM Fraction	DMM Fractionation Scheme	
	Pilot-Scale (k' = 30)	*Preparative-Scale (k' = 88)
HPO-A	75.4	58.7
HPO-B	1.71	0.73
HPO-N	5.02	1.42
HPI-A	4.81	27.1
HPI-B	1.80	3.87
HPI-N	11.3	8.12

*From reference (*76*)

Review of the literature indicates that the distribution of iron and aluminum among the discrete chemical fractions isolated by the DMM Fractionation Protocol has not been previously reported. The results of this work indicate that recovered iron and aluminum were distributed differently following DMM fractionation: greater than 80 % of recovered iron was present in the HPO-A fractions of both untreated waters, while significant portions of recovered aluminum were present in the HPO-B and HPI-B fractions in addition to the HPO-A fractions. However, DOM-metal complexation and sorption interactions in an unfractionated water may not be accurately represented by the observed distribution of iron and aluminum among its DMM fractions due to pH induced solublization of colloidal iron and aluminum oxides and differing relative affinities of DOM and strong cation exchange resins for these metals. Soluble metals may be complexed by DOM at acidic pH, resulting in a net increase in the fraction of soluble iron and aluminum. Furthermore, soil derived humic material has been observed to have a higher affinity for iron than aluminum at acidic pH (*77*), which may lead to the preferential replacement of complexed aluminum by iron. The preferential affinity of humic material for iron over aluminum may account for the fact that a significantly higher proportion of recovered iron was present in the HPO-A

DMM fraction, since this DMM fraction is composed primarily of DOM which would be classified as humic material by other extraction methods (*29,56*).

Influence of DMM Component Properties on Coagulation Behavior

Comparison of the NPDOC and UV_{254} absorbing material distributions of the DMM fractions reveals several noteworthy points regarding the physicochemical properties of DOM in the source waters examined in this study. Although the majority of both NPDOC and UV_{254} absorbing material was isolated in the hydrophobic DMM fractions of both source waters, UV_{254} absorbing material had a more pronounced bias toward the hydrophobic DMM fractions compared to NPDOC: the hydrophobic DMM fractions accounted for 88.8 and 87.3 percent of UV_{254} absorbing material, but only 78.8 and 74.3 percent of NPDOC, in Lake Drummond and Chickahominy River raw working solutions, respectively. A similar bias of UV_{254} absorbing material toward hydrophobic DOM fractions has been previously observed for XAD-8 fractionated DOM in several river waters (*63,78*). Also, Lake Drummond DOM was generally more hydrophobic than Chickahominy River DOM, since the specific UV_{254} absorbance (SUVA = $100 \times UV_{254}/DOC$) values of the two raw waters were 4.4 and 2.9, respectively.

SUVA has been proposed as an index of DOM hydrophobicity in natural waters: SUVA values of 4 to 5 indicate that DOM in a given water is relatively hydrophobic, aromatic, and of high molecular weight compared to waters with lower SUVA values, while SUVA values of less than 3 indicate that DOM in the given water is relatively hydrophilic, less aromatic, and of low molecular weight when compared to waters with higher SUVA values (*79*). In general, water sources in which DOM is primarily of autochthonous origin may be expected to exhibit low SUVA values, while water sources which have significant input of allochthonous DOM characteristic of soil organic matter may be expected to exhibit higher SUVA values. Review of SUVA values reported in the literature for surface and groundwater sources from the United States and Europe indicate that some degree of correlation exists between the origin of source water DOM and the associated SUVA value (*62,63,78-81*).

The distributions of residual DOM present in coagulated waters were significantly altered compared to the DOM distributions of the respective untreated waters. The overall removal of organic material in the two source waters by coagulation with alum was similar, as the NPDOC and UV_{254} absorbing material contents of Lake Drummond and Chickahominy River working solutions decreased by 50.5 and 48.6 percent, and 75.5 and 70.8 percent respectively following coagulation. Preferential removal of UV_{254} absorbing material compared to NPDOC has been frequently observed for coagulation of natural waters (*18,59,63,78,80,82*). As manifested by the preferential removal of UV_{254} absorbing material by coagulation, significantly different removals of hydrophobic and hydrophilic DOM were observed for both source waters examined. Removal of hydrophobic DOM from the two source waters was similar, as hydrophobic NPDOC decreased by 59.1 percent and 55.1 percent for Lake Drummond and Chickahominy River working solutions, while hydrophobic UV_{254} absorbing material decreased by 82.5 percent and 76.0 percent for the two waters, respectively. In contrast, the removal of hydrophilic DOM was markedly different for the two source waters. The hydrophilic DOM content of Lake Drummond water actually increased slightly, with increases in NPDOC and UV_{254} absorbing material of 4.48 and 15.8 percent. Hydrophilic DOM decreased following coagulation of Chickahominy River working solution, with NPDOC and UV_{254} removals of 33.6 and 44.1 percent, respectively.

The apparent shift in organic matter among Lake Drummond DMM fractions following coagulation was most prominant for the HPI-B DMM fraction, which had two to three fold increases in NPDOC and UV_{254} absorbing material (Figure 1.2 and Figure 1.3). The aluminum content of coagulated Lake Drummond water also increased by approximately 2.5 times, with all of the additional aluminum distributed in the basic DMM fractions (Figure 1.5). The unexpected shift in organic material between DMM fractions of the Lake Drummond untreated water due to coagulation cannot be explained by an experimental anomaly in either post-coagulation filtration (1 μm) or subsequent DMM fractionation. Since filtration of coagulated samples preceded DMM fractionation, membrane failure would have been reflected in unrepresentative distributions of all DMM properties among all DMM fractions, not simply the NPDOC and UV_{254} absorbing material values of the basic fractions. For example, the iron content of all DMM fractions in Lake Drummond water decreased dramatically following coagulation. Nor is the observed shift in DOM between DMM fractions resulting from coagulation readily explained by an artifact in the DMM fractionation step, as the cumulative recovery of DMM properties associated with organic material was virtually complete. Interestingly, an apparently anomalous increase in hydrophobic base DOM has been previously observed following lime treatment of Mississippi River water (*59*).

It is possible that the shift in DOM among DMM fractions following coagulation of Lake Drummond water was the result of interaction between HPO-A DOM molecules and soluble aluminum species or colloidal particles. The formation of soluble aluminum-humate complexes and DOM-mineral phase aluminum colloids during coagulation of natural waters with alum has been widely reported in the literature (*83-89*). Furthermore, the filterability of soluble and colloidal DOM-aluminum species has been demonstrated by passage of substantial portions of the DOM and aluminum present in previously coagulated natural waters through 0.45 μm and 0.1 μm membrane filters (*86*,*90*). The absence of any observable shift in DOM between DMM fractions, and only slight increase in aluminum recovered in the HPO-B DMM fraction, of coagulated Chickahominy River water may be due to a decreased tendency to form soluble or colloidal aluminum-DOM species. As previously noted, the DOM in Chickahominy River water was characteristically less hydrophobic than DOM from Lake Drummond water.

Conclusions

Pilot-scale application of the DMM Fractionation protocol allows distribution of organic constituents between hydrophobic and hydrophilic acid, base, and neutral fractions to be determined with modest sample volumes on the order of several liters. Mass balance results of NPDOC and UV_{254} absorbing material for both untreated and coagulated Lake Drummond and Chickahominy River working solutions indicate quantitative recovery (100 ± 2 percent) of DOM was achieved using the DMM Fractionation Protocol. Quantitative recovery of iron and aluminum was not achieved using the DMM Fractionation Protocol as described. Lack of complete iron and aluminum recovery was hypothesized to be incomplete elution of metals from the MSC-1 cation exchange resin. Quantitative recovery was achieved when iron retained following the standard DMM Fractionation Protocol elution of MSC-1 resin was included in the mass balance. Further refinement of the MSC-1 resin elution step to enhance metal recovery appears warranted.

Unrecovered iron and aluminum appeared to consist primarily of colloidal mineral oxides solublized by low pH conditions imposed during the DMM Fractionation Protocol. Removal of a portion of the colloidal metals in whole waters by coagulation increased recovery of both iron and aluminum in the DMM fractions. Redistribution of DOM among DMM fractions due to coagulation was also observed, as evidenced by mass increases in NPDOC, UV_{254} absorbing material, and aluminum of several DMM fractions recovered from previously coagulated Lake Drummond water. Although quantitative DOM recovery can be achieved, the results of studies using chemically extracted DOM should be critically evaluated with respect to the potential loss or redistribution of metals present as mineral oxides in the unfractionated source water.

In situations where the distribution of metals between colloidal and DOM-complexed forms is of interest, use of an additional pre-filtration step may help avoid pH induced changes in metal speciation associated with use of the DMM Fractionation Protocol. Colloidal material could be isolated by ultrafiltration against a 100 kDa apparent molecular weight cut-off membrane, acidified to solublize metal oxides, and then passed through a cation exchange column to remove free metal ions. Previously sorbed DOM and associated complexed metal in the column effluent would be added to the prefiltered source water prior to separation into DMM fractions. Colloidal metals would be recovered by regenerating the cation exchange resin and quantified. A more representative speciation of metals present in natural waters may be possible using this modification to the DMM Fractionation Protocol.

Literature Cited

1. Buffle, J., A. Tessier, and W. Haerdi. (1984). Interpretation of Trace Metal Complexation by Aquatic Organic Material. In Complexation of Trace Metals in Natual Waters. C. J. M. Kramer and J. C. Duinker, editors. Developments in Biogeochemistry. Martinus Nijhoff/Dr W. Junk Publishers, The Hague. 301-316.

2. Senesi, N. and Y. Chen. (1989). Interactions of Toxic Organic Chemicals with Humic Substances. In Toxic Organic Chemicals in Porous Media. Z. Gerstl, Y. Chen, U. Mingelgrin, and B. Yaron, editors. Ecological Studies, Vol. 73. Springer-Verlag, Berlin. 37-90.

3. Leenheer, J. A. (1991). Organic Substances That Facilitate Contaminant Transport and Transformations in Aquatic Sediments. In Humics and Soils. R. A. Baker, editor. Organic Substances in Sediments and Water. Lewis Publishers, Chelsea. 3-22.

4. Wershaw, R. L. (1991). The importance of Humic Substance-Mineral Particle Complexes in the Modeling of Contaminant Transport in Sediment-Water Systems. In Humics and Soils. R. A. Baker, editor. Organic Substances in Sediments and Water. Lewis Publishers, Chelsea. 23-34.

5. Kozak, J. (1996). Soil Organic Matter as a Factor Influencing the Fate of Organic Chemicals in the Soil Environment. In Humic Substances in Terrestrial Ecosystems. A. Piccolo, editor. Elsevier, Amsterdam. 625-664.

6. Kukkonen, J., J. F. McCarthy, and A. Oikari. (1991). Binding and Bioavailability of Organic Micropollutants in Natural Waters: Effects of the Quality and Quantity of Dissolved Organic Material. In Biological. R. A. Baker, editor. Organic Substances in Sediments and Water. Lewis Publishers, Chelsea. 111-127.

7. Müller-Wegener, U. (1988). Interaction of Humic Substances with Biota. In Humic Substances and Their Role in the Environment. F. H. Frimmel and R. F. Christman, editors. Dahlem Workshop Report. John Wiley & Sons, Chichester. 179-192.

8. Shapiro, J. (1957). Chemical and Biological Studies on the Yellow Organic Acids of Lake Waters. *Limnol. Oceanog.* 2:161-179.

9. Mathur, S. P. and E. A. Paul. (1967). Microbial Utilization of Soil Humic Acids. *Can. J. Microbiol.* 13:573-580.

10. Bhardwaj, K. K. R. and A. C. Gaur. (1972). Growth Promoting Effect of Humic Substances on *Rhizobium trifolia*. *Indian J. Microbiol* 12:19-21.

11. De Haan, H. (1974). Effect of a Fulvic Acid Fraction on the Growth of a *Pseudomonas* from the Tjeukemeer (The Netherlands). *Freshwater Biol.* 4:301-310.

12. Insam, H. (1996). Microorganisms and Humus in Soils. In Humic Substances in Terrestrial Ecosystems. A. Piccolo, editor. Elsevier, Amsterdam. 265-292.

13. Toledo, A. P. P., J. C. Tundisi, and V. A. D'aquino. (1980). Humic Acid Influence on the Growth and Copper Tolerance of *Chlorella* sp. *Hydrobiologia* 71:261-263.

14. Hoeffner, S. L. and S. E. Manahan. (1980). Influence of Coal Humic Acid on the Growth of *Chlorella vulgaris* Algae. *J. Environ. Sci. Health* A15:149-161.

15. Prakash, A. and D. J. MacGregor. (1983). Environmental and Human Health Significance of Humic Materials: An Overview. In Aquatic and Terrestrial Humic Materials. R. F. Christman and E. T. Gjessing, editors. Ann Arbor Science, Ann Arbor. 481-494.

16. Vaughan, D. and R. E. Malcolm. (1985). Influence of humic substances on growth and pysiological processes. In Soil Organic Matter and Biological Activity. D. Vaughan and R. E. Malcolm, editors. Martinus Nijhoff/Dr. W. Junk Publishers, Dordrecht. 37-75.

17. Nardi, S., G. Concheri, and G. Dell'Agnola. (1996). Biological Activity of Humus. In Humic Substances in Terrestrial Ecosystems. A. Piccolo, editor. Elsevier, Amsterdam. 361-406.

18. Edzwald, J. K. (1993). Coagulation in Drinking Water Treatment: Particles, Organics, and Coagulants. *Wat. Sci. Tech.* 27:21-35.

19. Glaze, W. H. (1990). Chemical Oxidation. In Water Quality and Treatment: A Handbook of Community Water Supplies. F. W. Pontius, editor. McGraw-Hill, Inc. New York. 747-779.

20. Krasner, S. W., M. J. McGuire, J. G. Jacangelo, N. L. Patania, K. M. Reagan, and E. M. Aieta. (1989). The Occurrence and Distribution of Disinfection By-products in US Drinking Water. *Jour. AWWA* 81:41-53.

21. Reckhow, D. A., P. C. Singer, and R. L. Malcolm. (1990). Chlorination of Humic Materials: Byproduct Formation and Chemical Interpretations. *Environ. Sci. Technol.* 24:1655-1664.

22. Leenheer, J. A., R. L. Malcolm, P. W. McKinley, and L. A. Eccles. (1974). Occurence of Dissolved Organic Carbon in Selected Groundwater Samples in the United States. *U. S. Geol. Surv. J. Res.* 2:361-369.

23. Thurman, E. M. (1985). Organic Geochemistry of Natural Waters. Martinus Nijhoff/Dr W. Junk Publishers, Dordrect.

24. Buffle, J. (1988). The Components of Aquatic Systems and Their Reactivity. In Complexation Reactions in Aquatic Systems: An Analytical Approach. Ellis Horwood Series in Analytical Chemistry. Ellis Horwood Limited, Chichester. 16-89.

25. Malcolm, R. L. (1991). Factors to be Considered in the Isolation and Characterization of Aquatic Humic Substances. In Humic Substances in the Aquatic and Terrestrial Environment. B. Allard, H. Borén, and A. Grimval, editors. Lecture Notes in Earth Sciences. Springer-Verlag, Berlin. 9-36.

26. Jolley, R. L., S. Katz, J. E. Mrochek, W. W. Pitt, and W. T. Rainey. (1975). Analyzing Organics in Dilute Aqueous Solutions. *Chemtech* 5:312-318.

27. Malcolm, R. L. (1968). Freeze-Drying of Organic Matter, Clays, and Other Earth Materials. *U. S. Geol. Surv. Prof. Paper 600C* 211-216.

28. Deinzer, M., R. Melton, and D. Mitchell. (1975). Trace Organic Contaminants in Drinking Water; Their Concentration by Reverse Osmosis. *Water Res.* 9:799-805.

29. Thurman, E. M. and R. L. Malcolm. (1981). Preparative Isolation of Aquatic Humic Substances. *Environ. Sci. Technol.* 15:463-466.

30. Shapiro, J. (1961). Freezing-Out, a Safe Technique for Concentration of Dilute Solutions. *Science* 133:2063-2064.

31. Black, A. P. and R. F. Christman. (1963). Characteristics of Colored Surface Waters. *Jour. AWWA* 55:753-770.

32. Black, A. P. and R. F. Christman. (1963). Chemical Characteristics of Fulvic Acids. *Jour. AWWA* 55:897-912.

33. Baker, R. A. (1967). Trace Organic Contaminant Concentration by Freezing. I. Low Inorganic Aqueous Solutions. *Water Res.* 1:61-77.

34. Baker, R. A. (1970). Trace Organic Contaminant Concentration by Freezing. IV. Ionic Effects. *Water Res.* 4:559-573.

35. Sridharan, N. and G. F. Lee. (1972). Coprecipitation of Organic Compounds from Lake Water by Iron Salts. *Environ. Sci. Technol.* 6:1021-1023.

36. Otsuki, A. and R. G. Wetzel. (1973). Interaction of Yellow Organic Acids with Calcium Carbonate in Freshwater. *Limnol. Oceanogr.* 18:490-493.

37. Milanovich, F. P., R. R. Ireland, and D. W. Wilson. (1975). Dissolved Yellow Acids: Quantitative and Qualitative Aspects of Extraction by Four Column Techniques. *Anal. Lett.* 8:337-344.

38. Kopfler, F. C., R. Melton, J. L. Mullaney, and R. G. Tardiff. (1975). Human Exposure to Water Pollutants. In Fate of Pollutants in the Air and Water Environments, Pt. 2. I. H. Suffet, editor. Wiley-Interscience, New York. 419-433.

39. Odegaard, H. and S. Koottatep. (1982). Removal of Humic Substances from Natural Waters by Reverse Osmosis. *Water Res.* 16:613-620.

40. Clair, T. A., J. R. Kramer, M. Sydor, and D. Eaton. (1991). Concentration of Aquatic Dissolved Organic Material by Reverse Osmosis. *Water Res.* 25:1033-1037.

41. Eberle, S. H. and K. H. Schweer. (1974). Bestimmung von Huminsaure und Ligninsulfonsaure im Wasser durch Flussig-Flussingextraktion. *Vom Wasser* 41:27-44.

42. Snyder, L. R. (1968). Principles of Adsorption Chromatography. Marcel-Dekkar, New York.

43. Moed, J. R. (1970). Aluminum Oxide as Adsobent for Natural Water-Soluble Yellow Material. *Limnol. Oceanogr.* 15:140-142.

44. Laitinen, H. A. and W. E. Harris. (1975). Chemical Analysis. McGraw-Hill, Inc, New York.

45. Kerr, R. A. and J. G. Quinn. (1975). Chemical Studies on the Dissolved Organic Matter in Seawater: Isolation and Fractionation. *Deep-Sea Res.* 22:107-116.

46. Mantoura, R. F. C. and J. P. Riley. (1975). The Analytical Concentration of Humic Substances from Natural Waters. *Anal. Chim. Acta* 76:97-106.

47. Weber, J. H. and S. A. Wilson. (1975). The Isolation and Characterization of Fulvic Acid and Humic Acid from River Water. *Water Res.* 9:1079-1084.

48. Kunin, R. (1977). Polymeric Adsorbents for Treatment of Waste Effluents. *Polym. Eng. Sci.* 17:58-62.

49. Tilsley, G. M. (1979). Interaction of Organic Matter with Anion Resins. *Chem. Ind.* 5:142-149.

50. Miles, C. J., J. R. Tuschall,Jr., and P. L. Brezonik. (1983). Isolation of Aquatic Humus with Diethylaminoethylcellulose. *Anal. Chem.* 55:410-411.

51. Aiken, G. R. (1987). Isolation of Organic Acids from Large Volumes of Water by Adsorption on Macroporous Resins. In Organic Pollutants in Water: Sampling, Analysis, and Toxicity Testing. I. H. Suffet and M. Malaiyandi, editors. ACS Advanced Chemistry Series, Vol. 214. Americal Chemical Society, Washington,D.C. 295-307.

52. Aiken, G. R. (1985). Isolation and Concentration Techniques for Aquatic Humic Substances. In Humic Substances in Soil, Sediment, and Water: Geochemistry, Isolation, and Characterization. G. R. Aiken, D. M. McKnight, R. L. Wershaw, and P. MacCarthy, editors. John Wiley & Sons, New York. 363-386.

53. Leenheer, J. A. (1985). Fractionation Techniques for Aquatic Humic Substances. In Humic Substances in Soil, Sediment, and Water: Geochemistry, Isolation, and Characterization. G. R. Aiken, D. M. McKnight, R. L. Wershaw, and P. MacCarthy, editors. John Wiley & Sons, New York. 409-420.

54. Thurman, E. M., G. R. Aiken, M. Ewald, W. R. Fischer, U. Förstner, A. H. Hack, R. F. C. Mantoura, J. W. Parsons, R. Pocklington, F. J. Stevenson, R. S. Swift, and B. Szpakowska. (1988). Isolation of Soil and Aquatic Humic Substances: Group Report. In Humic Substances and Their Role in the Environment. F. H. Frimmel and R. F. Christman, editors. Dahlem Workshop Report. John Wiley & Sons, Chichester. 31-43.

55. Leenheer, J. A. and E. W. D. Huffman,Jr. (1976). Classification of Organic Solutes in Water Using Macroreticular Resins. *J. Res. U. S. Geol. Surv.* 4:737-751.

56. Leenheer, J. A. (1981). Comprehensive Approach to Preparative Isolation and Fractionation of Dissolved Organic Carbon from Natural Waters and Wastewaters. *Environ. Sci. Technol.* 15:578-587.

57. Leenheer, J. A. and T. I. Noyes. (1984). A Filtration and Column-Adsorption System for Onsite Concentration and Fractionation of Organic Substances from Large Volumes of Water. In U.S. Geological Survey Water-Supply Paper 2230. United States Government Printing Office, Washington. 1-16.

58. McKnight, D., E. M. Thurman, R. L. Wershaw, and H. Hemond. (1985). Biogeochemistry of Aquatic Humic Substances in Thoreau's Bog, Concord, Massachusetts. *Ecology* 66:1339-1352.

59. Semmens, M. J. and A. B. Staples. (1986). The Nature of Organics Removed During Treatment of Mississippi River Water. *Jour. AWWA* 78:76-81.

60. Bourbonniere, R. A. (1989). Distribution Patterns of Dissolved Organic Matter Fractions in Natural Waters from Eastern Canada. *Org. Geochem.* 14:97-107.

61. McCarthy, J. F., L. E. Roberson, and L. W. Burrus. (1989). Association of Benzo(a)pyrene with Dissolved Organic Matter: Prediction of Kdom from Structural and Chemical Properties of the Organic Matter. *Chemosphere* 19:1911-1920.

62. Reckhow, D. A., P. Bose, B. Bezbarua, E. Hesse, and A. MacNeill. (1992). Transformations of Natural Organic Material During Preozonation. Cincinnati, Ohio. United States Environmental Protection Agency. CR-814663-01-0: pp. 1-276.

63. Croué, J. P., E. Lefebvre, B. Martin, and B. Legube. (1993). Removal of Dissolved Hydrophobic and Hydrophilic Organic Substances During Coagulation/Flocculation of Surface Waters. *Wat. Sci. Tech.* 27:143-152.

64. Pohlman, A. A. and J. G. McColl. (1988). Soluble Organics from Forest Litter and Their Role in Metal Dissolution. *Soil Sci. Soc. J.* 52:265-271.

65. David, M. B., G. F. Vance, J. M. Rissing, and F. J. Stevenson. (1989). Organic Carbon Fractions in Extracts from O and B Horizons from a New England Spodsol: Effects of Acid Treatment. *J. Environ. Qual.* 18:212-217.

66. Vance, G. F. and M. B. David. (1989). Effect of Acid Treatment on Dissolved Organic Carbon Retention by a Spodic Horizon. *Soil Sci. Soc. J.* 53:1242-1247.

67. Abrams, M. M. and R. G. Burau. (1989). Fractionation of Selenium and Detection of Selenomethionine in a Soil Extract. *Commun. In Soil Sci. Plant Anal.* 20:221-237.

68. Abrams, M. M., R. G. Burau, and R. J. Zasoski. (1990). Organic Selenium Distribution in Selected California Soils. *Soil Sci. Soc. Am. J.* 54:979-982.

69. Hunt, G. (1987). Potential Organic Contamination Associated with Commercially Available Polymeric Sorbents. In Organic Pollutants in Water: Sampling, Analysis, and Toxicity Testing. I. H. Suffet and M. Malaiyandi, editors. ACS Advances in Chemistry Series Vol. 214. Americal Chemical Society, Washington, D.C. 245-265.

70. K.J. Pardue . (1993). Personal Communication; Supelco, Inc., Bellefonte, PA.

71. APHA, AWWA, and WEF. (1995). UV-Absorbing Organic Constituents. In Standard Methods for the Examination of Water and Wastewater. A. D. Eaton, L. S. Clesceri, and A. E. Greenberg, editors. American Public Health Association, Washington, D.C. 5-60-5-62.

72. Knocke, W. R., H. L. Shorney, and J. Bellamy. (1993). Impacts of Dissolved Organic Carbon on Iron Removal. AWWARF, Denver.

73. Tadanier, C. J., D. F. Berry and W. R. Knocke. (1997). Distribution of Iron Between Colloidal and Organically Complexed Forms -- Implications for Drinking Water Treatment. Proceedings of the CSCE-ASCE Joint Environmental Conference. Edmonton, Alberta.

74. Dean, J. A. (1995). Preliminary Separation Methods. In Analytical Chemistry Handbook. McGraw-Hill, Inc. New York. 2.1-2.128.

75. Leenheer, J. A. and E. W. D. Huffman,Jr. (1979). Analytical Method for Dissolved-Organic-Carbon Fractionation. *U. S. Geol. Surv. Water Resour. Invest.* 79:1-16.

76. Tadanier, C. J. (1998). Influence of Operational Characterization Methods on DOM Physicochemical Properties and Reactivity with Aqueous Chlorine. Doctoral Dissertation, Chapter 3. Virginia Polytechnic Institute & State University.

77. Kerndorf, H. and M. Schnitzer. (1980). Sorption of Metals on Humic Acid. *Geochim. Cosmochim. Acta* 44:1701-1708.

78. Kuo, C. and G. L. Amy. (1988). Factors Affecting Coagualtion with Aluminum Sulfate -- II. *Water Res.* 22:863-872.

79. Edzwald, J. K. and J. E. Van Benschoten. (1990). Aluminum Coagulation of Natural Organic Material. In Chemical Water and Wastewater Treatment. H. H. Hahn and R. Klute, editors. Springer-Verlag, Berlin. 341-359.

80. Edzwald, J. K., W. C. Becker, and K. L. Wattier. (1985). Surrogate Parameters for Monitoring Organic Matter and THM Precursors. *Jour. AWWA* 77:122-131.

81. Amy, G. L., M. R. Collins, C. Kuo, and P. H. King. (1987). Comparing Gel Permeation Chromatography and Ultrafiltration for the Molecular Weight Characterization of Aquatic Organic Matter. *Jour. AWWA* 79:43-49.

82. Collins, M. R., G. L. Amy, and C. Steelink. (1986). Molecular Weight Distribution, Carboxyl Acidity, and Humic Substances Content of Aquatic Organic Matter: Implications for Removal During Water Treatment. *Environ. Sci. Technol.* 20:1028-1032.

83. Narkis, N. and M. Rebhun. (1977). Stoichiometric Relationship Between Humic and Fulvic Acids and Flocculants. *Jour. AWWA* 69:325-328.

84. Dempsey, B. A., R. M. Ganho, and C. R. O'Melia. (1984). The Coagulation of Humic Substances by Means of Aluminum Salts. *Jour. AWWA* 76:141-150.

85. Edwards, G. R. and A. Amirtharajah. (1985). Removing Color Caused by Humic Acids. *Jour. AWWA* 77:50-57.

86. Jekel, M. R. (1986). The Stabilization of Dispersed Mineral Particles by Adsorption of Humic Substances. *Water Res.* 20:1543-1554.

87. Hundt, T. R. and C. R. O'Melia. (1988). Aluminum-Fulvic Acid Interactions: Mechanisms and Applications. *Jour. AWWA* 80:176-186.

88. Van Benschoten, J. E. and J. K. Edzwald. (1990). Chemical Aspects of Coagulation Using Aluminum Salts-I. Hydrolytic Reactions of Alum and Polyaluminum Chloride. *Water Res.* 24:1519-1526.

89. Van Benschoten, J. E. and J. K. Edzwald. (1990). Chemical Aspects of Coagulation Using Aluminum Salts-II. Coagulation of Fulvic Acid Using Alum and Polyaluminum Chloride. *Water Res.* 24:1527-1535.

90. Diamadopoulos, E. and D. R. Woods. (1984). The Effect of Filter Pore Size on the Evaluation of Aluminum Coagulants to Remove Fulvic Acid From Water. *Water Res.* 18:1455-1459.

Appendix A

Preparation steps for XAD-8, MSC-1, and Duolite A-7 resins.

Resin	Preparation Scheme
XAD-8	• Immerse resin in dilute NaOH (pH 10) for 24 h. • Decant NaOH and rinse 3 times in ultra-pure water. • Remove resin fines by counter-flow floatation in ultra-pure water. • Air dry and sieve resin to isolate 20/50 mesh beads. • Soxhlet extract resin sequentially in methanol for 24 h, acetonitrile for 6 h, and methylene chloride for 6 h. • Store resin in methanol until use.
MSC-1	• Immerse resin in dilute NaOH (pH 10) for 24 h. • Decant NaOH and rinse 3 times in ultra-pure water. • Air dry and sieve resin to isolate 20/50 mesh beads. • Soxhlet extract resin in methanol for 24 h. • Slurry resin with ultra-pure water and decant. Repeat until TOC of rinse water is less than 1 mg/L. • Store resin in ultra-pure water until use.
Duolite A-7	• Immerse resin in dilute NaOH (pH 10) for 24 h. • Decant NaOH and rinse 3 times in ultra-pure water. • Repeat steps 1 and 2 three times. • Air dry and sieve resin to isolate 14/50 mesh beads. • Soxhlet extract resin in acetone for 24 h. • Slurry resin with ultra-pure water and decant. Repeat until TOC of rinse water is less than 1 mg/L. • Store resin in ultra-pure water until use.

Appendix B

Column Preparation, Sample Application, and DMM Fraction Recovery

Resin	Column Preparation
XAD-8	• Rinse with ultra-pure water until column effluent NPDOC is ≤ 0.1 mg/L above the NPDOC of ultra-pure water. • Rinse column with 1 BV of 0.1 N NaOH. • Rinse column with 1 BV of 0.1 N HCl. • Rinse with ultra-pure water until column effluent is ≤ 0.1 pH unit below the pH of ultra-pure water.
MSC-1	• Rinse with ultra-pure water until column effluent NPDOC is ≤ 0.1 mg/L above the NPDOC of ultra-pure water. • Rinse column with 1 N NaOH until breakthrough (approximately 3 BV). • Rinse column with 4 BV of 2 N HCl to hydrogen saturate the resin. • Rinse column with ultra-pure water until the specific conductance of the column effluent is ≤ 0.1 μmho/cm.
Duolite A-7	• Rinse with ultra-pure water until column effluent NPDOC is ≤ 0.1 mg/L above the NPDOC of ultra-pure water. • Rinse column with 1 N HCl until effluent NPDOC ≤ 1 mg/L. • Rinse column with 1 N NaOH to convert resin to free-base form (color change from brown to yellow complete). • Rinse column with ultra-pure water until the specific conductance of the column effluent is ≤ 0.1 μmho/cm.

Resin	Sample Application
	• Pre-filter desired sample volume with 0.45 μm filter cartridges (Submicronic Filter – Fisher Scientific Cat. No. H-02913-20). • Adjust filtered sample pH to 6.3±0.1 with Na_2CO_3, sparge vigorously for 15 min with filtered air to equilibrate with atmosphereic CO_2. Check pH, repeat step if necessary.
XAD-8	• Apply sample to XAD-8 column at 10±0.2 BV/h (Carbuoy pressure ~ 10 psig) • Monitor effluent NPDOC for column breakthrough. • Displace residual sample from column with 2.5 BV ultra-pure water rinse. Add rinse volume to processed sample volume. • Elute HPO-B DMM fraction as described below. • Acidify processed sample to pH 2 with 3 N HCl. • Apply acidified sample to XAD-8 column at 10±0.2 BV/h (Carbuoy pressure ~ 10 psig). • Monitor effluent NPDOC for column breakthrough. • Displace residual sample from column with 1.0 BV 0.01 N HCl rinse. Add rinse volume to processed sample volume.
MSC-1	• Apply acidified sample to MSC-1 column at 10±0.2 BV/h (Carbuoy pressure ~ 10 psig). • Monitor effluent NPDOC and $[Na^+]$ for column breakthrough. • Displace residual sample from column with 1.0 BV 0.01 N HCl rinse. Add rinse volume to processed sample volume.
Duolite A-7	• Apply acidified sample to Duolite A-7 column at 10±0.2 BV/h (Carbuoy pressure ~ 10 psig). • Monitor effluent NPDOC and specific conductance for column breakthrough. • Displace residual sample from column with 1.0 BV ultra-pure water rinse. Add rinse volume to processed sample volume.

Fraction	DMM Fraction Recovery
HPO-B	• Backflush elute XAD-8 column after first sample pass (Figure 1.1 – Step 3). Apply 0.25 BV 0.1 N HCl followed by 1.5 BV 0.01 N HCl. • Immediately neutralize eluent to pH 7.0±0.1 with 3 N NaOH and store at 4°C.
HPO-A	• Backflush elute XAD-8 column after second sample pass (Figure 1.1 – Step 5). Apply 0.25 BV 0.1 N NaOH followed by 1.5 BV 0.01 N NaOH. • Immediately neutralize eluent to pH 7.0±0.1 with 3 N HCl and store at 4°C.
HPO-N	• Rinse XAD-8 column with ultra-pure water until influent and effluent differ by ≤ 0.1 pH unit. Unpack column and air dry resin (Figure 1.1 – Step 6). • Soxhlet extract resin in methanol for 1 h. • Dilute methanol 1:1 with ultra-pure water • Remove methanol by vacuum-rotary evaporation at 40°C. • Adjust pH to 7.0±0.1 as necessary and store at 4°C.
HPI-B	• Forward elute loaded MSC-1 column with 1 N NaOH until Na^+ breakthrough (Figure 1.1 – Step 8). • Immediately neutralize eluent to pH 7.0±0.1 with 3 N HCl and store at 4°C.
HPI-A	• Backflush elute loaded Duolite A-7 column with 1 N NaOH (Figure 1.1 – Step 10). Monitor effluent specific conductance, pH and NPDOC for elution endpoint (~ 2 BV). • Immediately neutralize eluent to pH 7.0±0.1 with 3 N HCl and store at 4°C.
HPI-N	• Reduce volume of processed sample by vacuum rotary evaporation at 40°C. • Adjust pH to 7.0±0.1 as necessary and store at 4°C.

Chapter 2

Apparent Molecular Weight Distribution of Dissolved Organic Material in Environmental Samples by Ultrafiltration

Abstract

Knowledge of the size distribution of dissolved organic material (DOM) is of tremendous practical significance in the study of both natural and engineered aquatic and terrestrial systems. This study was conducted to demonstrate the validity of using batch ultrafiltration data in conjunction with an appropriate membrane permeation model as a means of determining both average and distributed AMW information for solutes in dilute heterodisperse mixtures such as natural waters. An ultrafiltration protocol was developed by combining carefully controlled experimental procedures with an existing membrane permeation model. The protocol was systematically validated with respect to implicit permeation model assumptions and near-membrane surface hydraulic environment effects. Linear independence of membrane solute transport was theoretically described using non-equilibrium thermodynamics and experimentally demonstrated for the moderately hydrophilic YC/YM series of AMICON® UF membranes. The distribution of DOM with AMW and number average AMW were determined for several natural waters by fitting an appropriate statistical cummulative probability distribution function (Weibel cdf) to batch UF data determined in conjunction with the permeation coefficient model. Batch ultrafiltration provides a flexible and relatively straightforward alternative for examining the size distribution of DOM in environmental samples which is not subject to uncorrectable analytical bias.

Introduction

Knowledge of the size distribution of dissolved organic material (DOM) is of tremendous practical significance in the study of both natural and engineered aquatic and terrestrial systems. The design, evaluation, and integration of water treatment processes such as coagulation (*1,2*), solid media and membrane filtration (*3*), disinfection (*4-6*), and sorption on granular activated carbon (*7,8*) are strongly influenced by DOM size distribution. Dissolved organic material size distribution also has implications for the treatment and potential reuse of municipal and industrial wastewaters by impacting the performance of solid-liquid separation unit operations through production of soluble microbial products (*9-11*). In terrestrial and sedimentary environments, the fate and transport of synthetic organic chemicals (*12,13*), complexation of metals (*14*), and fertility of soil (*15*) have been shown to be intimately related to DOM size. Ecological studies of the primary productivity (*16-18*) and sources of DOM (*19-22*) in natural waters, and elemental cycling in the environment (*23*) also involve consideration of DOM size distribution.

Numerous analytical techniques have been used to obtain molecular size information for DOM in environmental samples including gel permeation chromatography, ultrafiltration, scattering of electromagnetic radiation, electron microscopy, ultracentrifugation, viscometry, and several colligative property measurements (*24*). Gel permeation chromatography (GPC) and ultrafiltration (UF) have been the most commonly used methods for determining DOM size data due to their versatility and relative ease of application, modest equipment requirements, and ability to simultaneously generate both average and distributed size information. However, GPC and UF use fundamentally different physicochemical processes to produce solute separation: GPC is based on size dependent exclusion of solutes from a porous gel matrix, while UF is based on concentration dependent membrane equilibrium. Based on the different physicochemical processes which produce solute separation, GPC and UF yield average and distributed size estimates which have distinct inherent analytical biases. Gel permeation chromatography gives a weight average estimate which is biased toward higher molecular weight DOM molecules; whereas, ultrafiltration results in a number average estimate which is biased toward lower molecular weight DOM molecules (*24,25*).

Membrane based separation techniques are subject to membrane rejection, a phenomenon in which membrane-solute interactions retard solute transport. The effects of membrane rejection on solute transport can be mathematically accounted for by applying a two parameter membrane permeation coefficient model to batch ultrafiltration data (*26*). Chromatographic techniques based on solute size (weight) are susceptible to solute detection related biases. Due to dilution by the mobile phase, adequate solute detection in column effluent either requires pre-concentration of solute or use of a sensitive detection method such as uv-visible absorbance. Concentration may result in DOM aggregation through intermolecular interaction (*27*); whereas, uv-visible absorbance does not detect non-aromatic DOM constituents such as low molecular weight aliphatics and carbohydrates due to the lack of conjugated bonding in their structures.

The bias inherent in any operationally defined analytical method used to obtain DOM molecular weight information in an environmental sample must be carefully considered whenever physicochemical property or chemical reactivity data are interpreted. Selection of an appropriate analytical method ultimately depends on the type of molecular weight information desired, and constraints which may be imposed by the sample matrix or objectives of the study. From the perspective of evaluating the chemical reactivity of DOM, solute concentration based methods such as ultrafiltration may be more appropriate as both the thermodynamics and kinetics of dilute aqueous phase chemical reactions are generally more closely related to the concentrations of reacting species than to their sizes.

Based on parameter estimate errors observed for a mathematically simulated UF fractionation of a two component mixture, it has been suggested that the adequacy of the membrane permeation coefficient model for determining DOM size information is limited (*26,28*). The primary focus of this research was to demonstrate the utility of the permeation coefficient model for determination of solute apparent molecular weight distribution and average AMW information in heterodisperse mixtures such as natural waters. The objectives of this research were (i) to demonstrate the adequacy of the permeation coefficient model for describing the size fractionation of heterodisperse mixtures by batch ultrafiltration based on theoretical consideration of non-equilibrium thermodynamics, and (ii) to use batch ultrafiltration data in conjunction with the permeation coefficient model to determine the number average molecular weight (AMW_N) and AMW distribution information of DOM in natural waters.

Materials and Methods

Permeation Coefficient Model

The continuously coupled manner in which permeate and retentate concentrations vary with volume filtered during batch ultrafiltration provides a logical approach for developing a permeation based model. A membrane permeation based model has been developed previously which relates the actual solute concentration with size less than the membrane AMW cutoff to permeate volume and concentration using two adjustable parameters, and has been termed the *permeation coefficient model* (*26*). If membrane permeation behavior is assumed to remain constant during an ultrafiltration cycle, the permeation coefficient is defined as,

$$p = \frac{C_p}{C_r} \qquad (1)$$

where C_p and C_r are the instantaneous membrane permeate and retentate concentrations. A differential mass balance applied to a pressurized batch ultrafiltration cell results in a first order linear differential equation of the form,

$$\frac{d\left(VC_r\right)}{dt} = -pC_rQ \qquad (2)$$

with quantities as defined in Figure 2.1.

Relating the filtration flow rate Q to the change in retentate volume V by $Q = -dV/dt$, expanding the differential, and collecting terms in Eq. 2 the differential mass balance becomes,

$$\frac{1}{C_r}\frac{dC_r}{dt} = \left(p-1\right)\frac{1}{V}\frac{dV}{dt}\,. \qquad (3)$$

Eliminating dt from both sides of the equation, the mass balance expression in Eq. 3 can be solved by integration. Integration of Eq. 3 between the initial condition $C_r(V_0) = C_{r0}$ and any arbitrary point during filtration where $C_r(V) = C_r$ yields,

$$C_r = C_{r0}\left(\frac{V_r}{V_{r0}}\right)^{p-1}. \qquad (4)$$

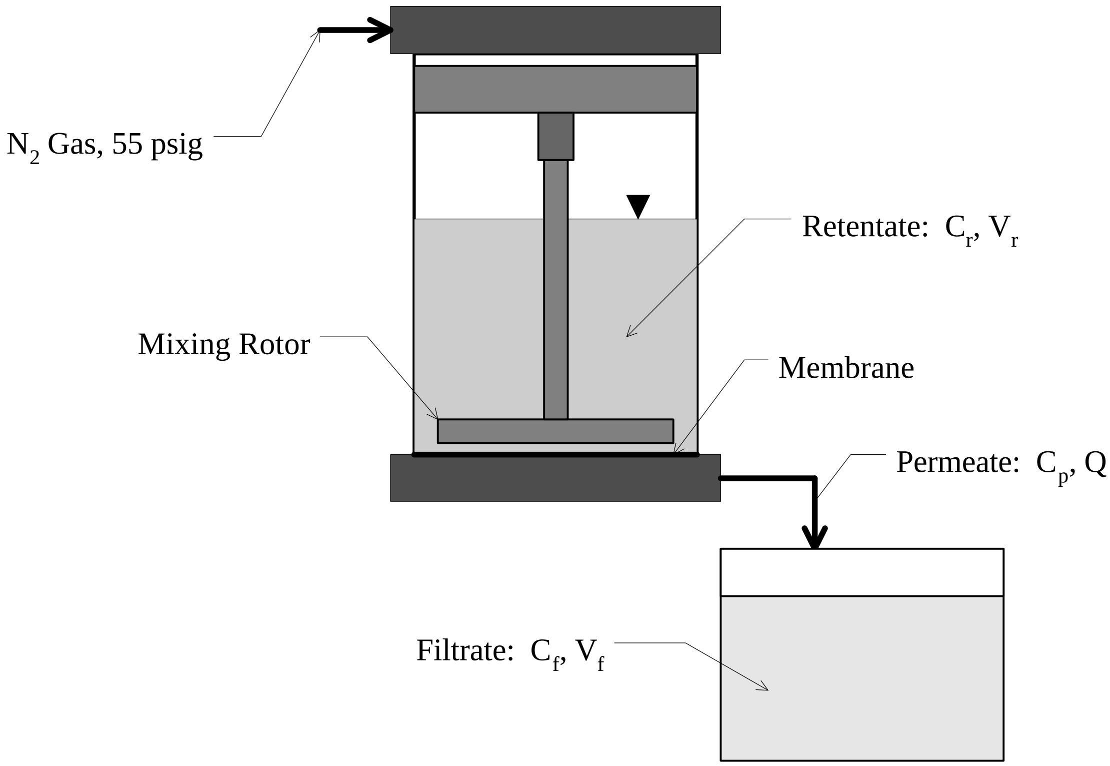

Figure 2.1: Nomenclature for a pressurized batch ultrafiltration cell.

Since the objective of a permeation based model is to relate membrane permeation behavior to permeate characteristics, the instantaneous retentate concentration C_r is eliminated from the integrated mass balance by substituting Eq. 1 into Eq. 4, and expressing retentate volume as $V_r = V_{r0} - V_p$. Elimination of V_r is required as it cannot be reliably determined due to the surface vortex produced by mixing. With these substitutions, the integrated mass balance expression becomes,

$$C_p = pC_{r0}F^{p-1} \tag{5}$$

where $F = 1-(V_p/V_0)$ is the instantaneous fractional reduction in retentate volume.

The permeation coefficient model as defined in Eq. 5 allows determination of the actual concentration C_{r0} of a solute with AMW less than the AMW cutoff of any given membrane solely from permeate data. The values of p and C_{r0} are easily determined from the linearized form of Eq. 5,

$$\ln C_p = \ln\left(pC_{r0}\right) + \left(p-1\right)\ln F \tag{6}$$

where ln (pC_{r0}) and $(p$-1) are the y-intercept and slope of the line, respectively. Alternatively, p and C_{r0} can be determined using nonlinear regression to fit the permeation coefficient model in the form of Eq. 5 to ultrafiltration permeate data. Although the linearized form of the permeation coefficient model provides an intuitive and mathematically straightforward means of calculating p and C_{r0}, evaluation of the uncertainty associated with the point estimates of these model parameters is cumbersome, as standard errors determined from the logarithmically transformed form of the model are not directly transformable to the linear domain. However, the uncertainty of p and C_{r0} parameter estimates can be evaluated directly from nonlinear regression of permeate data; standard errors represent a measure of model parameter uncertainty since transformation from the linear domain is not required.

The permeation coefficient model can also be used to demonstrate the dependence of collected permeate DOM concentration, termed the filtrate concentration C_f, on the volume of sample filtered and the magnitude of the permeation coefficient p (*26*). Substitution of the total solute mass balance $C_{r0}V_{r0} = C_rV_r + C_fV_f$ into Eq. 4 gives,

$$C_f = C_{r0}\frac{\left(1 - F^{p}\right)}{\left(1 - F\right)} \qquad (7)$$

The relationship between C_f and C_{r0} expressed in Eq. 10 is useful for evaluating the effect of permeation coefficient on ultrafiltration performance. In order to facilitate subsequent mathematical curve fitting and graphical representation of experimental UF data, the actual concentration of DOM which was nominally sized small enough to pass each ultrafiltration membrane was nondimensionalized as,

$$C_{r0}^{\ *} = \frac{C_{r0}}{C_0} \qquad (8)$$

where C_0 is the total DOM concentration in the given sample.

Determination of AMW_N from Batch Ultrafiltration Data

The Weibell probability density function (pdf) and its associated cumulative distribution function (cdf) given in Eq. 9 and Eq. 10, respectively,

$$f(x) = abx^{b-1}e^{-ax^b} \tag{9}$$

$$F(x) = 1 - e^{-ax^b} \tag{10}$$

where x equals log AMW,

were used to determine the AMW_N values of Lake Drummond DMM fractions, unfractionated whole water, and whole water mathematically reconstituted from DMM fractions using C_{r0}^* ultrafiltration data. The scale parameter a and shape parameter b for each DOM fraction were determined by fitting the cumulative distribution function Eq. 10 to C_{r0}^* ultrafiltration data. A non-linear least squares regression routine based on the Levenberg-Marquardt algorithm was used to perform all curve fitting of Eq. 10 to UF data (*29*). Best-fit values for a and b were determined by minimizing the sum of squares of deviations (c^2) between the C_{r0}^* data points and the Weibell cdf. The mean m and variance s^2 of the Weibell pdf (Eq. 9) were expressed in terms of the parameters a and b as,

$$m = a^{-1/b}\Gamma\left(1 + \frac{1}{b}\right) \tag{11}$$

and,

$$s^2 = a^{-2/b}\Gamma\left(1 + \frac{2}{b}\right) - m^2 \tag{12}$$

where Γ is the gamma function (*30*).

Sample Handling and Analytical Methods

The natural water used in this study was collected as a surface sample form Lake Drummond in Southeastern Virginia. The sample was transported to the laboratory where it was immediately (within 24 hr) processed to produce a stock sample solution for use in all further experiments. The raw water was pre-filtered through a 0.45 μm membrane filter cartridge to remove large particulate matter and detritus. Following pre-filtration, the sample was diluted with ultra-pure water to achieve a DOM concentration of approximately 10 mg/L C. The pH of the diluted sample was adjusted to 6.3 with Na_2CO_3, and the ionic strength adjusted to 0.01 with reagent grade NaCl. The stock sample was stored in 20 L aliquots at 4°C in the dark. Additional processing of the stock sample consisted of fractionating DOM into chemically discrete hydrophobic and hydrophilic acid, base, and neutral fractions using a resin based procedure (*31*,*32*).

The non-purgable dissolved organic carbon content (NPDOC) in all Lake Drummond derived water samples was measured using a Shimadzu TOC-5000 Total Carbon Analyzer operated in the non-purgable organic carbon mode. A high sensitivity tungstun impregnated glass wool thermal combustion catalyst was used throughout this study to improve the accuracy and precision of NPDOC measurements at low carbon concentrations. With the high sensitivity catalyst installed, the coefficient of variation for replicate NPDOC measurements was routinely less than 1 %, even at carbon levels as low as 0.5 mg/L. A five point calibration curve was generated for the range of 0 to 10 mg/L carbon, using analytical grade potassium hydrogen phthalate as a carbon source. The performance of the carbon analyzer was monitored by including several QA/QC standards with each batch of samples analyzed. All standards and samples were acidified to pH 2 with 3 N HCl and sparged with TOC grade air for 2 min. prior to analysis, in order to remove trace volatile compounds and inorganic carbon (CO_2).

The DOM in the subject water was size fractionated by passing aliquots of sample through a series of ultrafiltration membranes operated in parallel and the NPDOC of the filtrates used to determine the amount of organic carbon in each size range by difference. Amicon® YC-05 and YM-1, YM-3, YM-10, and YM-30 series membranes were selected for the low specific binding and associated high solute recovery characteristics they exhibit (*33*). The apparent molecular weight cutoff values specified by the manufacturer for these membranes are 0.5, 1, 3, 10, and 30 kDa, respectively. Substantial preparation of the as received membranes was required, as they are treated with glycerin to stabilize the ultrafiltration emulsion and sodium azide to inhibit microbial growth (*33*). Initial preparation of the membranes consisted of a 1 h equilibration period in ultra-pure water to remove the bulk of storage preservatives. Membranes were then placed in individual Amicon® 8200 series stirred cells and ultra-pure water passed through each, at the nominal operating pressure specified by the manufacturer (55 psig), until the NPDOC of the permeate was equal to that of ultra-pure water.

An operationally defined experimental protocol was used to evaluate the apparent molecular weight distribution of DOM in natural water samples. The operational protocol consisted of the ultrafiltration procedure used to size fractionate samples and use of the two parameter permeation coefficient model to correct for membrane rejection effects. The ultrafiltration procedure was designed to minimize variation in membrane permeability caused by filtration conditions; therefore, ultrafiltration cell operation and sample solution conditions were rigidly controlled during all filtration experiments.

Since DOM conformation and charge is strongly influenced by solution pH and ionic strength, the pH of all samples was adjusted to 6.3±0.05 with 3N HCl or NaOH as appropriate and ionic strength adjusted to 0.01 with reagent grade NaCl. The filtered volume was set at 140 ml, which corresponded to filtration from the full cell volume of 200 ml to a final volume of 60 ml. Stir speed was maintained at 200 ± 10 RPM throughout each filtration run by continuous monitoring with an optical tachometer. Each ultrafiltration membrane was used a maximum of 10 filtration cycles, then discarded. Membranes were regenerated with 0.1 N NaOH following each use, and the clean water flux verified to be within the nominal range specified by the manufacturer. Eight 10 mL aliquots were collected during each filtration run to allow the effect of membrane rejection to be accounted for when calculating C_{r0} (*26*).

Results and Discussion

Experimental Procedure Validation

Overall compliance of the ultrafiltration procedure used in this work with the implicit operational requirements imposed by use of the permeation coefficient model to describe membrane transport behavior was evaluated by performing a repeatability study consisting of a series of 10 ultrafiltration cycles applied to YM-1, YM-3, and YM-10 membranes. Each membrane was initially prepared as previously described, and regenerated between filtration cycles. Clean water flux was measured before each run, and sample flux measured at selected points during each ultrafiltration cycle. An applied nitrogen pressure of 55 psig was used to allow direct comparison of experimentally observed and manufacturer specified nominal solvent flowrates. Solute recovery was evaluated by performing a mass balance on the filtrate and retentate following each run. The constancy of permeation behavior during ultrafiltration runs was assessed by examining the linearity of logarithmically transformed permeate data.

Based on results of the repeatability study, no significant degradation in membrane flux was noted due to membrane reuse. The average clean water flux for each membrane tested was within the nominal range specified by the manufacturer (*33*), as were each of the individual cycle flowrates, and the coefficient of variation for the mean flux values was less than 2%. Average sample flux values were slightly lower than clean water flux values, but were again within the nominal range for the given membrane. The coefficient of variation for the mean sample flowrates was also less than 2%. No systematic trends in flux behavior were observed either within or between individual filtration cycles. Therefore, the permeation coefficient model assumption of constant membrane solvent flux was deemed to be satisfied by the operational ultrafiltration procedure used in this research effort.

Solute recovery was estimated by performing a mass balance on NPDOC following each ultrafiltration cycle. Each cell was allowed to recirculate for 10 min. after flow was stopped to ensure complete redistribution of solute in the retentate, and then a retentate sample taken. The mass balance was performed by comparing the initial mass of NPDOC in the sample before ultrafiltration with the cumulative NPDOC present in the retentate and permeate. Observed solute recovery was generally complete, with average differences between initial and recovered NPDOC masses of 1.08, 0.96, and 0.27 percent for YM-1, YM-3, and YM-10 membranes, respectively. No systematic trends in solute recovery were noted and the observed deviations were relatively evenly divided between positive and negative values. Error induced by the large number of volume measurements required to perform the mass balance is most likely a large contributing factor to the observed variation in solute recovery.

Since the permeation coefficient may be determined from the slope of a plot of logarithmically transformed permeate concentration and fractional filtration data (ln C_p vs. ln F), any variation in permeation behavior during an ultrafiltration cycle is manifested as nonlinearity in this plot. The linearity of logarithmic permeate data plots, and hence the constancy of permeation behavior, was examined by calculating the R^2 value associated with linear regression of the transformed permeate data and by visual inspection of the plots for systematic nonlinear deviation. The R^2 values for all 30 ultrafiltration cycles comprising the repeatability study exceeded 0.99 and nonlinear trends were not observed in the logarithmic permeate data plots. Thus, under the ultrafiltration conditions specified by the operational ultrafiltration procedure, the permeation coefficient model requirement of constant membrane permeation behavior was satisfied.

The cumulative effects of small errors in sample volume and NPDOC measurement, as well as minor variations in ultrafiltration conditions such as applied pressure, temperature, and mixing intensity, are manifested as variability in permeation coefficient model parameter estimates. The inherent uncertainty associated with the operational AMW distribution protocol used in this study was evaluated using membrane permeation data from the ultrafiltration repeatability study previously outlined. Parameter estimates for p and C_{r0} were calculated for each ultrafiltration cycle from permeate NPDOC measurements using the linearized form of the permeation coefficient model given by Eq. 6. Table 2.1 lists the mean values for p and C_{r0} and the associated coefficients of variation for these model parameter estimates. The coefficient of variation for the permeation coefficient was 3 % or less for each membrane tested, indicating that the variability in membrane permeation behavior associated with the operational AMW protocol is quite low. Perhaps more importantly, apparent molecular weight distribution information provided by the operational AMW protocol is highly reproducible, since the uncertainty of repeatability study C_{r0} estimates was 3 % or less for each AMW cutoff value examined.

Table 2.1: Precision of Permeation Coefficient model parameter estimates.

Membrane	p	C.V. (%)	C_{r0} (mg/L)	C.V. (%)
YM-1	0.30 ± 0.01	3.00	2.53 ± 0.08	2.97
YM-3	0.38 ± 0.01	2.98	4.69 ± 0.11	2.43
YM-10	0.66 ± 0.02	2.46	5.95 ± 0.11	1.79

Effect of Hydraulic Environment on Membrane Permeation Behavior

Membrane permeation behavior is intimately related to the near-surface solute concentration profile, which is in turn determined by solute physiochemical properties and hydraulic conditions imposed by the ultrafiltration procedure. A series of experiments was conducted to assess the impact of hydraulic environment on membrane permeation behavior. Lake Drummond water was fractionated against a YM-10 membrane with varying degrees of mixing, as determined by the rotational speed of the ultrafiltration module stirring impeller, and the permeation coefficient model applied to determine the permeation coefficient p and actual rejected solute concentration C_{r0} for each hydraulic condition. The influence of hydraulic environment on model parameters for rotational speeds between 100 rpm and 300 rpm is illustrated in Figure 2.2. Clearly, membrane permeation behavior in stirred batch ultrafiltration cells is dependent on the degree of mixing. Similar dependence of membrane permeation behavior on mixing intensity of dilute protein solutions in rotating membrane ultrafiltration has been observed (*34*).

The relationship between hydraulic environment and membrane permeation behavior shown in Figure 2.2 was qualitatively interpreted through visualization of the mixing conditions present in the ultrafiltration module as a function of impeller rotational speed. A dilute dispersion containing MnO_2 particles in ultra-pure water was filtered through a YM-10 membrane and the hydraulic circulation pattern of the retained particles observed visually. At low impeller rotational speeds circulation in the module was incomplete and tangential velocity across the membrane face was minimal. As expected, recirculation increased with impeller rotational speed, encompassing the entire cell volume at 200 rpm. Tangential fluid velocity across the membrane surface also progressively increased with impeller rotational speed. At rotational speeds greater than 200 rpm large scale turbulent structures were observed in the lower portions of the module, resulting in significant vertical fluid velocity at the membrane surface. Similar large scale turbulent structures termed Taylor vorticies have been visually observed in a rotating membrane ultrafiltration apparatus (*35*). These Taylor vortices overlapped one another at high rotational speeds due to flow instability resulting in increased turbulence.

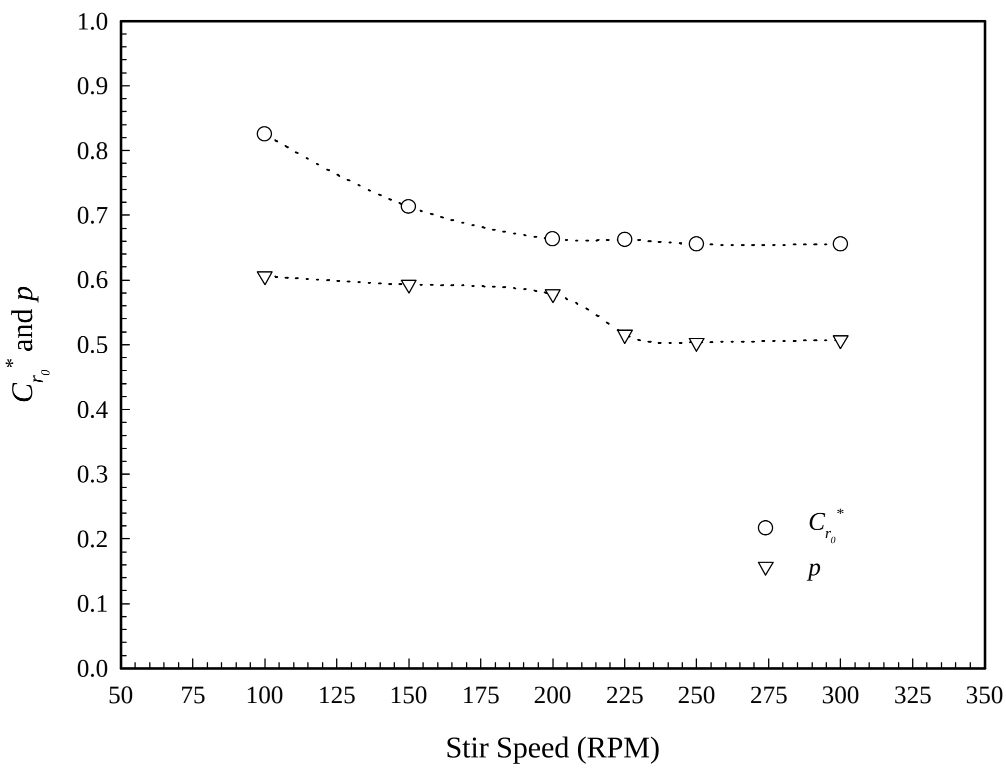

Figure 2.2: Effect of hydraulic environment on membrane permeation behavior.

The influence of hydraulic environment on the observed membrane permeation behavior at impeller rotational speeds less than 200 rpm displayed in Figure 2.2 may be explained by the presence of a semi-viscous solute layer at the membrane-solution interface. For dilute solutions ultrafiltered at low trans-membrane pressure difference the solute layer which forms due to membrane polarization remains relatively fluid, and solute molecules are relatively mobile within the layer (*36*). In contrast to the inhibition of solvent flow and decreased membrane permeation resulting from the gel-like properties of truly viscous solute layers, in the presence of a relatively fluid solute layer solvent flux remains linearly dependent on applied pressure and membrane permeation behavior is constant and independent of pressure (*37*). As tangential velocity across the membrane surface increases, the fluidity of the solute layer increases and the local solute concentration at the surface approaches that of the bulk solution. The relatively constant permeation coefficient and increase in rejected solute fraction with increased mixing observed in this study is consistent with the progressive fluidization of a semi-viscous solute layer. At an impeller speed of 200 rpm the rejected solute fraction became constant, indicating complete dissolution of the semi-viscous gel layer.

The decline in the permeation coefficient observed at rotational speeds above 200 rpm was attributed to disruption of the membrane surface concentration boundary layer due to turbulence. Excessive turbulence in the near membrane-surface region under high mixing conditions can disrupt the surface solute boundary layer, resulting in rapid return of retained solute molecules to the bulk solution by convective transport. Although turbulent scouring of retained solute from the membrane surface prevents concentration polarization from occurring, premature removal of retained solute from the membrane surface may adversely effect the observed solute separation. Since ultrafiltration membranes typically exhibit a range of pore sizes (*38,39*), solute molecules which are near in size to the nominal pore diameter may travel some distance across the membrane surface before encountering a pore of sufficient size to allow passage. If a heterodisperse mixture contains a relatively high fraction of solute molecules of approximately the same size as the membrane nominal pore diameter, excessively rapid removal of nominally retained solutes from the vicinity of the membrane surface may result in underestimation of the actual rejected solute concentration C_{r0}.

Previous Permeation Coefficient Model Error Analysis

The accuracy of parameter estimates obtained by applying the permeation coefficient model to ultrafiltration permeate data has been previously examined by simulating the permeation behavior of a solution composed of two homogeneous solute fractions (*26*). Each of the solute fractions was assumed to be physically and chemically homogeneous and relative mass fractions and permeation coefficients were arbitrarily selected for each component. The permeation behavior of the composite solution was modeled by first calculating simulated filtrate concentration data sets for the individual solute fractions C_{fa} and C_{fb} using Eq. 7, and then constructing a simulated solution filtrate concentration $C_{f(a+b)}$ data set by adding the filtrate concentration data sets of the individual components. The permeation coefficient model parameters p and C_{r0} were calculated for the composite solution through fitting the simulated solution filtrate data set ($C_{f(a+b)}$ vs. F) to Eq. 7 using nonlinear regression analysis (*40*).

Except for the special case where the permeation coefficients of the two solution components were selected to be the same, the C_{r0} value predicted for the simulated solution underestimated the assumed total solute concentration. The magnitude of parameter estimation error increased dramatically if either of the solute component permeation coefficients were assumed to be relatively small ($p \leq 0.3$) or as the difference between the assumed permeation coefficient values became larger (*26*). Based on the possible parameter estimation error indicated by this error analysis simulation, the unrestricted use of the permeation coefficient model for determination of the apparent molecular weight distribution of solutes in heterodisperse mixtures such as natural waters has been questioned (*26*,*28*).

Although the preceding simulation of ultrafiltration permeation behavior provides a convenient and computationally straightforward means of evaluating the accuracy of permeation coefficient model parameter estimates, the mathematical foundation of this error analysis approach is fundamentally flawed. The unsuitability of this simulated error analysis results from the inherently nonlinear character of the algebraic function (Eq. 5) which results from solution of the linear differential equation that defines the permeation coefficient model (Eq. 2). For the case at hand, the addition of individual solute fraction concentration data sets ($C_{fa} + C_{fb}$) to obtain the composite solution filtrate data set ($C_{f(a+b)}$), the nonlinear functional addition is represented by,

$$C_{r_{0(a+b)}}(1-F^{p_{(a+b)}}) = C_{r_{0a}}(1-F^{p_a}) + C_{r_{0b}}(1-F^{p_b})\,, \tag{13}$$

subject to the physical constraint,

$$C_{r_{0(a+b)}} = C_{r_{0a}} + C_{r_{0b}}\,. \tag{14}$$

Upon examination of Eq. 13 it is clear that, due to the exponential nature of the functions involved, the only condition under which the physical constraint imposed by Eq. 14 is satisfied occurs when p_a and p_b are equal. Stated in a mathematically more rigorous way, the computation of the composite solution filtration data set using Eq. 13 violates the *Laws of Exponents* for all but the special case when the constituent permeation coefficients p_a and p_b are equal (*41*). Moreover, as the value of either permeation coefficient deviates further from unity, the associated exponential function becomes more nonlinear and the error induced in Eq. 13 increases. Therefore, the composite filtrate concentration data set, as calculated by Eq. 13, does not accurately represent a solution to the linear differential equation which specifies the permeation coefficient model, and the parameter estimation error associated with the simulated error analysis outlined above is simply a mathematical artifact.

Linearly Independent Solute Transport in Dilute Heterogeneous Mixtures

The permeation coefficient model was derived assuming that UF membrane permeation behavior can be adequately described by a single model parameter p, which phenomenologically relates the effects of solution chemistry and membrane properties on observed permeate concentration. However, the use of a single lumped parameter p to mathematically model the composite solute permeation behavior observed during ultrafiltration of a heterodisperse mixture should not be misinterpreted as implying that the permeation behavior of individual solution components is the same. In fact, DOM present in environmental samples typically exhibits a continuum of physical and chemical properties, which would be expected to result in significant differences between observed permeation behaviors of various physiochemical solute categories. The permeation coefficient p obtained by applying the permeation coefficient model to heterodisperse solution permeate data; therefore, is more appropriately viewed as a composite parameter composed of contributions associated with the permeation of multiple physicochemically discrete solute fractions.

Consider a heterogeneous system composed of two homogeneous phases, with *n* chemically distinct solutes, separated from one another by a semi-permeable membrane as shown in Figure 2.3. Mass transport between the phases is due to an arbitrarily defined combination of convective and diffusive processes which are driven by differences in pressure ΔP, solute mole fraction Δx_i (concentration), and electrical potential $\Delta \boldsymbol{j}$. If the system is isothermal and mass transport sufficiently slow so that deviation from equilibrium at any point in the membrane is small, the simultaneous fluxes J_i of the *n* solutes in the system can be linearly related to generalized driving forces X_k by,

$$J_i = \sum_{k=1}^{n} \boldsymbol{a}_{ik} X_k \qquad (i = 1,2, \ldots,\mathrm{n}) \quad (15)$$

where the phenomenological coefficients $\boldsymbol{a}_{ik}$ collectively describe the influences of solution chemistry and membrane properties on the transport process (*42,43*). The generalized driving forces X_k are related to differences in solution composition and physical properties across the membrane by expressions of the form,

$$X_k = V_k \Delta P + \sum_{j=1}^{n} \left(\frac{\P m_k}{\P x_j} \right)_{T,P} \Delta x_j + z_k \boldsymbol{F} \Delta \boldsymbol{j} \qquad (k = 1,2, \ldots,\mathrm{n}) \quad (16)$$

where V_k denotes partial molar volume, m_k chemical potential, x_k mole fraction and z_k species charge of component *k*, and ***F*** is Faraday's constant (*44*).

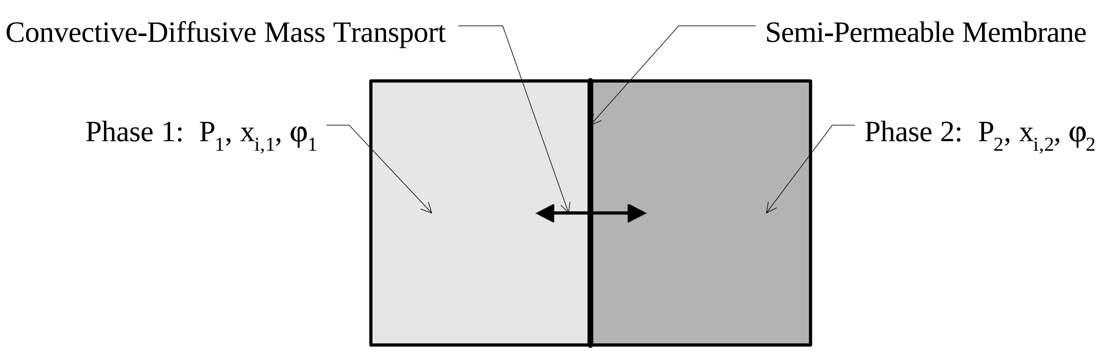

Figure 2.3: Convective-diffusive mass transport across a semi-permeable membrane in a heterogeneous two phase system.

In the most general sense, the phenomenological flux expressions given by Eq. 15 imply that the flux of any solute J_i is linearly dependent not only on its conjugate driving force $X_{k=i}$, but also to all non-conjugate driving forces $X_{k \neq i}$. Thus, non-equilibrium thermodynamics predicts the transport of solutes through a semi-permeable membrane may be represented by a coupled phenomenon, in which the extent of coupling is determined by the magnitude of the phenomenological coefficients $\boldsymbol{a}_{ik}$.

If the solution conditions imposed in Figure 2.3 are appropriately controlled – each phase is well mixed and solute concentrations are dilute enough so that concentration polarization of either membrane surface due to buildup of a solute gel layer is minimized – the non-equilibrium thermodynamic representation of trans-membrane solute transport given in Eq. 15 can be simplified considerably by setting the cross-coupling phenomenological coefficients $\boldsymbol{a}_{i \neq k}$ equal to 0. When the non-conjugate phenomenological coefficients $\boldsymbol{a}_{i \neq k}$ are neglected, Eq. 15 becomes,

$$J_i = \boldsymbol{a}_{ii} X_i \qquad (i = 1, 2, \ldots, \mathrm{n}) \quad (17)$$

from which membrane transport of each solution constituent is seen to be linearly independent of all others.

For ultrafiltration of dilute aqueous solutions, both theoretical and experimental justification for neglecting the effects of cross coupling have been presented in the literature. The theoretical framework of network thermodynamics, an extension of non-equilibrium thermodynamics which incorporates non-linear processes and the potential for chemical reactions within the membrane, has been used to demonstrate the relative insignificance of solute cross-coupling on membrane separation of dilute aqueous solutions (*45*). The effect of solute cross-coupling on pressure driven membrane transport of dilute aqueous binary salt solutions has been experimentally demonstrated to be negligible for flat cast cellulose acetate membranes (*46*). Although not explicitly recognized as such, the linear independence of solute fraction permeation behavior has also been previously observed for stirred batch ultrafiltration of a homogeneous synthetic solution composed of sucrose and vitamin B-12 with AMICON UF membranes similar to those used in this study (*26*). Under conditions of low trans-membrane pressure and high mixing intensity, the permeation behavior of several two protein mixtures separated by rotating membrane ultrafiltration has been observed to be nearly identical to that of the components separated individually (*47*). However, the uncoupled nature of ultrafiltration membrane transport processes has not been experimentally demonstrated for more complicated heterodisperse mixtures such as natural waters.

Thermodynamic Basis of the Permeation Coefficient Model

In situations where linear independence of solute fraction permeation is encountered, it may be possible to adequately describe the composite permeation behavior of a solute mixture with a linear combination of individual solute fraction permeation coefficient model parameter estimates. Since permeation of an individual solute depends on its relative abundance in solution, a logical linear apportionment of composite permeation behavior can be made using solute mass fractions as weighting factors. In terms of the permeation coefficient model, the linear independence of ultrafiltration permeation behavior can be expressed mathematically as,

$$p = \sum_{i=1}^{n} n_i \, p_i \qquad (i = 1,2,\ldots,\mathrm{n}) \qquad (18)$$

where p is the composite permeation coefficient parameter estimate calculated by linear recombination of individual solute fraction parameter estimates, p_i is the permeation coefficient parameter estimate of the i^{th} physiochemical solute fraction, n_i is the mass fraction of the i^{th} physiochemical solute fraction, and n is the number of discrete physiochemical solute fractions in the mixture.

Linear independence of solute transport during ultrafiltration of natural waters, and hence the ability of the permeation coefficient model to adequately describe their size fractionation by ultrafiltration, was experimentally evaluated by examining the extent to which a mass fraction weighted linear combination of physiochemical solute fraction permeation coefficient estimates approximated unfractionated whole water parameter estimates. The permeation coefficient model was applied to ultrafiltration permeate data for unfractionated Lake Drummond whole water and six hydrophobic and hydrophilic dissolved material matrix (DMM) DOM sub-fractions of the whole water, obtained as described elsewhere (*48*). Figure 2.4 illustrates the experimentally determined permeation coefficients for the DMM fractions and heterodisperse whole water DOM. The composite permeation coefficient p was calculated by linear combination of DMM fraction permeation coefficients p_i for each membrane AMW cutoff value using Eq. 18, and the dependence of predicted and experimentally observed permeation behavior on membrane AMW cutoff also plotted for comparison in Figure 2.4. Substantial variation existed among the permeation behaviors of the hydrophobic DMM fractions, while the permeation behaviors of the hydrophilic fractions were relatively similar to one another. The unfractionated and mathematically reconstituted whole water permeation coefficients were nearly identical over the molecular weight range observed, supporting linear independence of solute fraction ultrafiltration.

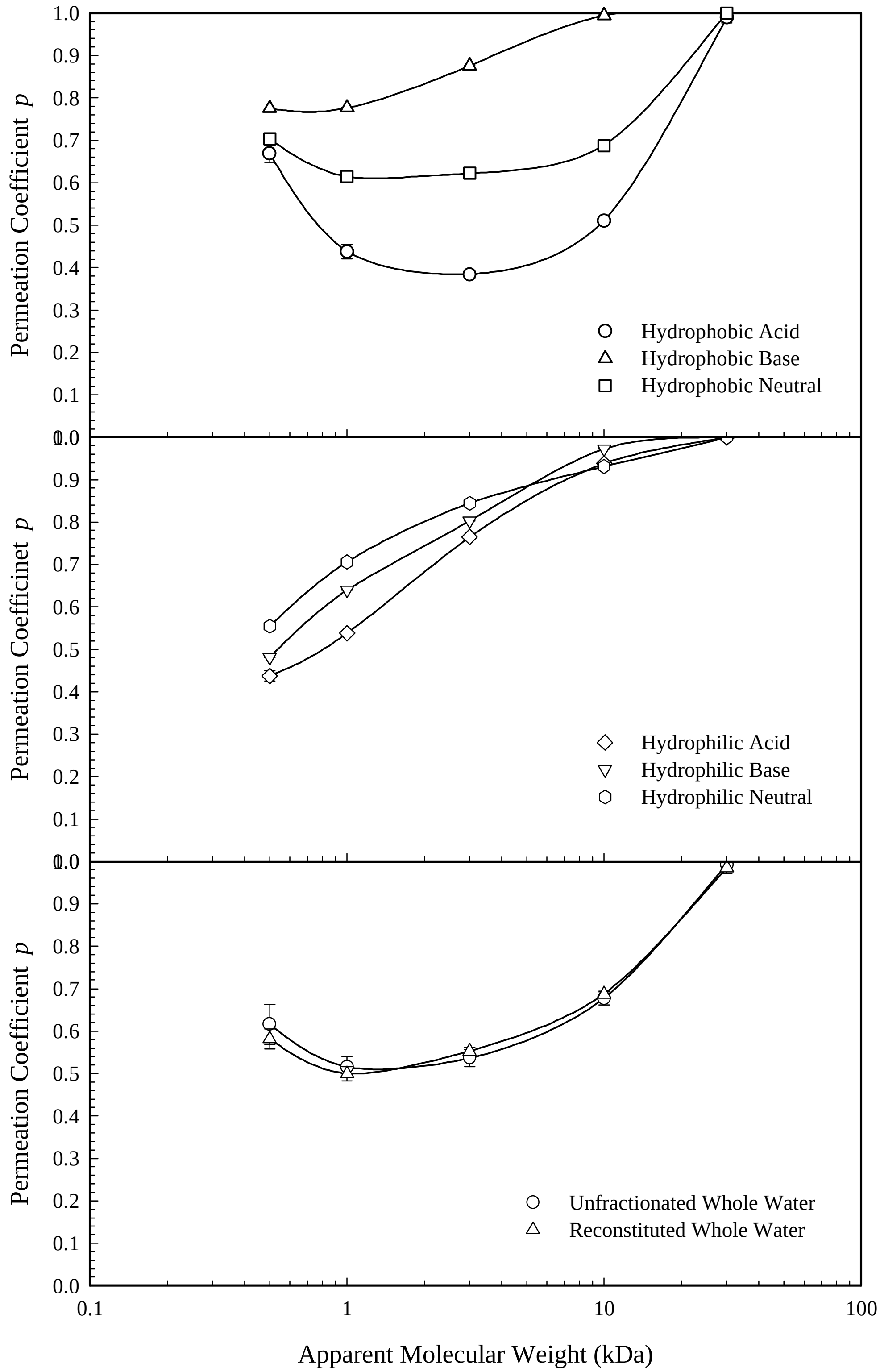

Figure 2.4: Permeation coefficients of Lake Drummond DMM fractions, unfractionated whole water, and whole water mathematically reconstituted from DMM fractions.

Determination of DOM AMW_N from Batch Ultrafiltration Data

The C_{r0}^* ultrafiltration data, associated curve-fit Weibell cdfs, and pdfs for Lake Drummond DMM fractions, unfractionated whole water, and whole water mathemaatically reconstituted from DMM fractions are given in Figure 2.5 through Figure 2.7. The average molecular weights of DOM in these samples are also graphically indicated in Figure 2.5 through Figure 2.7. Table 2.2 lists the numerical values of average molecular weight m determined using Eq. 11, the Weibell scale and shape parameters, and the χ^2 values which describe the goodness of fit of the Weibell cumulative distribution function (Eq. 10) to the respective sample C_{r0}^* ultrafiltration data. The probability density functions shown in Figure 2.5 through Figure 2.7 were nearly symmetrical about their respective means, as expected for shape parameter values of 4 and greater (*49*).

Table 2.2: Average Molecular Weight of Lake Drummond Derived DOM Samples.

DMM Fraction	AMW_{Ave} (Da)	Scale Parameter α	Shape Parameter β	χ^2
HPO-A	3910	$1.67 \cdot 10^{-4}$	6.44	0.0496
HPO-B	510	$4.79 \cdot 10^{-4}$	7.21	0.0202
HPO-N	930	$2.87 \cdot 10^{-3}$	4.99	0.0304
HPI-A	710	$2.74 \cdot 10^{-4}$	7.37	0.0706
HPI-B	520	$3.58 \cdot 10^{-4}$	7.47	0.0237
HPI-N	520	$1.98 \cdot 10^{-3}$	5.78	0.0690
Unfractionated	2590	$2.64 \cdot 10^{-4}$	6.34	0.0173
Reconstituted	1730	$1.89 \cdot 10^{-3}$	4.97	0.0666

Based on principles of calculus and probability theory, the molecular weights calculated using Eq. 11 and listed in Table 2.2 represent number average values. From calculus, the x-axis component of the centroid of the area bounded by a continuous function $g(x)$ and the x-axis is calculated as,

$$\bar{x} = \frac{M_x}{A} = \frac{\int_a^b xg(x)dx}{\int_a^b g(x)dx}, \tag{19}$$

where M_x is the first moment of $g(x)$ about the y-axis, A is the area bounded by $g(x)$, and a and b are the x-axis limits of $g(x)$ (*41*). If $g(x)$ represents an experimentally determined continuous size distribution (concentration as a function of molecular weight) of solutes in an aqueous sample, then the average value calculated by Eq. 19 represents an estimate of the number average molecular weight AMW_N of the solute dispersion (*50*). Similarly, the mean m or expected value $\mathrm{E}[x]$ of any continuously distributed random variable x with pdf $h(x)$ is defined by probability theory as,

$$m = \mathrm{E}[x] = \int_a^b xh(x)dx, \tag{20}$$

where a and b are the x-axis limits of $h(x)$, and is termed the first ordinary moment of x (*30*). Since the integrated area A under any pdf $h(x)$ is given by,

$$\int_a^b h(x)dx = 1, \tag{21}$$

the functional forms of Eq. 19 and Eq. 20 are identical. Thus, if $h(x)$ is taken as the Weibell pdf $f(x)$ defined in Eq. 9 with parameters a and b based on C_{r0}^* ultrafiltration data, then the average value calculated by Eq. 20 also represents an estimate of AMW_N.

The range of DOM molecular weights in natural waters generally spans several orders of magnitude with a mean value characteristically skewed toward smaller molecules, resulting in an asymmetric distribution of DOM with molecular weight. Due to the large range of DOM sizes encountered in natural waters, it is often convenient to express DOM molecular weight distribution in terms of log DOM molecular weight, and the distribution of log DOM molecular weight has often be adequately described by the normal distribution (*50,51*). The Weibell distribution was used to describe log DOM molecular weight in this study since it also provides a close approximation to the observed probability behavior of many natural phenomena (*30*,*49*), and has greater flexibility in fitting asymmetric pdfs due to its two parameters a and b.

For aqueous samples in which the distribution of DOM with log molecular weight is uni-modal – that is displays a single predominant peak with only minor shoulders – the Weibell pdf adequately describes the probability density of DOM and yields representative AMW_N estimates. Review of the literature indicates that the distribution of DOM with log molecular weight has often been observed to be uni-modal; however, examples are present in which the distribution of DOM with log molecular weight is more complex. The extent to which any given UF data satisfies the requirement of uni-modal DOM distribution can be qualitatively evaluated by observing the shape of the approximate DOM pdf generated by plotting the fraction of DOM in each UF size category, as determined by difference from C_{r0}^* data. Quantitatively, deviation from uni-modal distribution of DOM with log molecular weight is manifested as lack of fit of the Weibell cdf to C_{r0}^* data. It is recommended that use of the Weibell function to describe the probability distribution of DOM with log molecular weight be restricted to C_{r0}^* data which has c^2 ≤ 0.1 when fit with Eq. 10. More sophisticated numerical techniques must be developed to adequately describe the distribution of DOM with log molecular weight, and subsequently determine AMW_N, for waters which display more than one sizable pdf peak.

The impact of membrane rejection on DOM AMW distributions calculated with unadjusted batch UF permeation data (C_p) can be substantial. The error induced by use of an arbitrary C_p value to estimate the actual solute concentration sized to pass any given UF membrane (C_{r0}) depends on the volume of sample filtered and membrane AMW cut-off. If instantaneous permeate concentration C_p is used to estimate the filterable solute concentration for YC/YM series UF membranes the resulting C_{r0} estimate may be in error by as much as 50 percent, as shown in Figure 2.8. Use of unadjusted C_{r0} estimates (C_p) results in underestimation of filterable DOM fractions, which shifts C_{r0}^* data and the associated Weibell cdf and pdf functions toward higher AMW. For example, if the C_p values at a filtered sample fraction of 0.5 are used to estimate actual C_{r0} values, the calculated AMW_N for unfractionated Lake Drummond whole water increases from 2590 to 4180 Da.

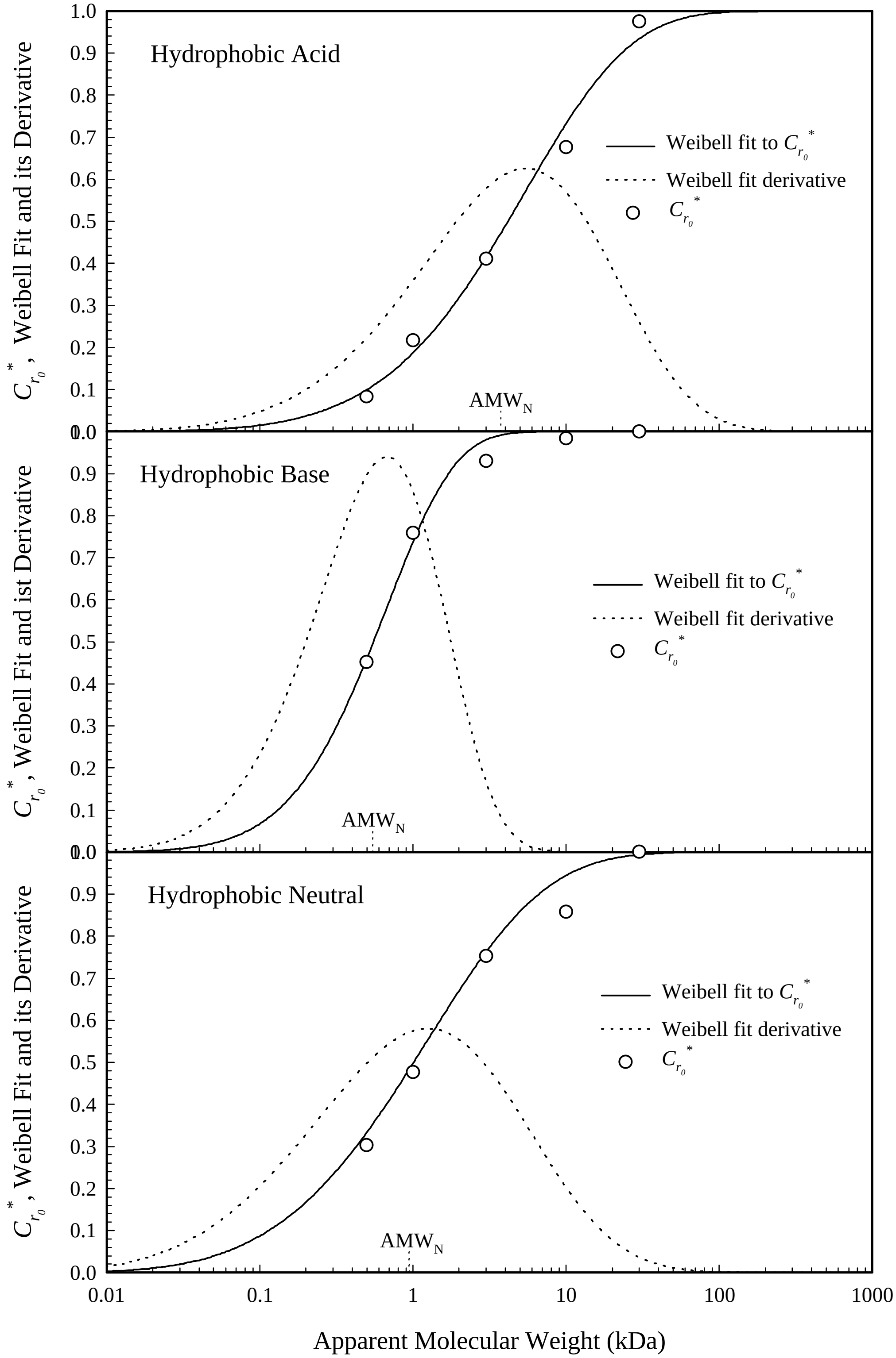

Figure 2.5: AMW$_N$ determination of Lake Drummond hydrophobic DMM fractions.

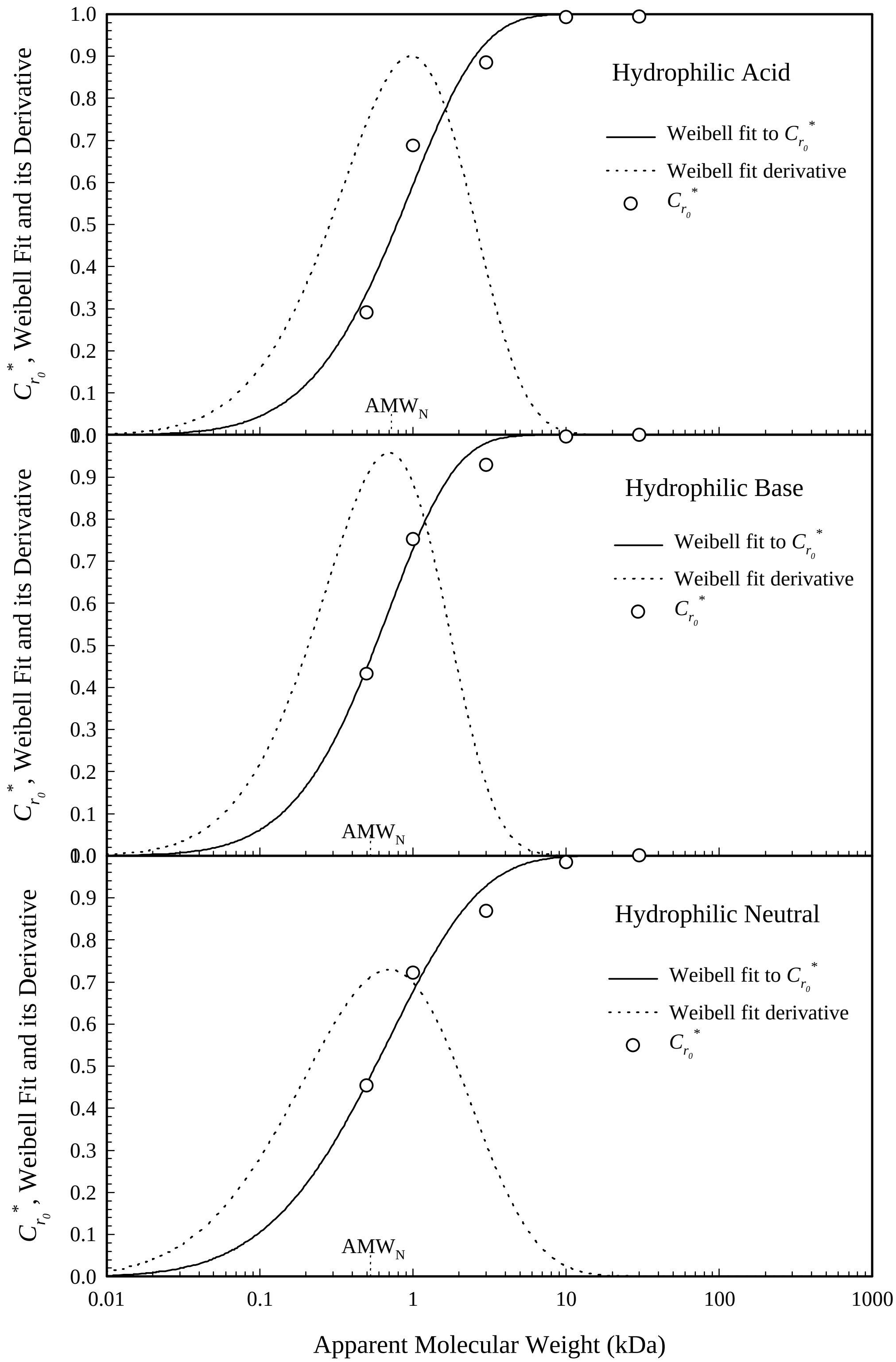

Figure 2.6: AMW$_N$ determination of Lake Drummond hydrophilic DMM fractions.

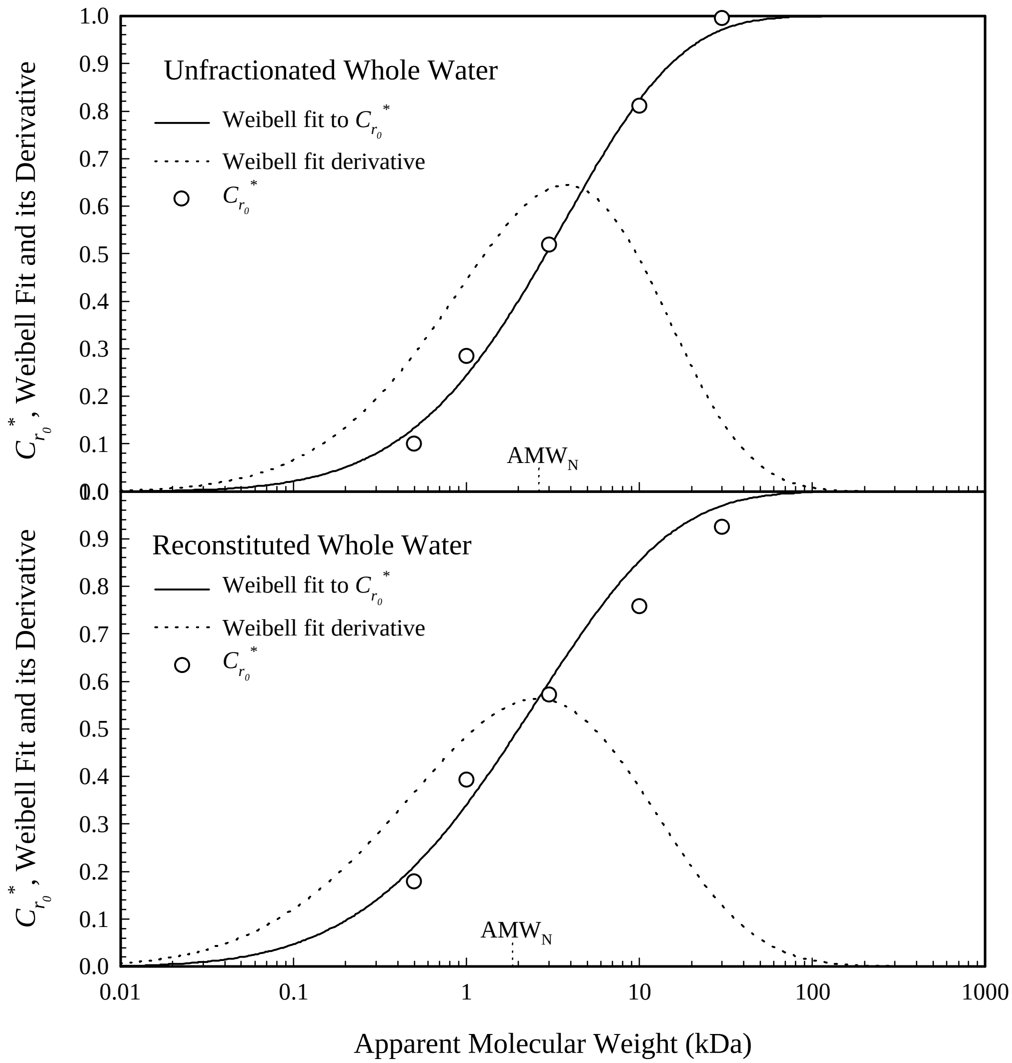

Figure 2.7: AMW$_N$ determination of Lake Drummond unfractionated and mathematically reconstituted whole waters.

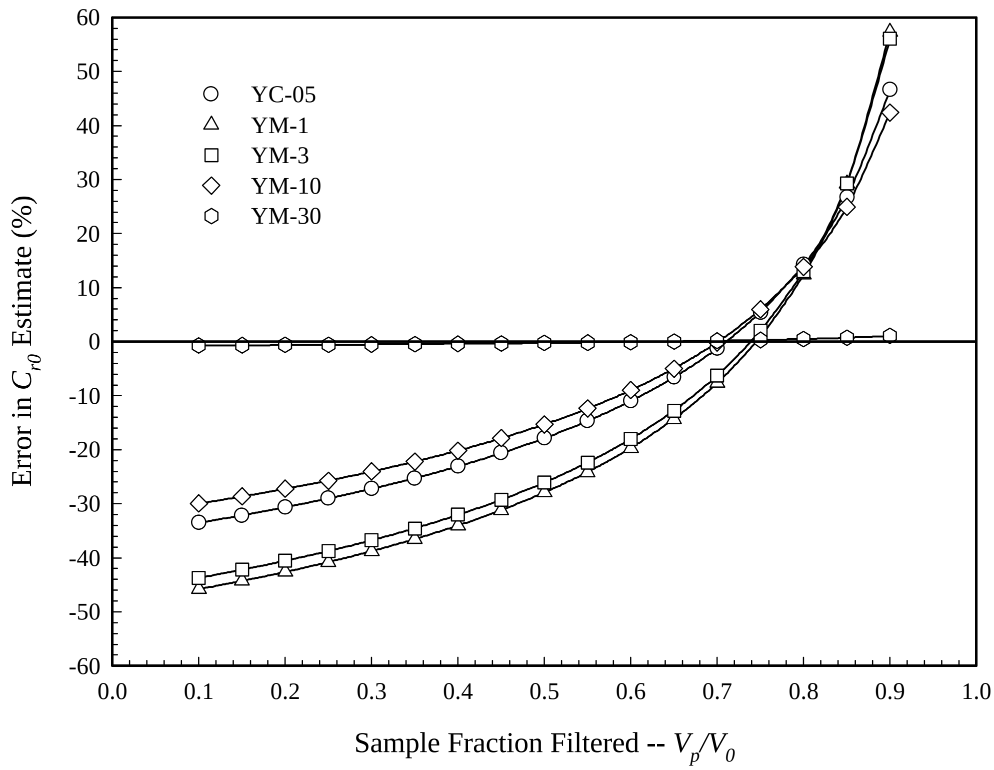

Figure 2.8: Error induced by use of C_p as an estimate of C_{r0}.

Conclusions

The permeation coefficient model adequately accounts for the effects of membrane rejection during batch ultrafiltration of dilute heterodisperse mixtures such as natural waters. The implicit assumptions of constant membrane solvent flux, absence of irreversible membrane-solute interactions, and constancy of membrane permeation behavior were demonstrated by the results of a ten cycle repeatability study using YM-1, YM-3, and YM-10 UF membranes. Effects of near membrane surface hydraulic environment on membrane permeation were examined and incorporated in an operational ultrafiltration procedure. Previous membrane permeation error estimates based on a simulated binary mixture separation were re-evaluated and shown to be artifact resulting from a mathematically flawed analysis.

Use of the permeation coefficient *p* as a single lumped parameter describing the complex permeation behavior of dilute heterogeneous mixtures such as natural waters was demonstrated, and shown to be consistent with the non-equilibrium thermodynamic foundation of membrane solute transport. Linear recombination of permeation coefficients measured for isolated hydrophobic and hydrophilic acid, base, and neutral DOM fractions successfully described the permeation coefficient of unfractionated whole water. Furthermore, linear independence of membrane solute transport was observed to be independent of membrane AMW cut-off for the Amicon® YC/YM series of moderately hydrophilic ultrafiltration membranes.

Batch ultrafiltration is a theoretically sound and experimentally viable method for average and distributed AMW information determination in dilute heterodisperse mixtures such as natural waters. The distribution of DOM with AMW and number average AMW were determined for several natural waters by fitting an appropriate statistical cummulative probability distribution function (Weibel cdf) to batch UF data determined in conjunction with the permeation coefficient model. Batch ultrafiltration provides a flexible and relatively straightforward alternative for examining the size distribution of DOM in environmental samples which is not subject to uncorrectable analytical bias.

Literature Cited

1. Randtke, S. J. (1988). Organic Contaminant Removal by Coagulation and Related Process Combinations. *Jour. AWWA* 80:40-56.

2. Kuo, C. and G. L. Amy. (1988). Factors Affecting Coagulation with Aluminum Sulfate--II Dissolved Organic Matter Removal. *Water Res.* 22:863-872.

3. Fu, P., H. Ruiz, K. Thompson, and C. Spangenberg. (1994). Selecting Membranes for Removing NOM and DBP Precursors. *Jour. AWWA* 86:55-72.

4. Schnoor, J. L., J. L. Nitzschke, R. D. Lucas, and J. N. Veenstra. (1979). Trihalomethane Yields as a Function of Molecular Weight. *Environ. Sci. Technol.* 13:1134-1138.

5. Sinsabaugh, R. L., R. C. Hoehn, W. R. Knocke, and A. E. Linkins. (1986). Precursor Size and Organic Halide Formation Rates in Raw and Coagulated Surface Waters. *J. Environ. Eng. -- ASCE* 112:139-153.

6. Amy, G. L., R. A. Sierka, J. Bedessem, D. Price, and L. Tan. (1992). Molecular Size Distributions of Dissolved Organic Matter. *Jour. AWWA* 84:67-75.

7. Kilduff, J. E., T. Karanfil, Y. Chin, and W. J. J. Weber. (1996). Adsorption of Natural Organic Polyelectrolytes by Activated Carbon: A Size-Exclusion Chromagography Study. *Environ. Sci. Technol.* 30:1336-1343.

8. Kilduff, J. E., T. Karanfil, and W. J. Weber,Jr. (1996). Competitive Interactions Among Components of Humic Acids in Granular Activated Carbon Adsorption Systems: Effects of Solution Chemistry. *Environ. Sci. Technol.* 30:1344-1351.

9. Chudoba, J. (1985). Inhibitory Effect of Refractory Organic Compounds Produced by Activated Sludge Micro-Organisms on Microbial Activity and Flocculation. *Water Res.* 19:197-200.

10. Boero, V. J., W. W. J. Eckenfelder, and A. R. Bowers. (1991). Soluble Microbial Product Formation in Biological Systems. *Wat. Sci. Tech.* 23:1067-1076.

11. Nagaoka, H., S. Ueda, and A. Miya. (1996). Influence of Bacterial Extracellular Polymers on the Membrane Separation Activated Sludge Process. *Wat. Sci. Tech.* 34:165-172.

12. Brusseau, M. L., R. E. Jessup, and P. S. Rao. (1991). Nonequilibrium Sorption of Organic Chemicals: Elucidation of Rate-Limiting Processes. *Environ. Sci. Technol* 25:134-142.

13. Brusseau, M. L. and P. S. Rao. (1991). Influence of Sorbate Structure on Nonequilibrium Sorption of Organic Compounds. *Environ. Sci. Technol.* 25:1501-1506.

14. Stevenson, F. J. (1994). Organic Matter Reactions Involving Metal Ions in Soil. In Humus Chemistry: Genesis, Composition, Reactions. John Wiley & Sons, Inc, New York. 378-404.

15. Nardi, S., G. Concheri, and G. Dell'Agnolla. (1996). Biological Activity of Humus. In Humic Substances in Terrestrial Environments. A. Piccolo, editor. Elsevier Science B. V. Amsterdam. 361-406.

16. Jüttner, F. and T. Matuschek. (1978). The Release of Low Molecular Weight Compounds by the Phytoplankton in an Eutrophic Lake. *Water Res.* 12:251-255.

17. Hoyer, O., B. Lüsse, and H. Bernhardt. (1985). Isolation and Characterization of Extracellular Organic Matter (EOM) from Algae. *Z. Wasser- Abwasser- Forsch.* 20:123-131.

18. Hino, S. (1988). Extracellular Relrease of Organic Matter Associated with the Pysiological State of Freshwater Blue-Green Algae. *Arch. Hydrobiol.* 113:307-317.

19. Steinberg, C. and U. Muenster. (1985). Geochemistry and Ecological Role of Humic Substances in Lakewater. In Humic Substances in Soil, Sediment, and Water: Geochemistry, Isolation, and Characterization. G. R. Aiken, D. M. McKnight, R. L. Wershaw, and P. MacCarthy, editors. John Wiley & Sons, New York. 106-145.

20. Malcolm, R. L. (1985). Geochemisrty of Stream Fulvic and Humic Substances. In Humic Substances in Soil, Sediment, and Water: Geochemistry, Isolation, and Characterization. G. R. Aiken, D. M. McKnight, R. L. Wershaw, and P. MacCarthy, editors. John Wiley & Sons, New York. 181-209.

21. Mayer, L. M. (1985). Geochemistry of Humic Substances in Estuarine Environments. In Humic Substances in Soil, Sediment, and Water: Geochemistry, Isolation, and Characterization. G. R. Aiken, D. M. McKnight, R. L. Wershaw, and P. MacCarthy, editors. John Wiley & Sons, New York. 211-232.

22. Harvey, G. R. and D. A. Boran. (1985). Geochemistry of Humic Substances in Seawater. In Humic Substances in Soil, Sediment, and Water: Geochemistry, Isolation, and Characterization. G. R. Aiken, D. M. McKnight, R. L. Wershaw, and P. MacCarthy, editors. John Wiley & Sons, New York. 233-247.

23. Tate, R. L., III. (1987). Soil Organic Matter as a Plant Nutrient Reservoir. In Soil Organic Matter: Biological and Ecological Effects. John Wiley & Sons, Inc. New York. 165-184.

24. Wershaw, R. L. and G. R. Aiken. (1985). Molecular Size and Weight Measurements of Humic Substances. In Humic Substances in Soil, Sediment, and Water: Geochemistry, Isolation, and Characterization. G. R. Aiken, D. M. McKnight, R. L. Wershaw, and P. MacCarthy, editors. John Wiley & Sons, New York. 477-492.

25. Moore, W. J. (1972). Physical Chemistry. Prentice-Hall, Englewood Cliffs. 977.

26. Logan, B. E. and Q. Jiang. (1990). Molecular Size Distributions of Dissloved Organic Matter. *J. Environ. Eng.* 116:1046-1062.

27. Leenheer, J. A., P. A. Brown, and T. I. Noyes. (1989). Implications of Mixture Characteristics on Humic-Substance Chemistry. In Aquatic Humic Substances: Influence on Fate and Treatment of Pollutants. I. H. Suffet and P. MacCarthy, editors. Advances in Chemistry. American Chemical Society, Washington, D.C. 25-39.

28. Kilduff, J. and W. J. Weber,Jr. (1992). Transport and Separation of Organic Macromolecules in Ultrfiltration Processes. *Environ. Sci. Technol.* 26:569-577.

29. Origin -- Technical Graphics and Data Analysis. Version 4.0 (1995). MICROCAL Software, Inc. Northampton.

30. Milton, J. S. and J. C. Arnold. (1995). Continuous Distributions. In Introduction to Probability and Sataistics: Principles and Applications for Engineering and the Computing Sciences. McGraw-Hill Series in Probability and Statistics. McGraw-Hill, New York. 99-155.

31. Leenheer, J. A. (1981). Comprehensive Approach to Preparative Isolation and Fractionation of Dissolved Organic Carbon from Natural Waters and Wastewaters. *Environ. Sci. Technol.* 15:578-587.

32. Leenheer, J. A. and T. I. Noyes. (1984). A Filtration and Column-Adsorption System for Onsite Concentration and Fractionation of Organic Substances from Large Volumes of Water. In U.S. Geological Survey Water-Supply Paper 2230. United States Government Printing Office, Washington. 1-16.

33. Amicon. (1995). Membrane Products Catalog.

34. Balakrishnan, M. and G. P. Agarwal. (1996). Protein Fractionation in a Vortex Flow Filter. I.: Effect of System Hydrodynamics and Solution Environment on Single Protein Transmission. *J. Membrane Science* 112:47-74.

35. Vigo, F. and C. Uliana. (1986). Influence of the Vorticity at the Membrane Surface on the Performances of the Ultrafiltration Rotating Module. *Sep. Sci. Technol.* 21:367

36. Blatt, W. F., A. Dravid, A. S. Michaels, and L. Nelson. (1970). Solute Polarization and Cake Formation in Membrane Ultrafiltration: Causes, Consequences, and Control Techniques. In Membrane Science and Technology: Industrial, Biological, and Waste Treatment Processes. J. E. Flinn, editor. Plenum Press, New York. 47-97.

37. Blatt, W. F. (1976). Principles and Practice of Ultrafiltration. In Membrane Separation Processes. P. Meares, editor. Elsevier Sci. Publ. Co. Amsterdam. 81-120.

38. Mulder, M. (1991). Polarization Phenomena and Membrane Fouling. In Basic Principles of Membrane Technology. Kluwer Academic Publishers, Dordrecht. 281-311.

39. Toyomoto, K. and A. Higuchi. (1992). Microfiltration and Ultrafiltration. In Membrane Science and Technology. Y. Osada and T. Nakagawa, editors. Marcel Dekkar, Inc. New York. 289-332.

40. B.E. Logan . (1997). Personal Communication.

41. Thomas, G. B., Jr. and R. L. Finney. (1992). The Calculus of Transcendental Functions. In Calculus and Analytic Geometry. Addison-Wesley Pub. Co. Reading. 397-478.

42. Onsager, L. (1931). Reciprocal Relations in Irreversible Processes -- Part I. *Phys. Rev.* 37:405-425.

43. Onsager, L. (1931). Reciprocal Relations in Irreversible Processes -- Part II. *Phys. Rev.* 38:2265-2279.

44. Haase, R. (1969). Processes in Heterogeneous (Discontinuous) Systems. In Thermodynamics of Irreversible Processes. Addison-Wesley Series in Chemical Engineering. Addison-Wesley Pub. Co., Inc. Reading. 157-214.

45. Simon, A. M., P. Doran, and R. Paterson. (1996). Assessment of Diffusion Coupling Effects in Membrane Separation. Part I. Network Thermodynamics Modelling. *J. Membrane Sci.* 109:231-246.

46. Bennion, D. N. and B. W. Rhee. (1969). Mass Transport of Binary Electrolytes in Membranes. *Ind. Eng. Chem. Fund.* 8:36-49.

47. Balakrishnan, M. and G. P. Agarwal. (1996). Protein Fractionation in a Vortex Flow Filter. II.: Separation of Simulated Mixtures. *J. Membrane Science* 112:75-84.

48. Tadanier, C. J. (1998). Influence of Operational Characterization Methods on DOM Physicochemical Properties and Reactivity with Aqueous Chlorine. Doctoral Dissertation, Chapter 3. Virginia Polytechnic Institute & State University.

49. Kottegoda, N. T. and R. Rosso. (1997). Probability Distributions. In Statistics, Probability, and Reliability for Civil and Environmental Engineers. McGraw-Hill, New York. 170-238.

50. Beyer, G. L. (1991). Determination of Particle Size. In Physical Methods of Chemistry. B. W. Rossiter and J. F. Hamilton, editors. John Wiley & Sons, New York. 445-513.

51. Buffle, J. (1988). The Components of Aquatic Systems and Their Reactivity. In Complexation Reactions in Aquatic Systems: An Analytical Approach. Ellis Horwood Series in Analytical Chemistry. Ellis Horwood Limited, Chichester. 16-89.

Chapter 3

Alteration of Dissolved Organic Matter Physicochemical Properties Produced by Resin Based Fractionation of the Dissolved Material Matrix of Natural Waters

Abstract

Dissolved organic matter (DOM) is often extracted and chemically fractionated from aquatic and terrestrial environments in order to facilitate the study of its physicochemical properties. The objective of this study was to evaluate the nature and extent of alteration induced in selected DOM physicochemical properties by simultaneous extraction and chemical fractionation from a natural water. The impact of chemical fractionation of aquatic DOM was evaluated by comparing the apparent molecular weight (AMW) distributions of selected unfractionated whole water physicochemical properties with comparable AMW distributions mathematically reconstituted from hydrophobic and hydrophilic acid, base, and neutral DOM fractions extracted from the whole water. The AMW distributions of non-purgable dissolved organic carbon (NDPOC), UV_{254} absorbing material, and DOM complexed iron were all shifted toward lower AMW due to chemical fractionation. A 54 percent decrease in iron content, predominantly colloidal in character, was observed in association with chemical fractionation. Evidence of pH induced partial hydrolysis of protein, polysaccharide, and ester DOM constituents was also observed: protein content decreased by 9 percent, $[NH_4^+]$ increased by 40 percent, and carboxylic and weakly acidic (phenolic) DOM functional group content increased by 8 percent and 74 percent, respectively. The fractionation induced shift of DOM physicochemical property size distributions toward lower AMW was attributed to reduced association of DOM with colloidal iron surfaces and formation of low AMW DOM hydrolysis products.

Introduction

Dissolved organic matter (DOM) in aquatic environments plays a number of key roles in determining the solubility and distribution of both organic and inorganic constituents which may be either naturally occurring or present as environmental pollutants. The presence of ionizable functional groups and the range in hydrophobicity typically exhibited by aquatic DOM results in a wide variety of complexation, sorption, and hydrophobic type interactions with both dissolved and particulate solution components. Environmentally significant effects of interaction between DOM and other solution components include solublizing metals – such as iron, manganese, aluminum, and trace heavy metal pollutants – due to DOM-metal complexation, influencing the fate and transport of organic pollutants due to electrostatic and sorptive interactions, and stabilizing colloidal mineral phase dispersions through surface sorption of DOM. The presence of DOM in aquatic environments also has significant implications in engineered settings such as drinking water and waste water treatment. Of particular concern is the formation of potentially carcinogenic halogenated disinfection by-products (DBPs) due to the reaction of aqueous chlorine with DOM during drinking water treatment.

In order to facilitate the study of the physicochemical properties and reactivity of aquatic DOM, numerous extraction and fractionation schemes have been developed, as reviewed in the literature (*1*-*3*). However, most methods are less than satisfactory due to incomplete recovery of DOM or impracticality of use for processing the large volumes of water required to obtain even modest amounts of extracted organic material. Perhaps the most appropriate preparative extraction scheme which has been developed is based on selective sorption of DOM constituents onto, and subsequent pH dependent elution from, non-ionic XAD-8, MSC-1 cation, and Duolite A-7 weakly basic anion exchange resins (*4*-*6*). This extraction scheme simultaneously extracts and fractionates DOM into chemically discrete hydrophobic and hydrophilic acid, base, and neutral fractions. Inorganic constituents are also segregated into one of the six chemically discrete fractions produced by this fractionation; therefore, this procedure has been termed the Dissolved Material Matrix Fractionation Protocol (*7*).

Since the ultimate objective of DOM extraction is generally to provide a source of material for physicochemical property characterization or for use in chemical reactivity studies, the extent of DOM alteration produced by extraction should be minimized. Alteration of DOM during extraction and fractionation may result from direct chemical modification of organic moieties due to extremes in pH, increased temperature, or reaction with extraction solvents. The physicochemical properties and associated reactivity of DOM also may be indirectly influenced by pH induced modification of DOM-metal sorption or complexation interactions. Possible sources of extraction induced alteration of DOM properties inherent in use of the DMM Fractionation Protocol include incomplete recovery and redistribution of mineral-phase colloidal material, principally iron and aluminum oxides (*7*); disruption of DOM-mineral phase associations (*8*); and pH dependent hydrolysis of certain DOM constituents.

Decreased association of DOM with colloidal iron oxide surfaces following application of the DMM Fractionation Protocol may be expected based on the effects of pH induced mineral oxide dissolution and/or formation of DOM hydrolysis products. DOM released and iron solublized due to colloidal dissolution at acidic pH would be expected to segregate into different DMM fractions based on potentially differing charge characteristics. Previously sorbed DOM molecules would be isolated in one of the DMM fractions based on their relative hydrophobicity and charge character, but solublized iron (Fe^{3+} ions at pH 2) would be strongly retained only by the MSC-1 cation exchange resin. Furthermore, substantially incomplete elution of iron from MSC-1 resin has been previously noted (*7*). The resulting redistribution and partial loss of colloidal iron in the DMM fractions could significantly reduce the degree of sorptive association with DOM. Hydrolysis of sorbed DOM also could result in decreased association with colloidal iron oxide surfaces.

pH induced hydrolysis of protein results in release of free amino acid residues, with a corresponding increase in carboxylic acid content (*9,10*). In addition, pH induced hydrolysis of proteinaceous material is known to result in the release of NH_4^+ due to the alteration of specific amino acid residues; notably the deamination of asparagine and glutamine to aspartic and glutamic acid, respectively, and degradation of the indole ring system of tryptophan under acidic conditions (*10-12*). Partial degradation of Cys, Ser, Thr, and Arg residues under alkaline conditions may also occur (*11*). Hydrolysis of ester moieties results in equimolar production of carboxylic acids and alcohols, while hydrolysis of polysaccharides produces lower molecular weight oligo and monosaccharide fragments (*9,10*). Overall, the pH dependent hydrolysis of DOM would be expected to result in production of lower molecular weight fragments along with an increase in carboxylic acidity and NH_4^+ content of the sample.

Review of the literature indicates that evidence of DOM alteration either by direct chemical modification or indirect influence on DOM-metal associations is quite limited. Ester hydrolysis at alkaline pH (*13,14*) and increased specific carboxyl acidity (mmol COOH/mmol NPDOC) have been observed associated with partial fractionation of aquatic DOM; however, no comprehensive study of possible alterations in the physicochemical properties or reactivity of DOM extracted with the DMM Fractionation Protocol has been reported. Therefore, the objectives of this study were to 1) evaluate the nature and extent of alterations in the association of DOM with colloidal iron oxides, and 2) examine the degree of DOM hydrolysis produced by the DMM Fractionation Protocol.

Materials and Methods

Sample Handling and Analytical Methods

The natural water analyzed in this study was collected as a surface sample from Lake Drummond near Suffolk, Virginia. Sample collection, initial processing, and storage were conducted using the procedures outlined in a previous study (*7*). A stock working solution containing approximately 10 mg/L non-purgable dissolved organic carbon (NPDOC) was prepared in sufficient volume for preparative-scale DMM fractionation. NPDOC, UV absorbance at 254 nm, and iron content were measured as described elsewhere (*7*). Organically complexed iron was operationally defined as that fraction of total iron which passed a 30 kDa ultrafiltration membrane (*8*). The number average apparent molecular weight (AMW) distributions based on NPDOC in the stock Lake Drummond sample and preparative-scale DMM fractions were determined by ultrafiltration as described elsewhere (*15*). The protein and carbohydrate concentrations of unfractionated Lake Drummond whole water and extracted DMM fractions were determined by the Lowry method with Hartree modifications and the DuBois method, respectively (*16-18*). Bovine serum albumin and glucose were used as protein and carbohydrate standards.

The net specific charge (meq_C/mmol DOM) associated with DOM in unfractionated Lake Drummond whole water and DMM fractions for any given pH was determined by charge balance as given by,

$$\text{Net Specific DOM Charge} = \frac{\left(\sum \text{inorganic anions} - \sum \text{inorganic cations}\right)}{\text{DOM}} \qquad (1)$$

where ion concentrations are expressed in meq_C/L and DOM is expressed as mmol/L. The concentrations of inorganic cations (Na^+, NH_4^+,K^+, Mg^{2+}, Ca^{2+}) and anions (F^-, Cl^-, NO_2^-, Br^-, NO_3^-, PO_4^{3-}, SO_4^{2-}) were determined by ion chromatography. Cations were measured using a Dionex (Sunnyvale, CA) 2010i Ion Chromatography System with conductivity detector, an APM-1 Analytical Pump, and a Dionex CS12 column and CSRSI autosuppressor operated in recycle mode. The mobile phase was 20 mM methane sulfonic acid delivered at 1.0 mL/min and 1500 psig. Due to low NH_4^+ concentration and proximity of the Na^+ and NH_4^+ peaks, NH_4^+

concentration could not be measured by ion chromatography for some DMM fractions. NH_4^+ concentration was also measured using *Standard Method* 4500-NH_3 F. (Phenate Method), which is not subject to Na^+ interference (*19*). Anions were measured using a Dionex Advanced Ion Chromatograph with a CDM-3 conductivity detector, an AGP-1 Advanced Gradient Pump, and an AS4A column and ASRSI autosuppressor operated in recycle mode. The mobile phase consisted of 1.7 mM $NaHCO_3$ and 1.8 mM Na_2CO_3 delivered at 2.0 mL/min and 1400 psig. Silica (as $H_4SiO_4^0$) was measured by atomic adsorption spectroscopy as described elsewhere (*7*).

The specific carboxyl acidity and specific weakly acidic functional group content of DOM in unfractionated Lake Drummond whole water and extracted DMM fractions were operationally defined as the difference in net specific organic charge between pH 3 and pH 8 and twice the difference in net specific organic charge between pH 8 and pH 10, respectively (*20*). The latter designation for weakly acidic functional group content was used to avoid practical difficulties associated with pH measurement and rapid hydrolysis of DOM under extremely alkaline conditions (*21*). The net specific organic charge of concentrated DOM samples (37 mg C/L to 107 mg C/L) was determined as a function of pH by direct potentiometric titration with 0.1 N NaOH. A 50 mL aliquot of each sample was adjusted to pH 3 with 3 N HCl, sparged with nitrogen gas for 15 min, and rapidly titrated to pH 10 with continuous sparging (~10 min).

Preparative-Scale DMM Fractionation Protocol

A preparative-scale version of the DMM Fractionation Protocol described previously (*7*) was used to extract and chemically fractionate DOM from large volumes of water. The preparative-scale procedure utilized three borosilicate glass chromatography columns with resin bed volumes (BV) of 1650 mL each and low pressure (8 psig) application of sample to the columns at 10 BV/hr. A total sample volume of 189 L of Lake Drummond stock solution was fractionated by sequential application of the entire sample volume to each resin column. The XAD-8 column capacity factor at the hydrophobic-hydrophilic break-point ($k'_{0.5r}$) was 88 for the preparative-scale DMM Fractionation Protocol. With the exception of the HPO-N fraction which required soxhlet extraction for recovery, the isolated DMM fractions were immediately recovered by appropriate pH adjustment, using the elution protocol described in an earlier study (*7*). The pH of each concentrated DMM fraction was promptly returned to a near neutral value to minimize pH dependent hydrolysis of susceptible organic moieties.

The HPO-B, HPI-A, and HPI-B DMM fractions were desalted prior to analysis due to their high as recovered ionic strength. Each fraction was reduced in volume by rotary evaporation at 40°C until salt saturation occurred, and the supernatant and salt precipitate saved separately. Supernatant was diluted to its original volume with meq water and reduced in volume again. Precipitated salt crystals were washed with methanol and the rinse saved separately. This process was repeated until ionic strength was decreased to 0.05. Finally, the collected methanol rinse was diluted with meq water, the methanol removed by rotary evaporation, and the residual aqueous phase combined with the desalted DMM fraction.

Evaluation of DOM Physicochemical Property Alteration

pH dependent hydrolysis of DOM constituents was expected to result in a shift of organic matter related physicochemical properties toward lower AMW values. Therefore, the extent of DOM physicochemical alteration due to chemical fractionation was evaluated by comparing size fractionated whole water DOM properties with corresponding properties mathematically reconstituted from size fractionated DMM fraction properties. NPDOC, UV_{254} absorbing material, and organically complexed iron (< 30 kDa) were used as the organic matter properties for these comparisons. The physical and chemical fractionation scheme used to evaluate the alteration of DOM properties is graphically illustrated in Figure 3.1. For each DOM property evaluated, a set of chemical fractionation coefficients $\langle f_j \rangle$ describes the segregation of that property into DMM fractions resulting from chemical fractionation, and a set of physical fractionation coefficients $\langle g_{ji} \rangle$ defines the proportion of the DOM property which passes each specified ultrafiltration membrane during subsequent size fractionation of the DMM fractions.

Since size fractionation by ultrafiltration does not chemically modify DOM, the alteration of DOM properties due to chemical fractionation was assessed by using the measured physical and chemical fractionation coefficients in Figure 3.1 to mathematically reconstitute size fractionated whole water DOM properties from size fractionated DMM properties. This process is represented mathematically as,

$$a^*_i = \sum_{j=1}^{6} f_j \, g_{ji} \qquad (i = 1, \ldots, 5) \qquad (2)$$

where a_i^* is the reconstituted value of a size fractionated whole water DOM property a_i. If no alteration of DOM physicochemical properties occurs due to chemical fractionation, then reconstituted and measured coefficients should be equal, or

$$a_i^* = a_i \qquad (i = 1, \ldots, 5). \qquad (3)$$

Thus, the extent to which the equality in Eq. (3) is not satisfied may be used as a measure of the alteration of DOM physicochemical properties due to chemical fractionation.

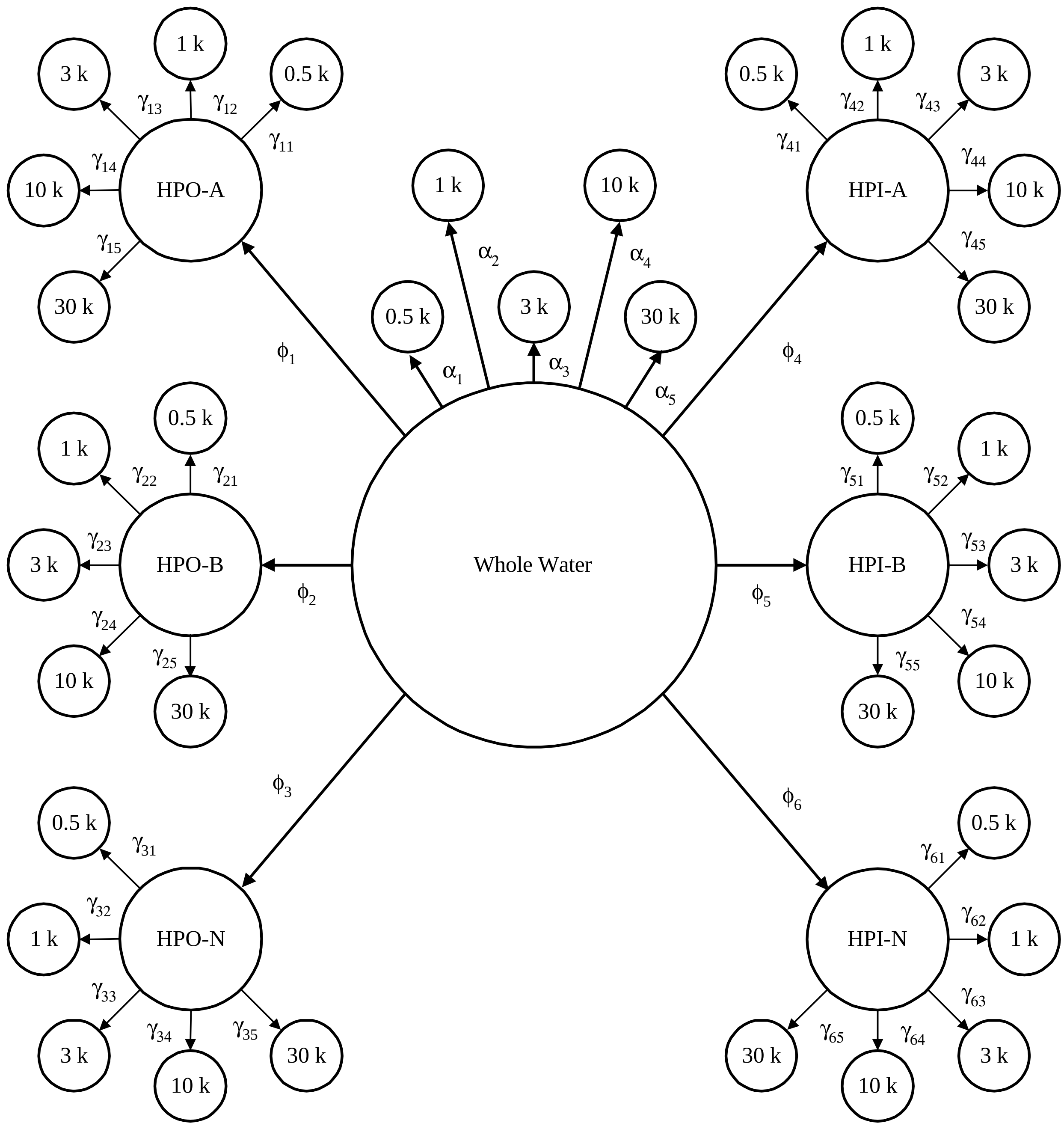

Figure 3.1: Schematic representation of DMM solute physicochemical fractionation scheme. Coefficients represent the proportion of a DOM property which passed the associated physical or chemical fractionation step.

Results

Alteration of Physicochemical Properties

Preparative-scale fractionation of Lake Drummond stock working solution resulted in distribution of NPDOC among the DMM fractions as shown in Table 3.1. Segregation of DOM was evaluated from column sorption data due to DOM loss during desalting. Overall recovery of DOM prior to desalting was 99 percent based on NPDOC. The recovery of NPDOC and iron in desalted HPO-B, HPI-A, and HPI-B DMM fractions was between 80.3 % and 86.5 %, and 3.6 % to 16.0 %, respectively. Compared to pilot-scale fractionation (*7*), preparative-scale fractionation of Lake Drummond water resulted in a shift of DOM from hydrophobic to hydrophilic DMM fractions of like acid-base character due to the higher XAD-8 column capacity factor ($k'_{0.5r}$) of the preparative fractionation scheme.

For the purpose of comparing the distribution of physicochemical properties with AMW of the DMM fractions, working solutions with approximately 10 mg/L NPDOC were prepared from each concentrated DMM fraction. Due to limited availability of DOM in the HPO-B DMM fraction, a lower NPDOC concentration (2.7 mg/L) was used in the working solution prepared from this fraction. The pH of each working solution was adjusted to 6.3 with HCl or NaOH, and the ionic strength adjusted to 0.01 with KCl, as appropriate. Table 3.2 lists the NPDOC, UV_{254} absorbance, and total iron content of the DMM working solutions. Each DMM working solution was size fractionated by ultrafiltration as previously described (*15*), and the distributions of NPDOC, UV_{254} absorbing material, and organically complexed iron with AMW determined. Due to the limited sub-sample volume (10 mL) used to correct for membrane rejection during ultrafiltration (*15*), the distributions of DOM net charge, acidic functional group content, and protein and polysaccharide content with AMW were not determined. Unless explicitly stated to the contrary, error bars in all plots represent ± 1 standard deviation of the given mean data value. For data expressed as a function of AMW, variability was determined as previously described (*15*), while for all other data variability was determined for the mean of 3 replicate measurements.

Table 3.1: Distribution of DOM among DMM fractions following preparative scale fractionation (XAD-8 $k'_{0.5r}$ 88) as measured by NPDOC.

DMM Fraction	Fraction of Whole Water NPDOC
HPO-A	0.587
HPO-B	0.0073
HPO-N	0.0142
HPI-A	0.271
HPI-B	0.0387
HPI-N	0.0812

Table 3.2: Selected properties of Lake Drummond whole water and DMM fraction working solutions used in AMW distribution determination.

DMM Fraction	AMW_N† (Da)	NPDOC (mg/L)	UV_{254} (L/mg·cm)	Fe_T (μg/L)
HPO-A	3910	10.67	0.4211	425
HPO-B	510	2.67	0.0431	121
HPO-N	930	10.33	0.1877	93
HPI-A	710	9.88	0.1174	33
HPI-B	520	10.38	0.2929	54
HPI-N	520	9.96	0.1068	21
Unfractionated	2590	9.83	0.3790	550
Reconstituted	1730	9.83	0.2922	251

†From reference (*15*)

Non-Purgable Dissolved Organic Carbon

The NPDOC based AMW distributions of DMM fractions recovered from Lake Drummond water, unfractionated Lake Drummond whole water, and whole water mathematically reconstituted from DMM fractions (Eq. 2) are shown in Figure 3.2. Lake Drummond DMM fractions contained a relatively small and invariant fraction of large DOM molecules, as greater than 85 percent of NPDOC in each fraction passed an ultrafiltration membrane with a 30 kDa AMW cutoff. However, there was considerable variation among the NPDOC based AMW distributions of the DMM fractions at AMW values less than 30 kDa. For AMW values less than approximately 25 kDa, the HPO-A DMM fraction displayed the lowest proportion of filterable NPDOC, indicating that this chemical fraction contained a disproportionately high fraction of the larger DOM molecules present in the unfractionated whole water. Compared to the HPO-A fraction, the NPDOC based AMW distribution of the HPO-N chemical fraction was shifted slightly toward lower AMW, while the NPDOC based AMW distributions of the four remaining DMM fractions were significantly skewed toward lower AMW. The DMM fractions which contained predominantly smaller molecules had similar NPDOC distributions below 3 kDa, but diverged at higher apparent molecular weights.

Examination of Figure 3.2 illustrates the lack of correspondence between the NPDOC based AMW distributions of Lake Drummond unfractionated and mathematically reconstituted whole waters. The reconstituted AMW distribution was shifted toward lower values over the entire AMW range examined, as evidenced by the higher fraction of reconstituted water NPDOC with AMW less than each respective ultrafiltration membrane cut-off value. The disparity between the unfractionated and reconstituted whole water NPDOC based AMW distributions was not constant, but decreased as AMW decreased from 30 kDa to 10 kDa, continuously increased as AMW decreased to 1 kDa, and then decreased at AMW values less than 1 kDa. The maximum and minimum fractional differences between unfractionated and reconstituted whole water NPDOC based AMW distributions were 0.147 and 0.054, and were observed at AMW values of 1 kDa and 10 kDa, respectively.

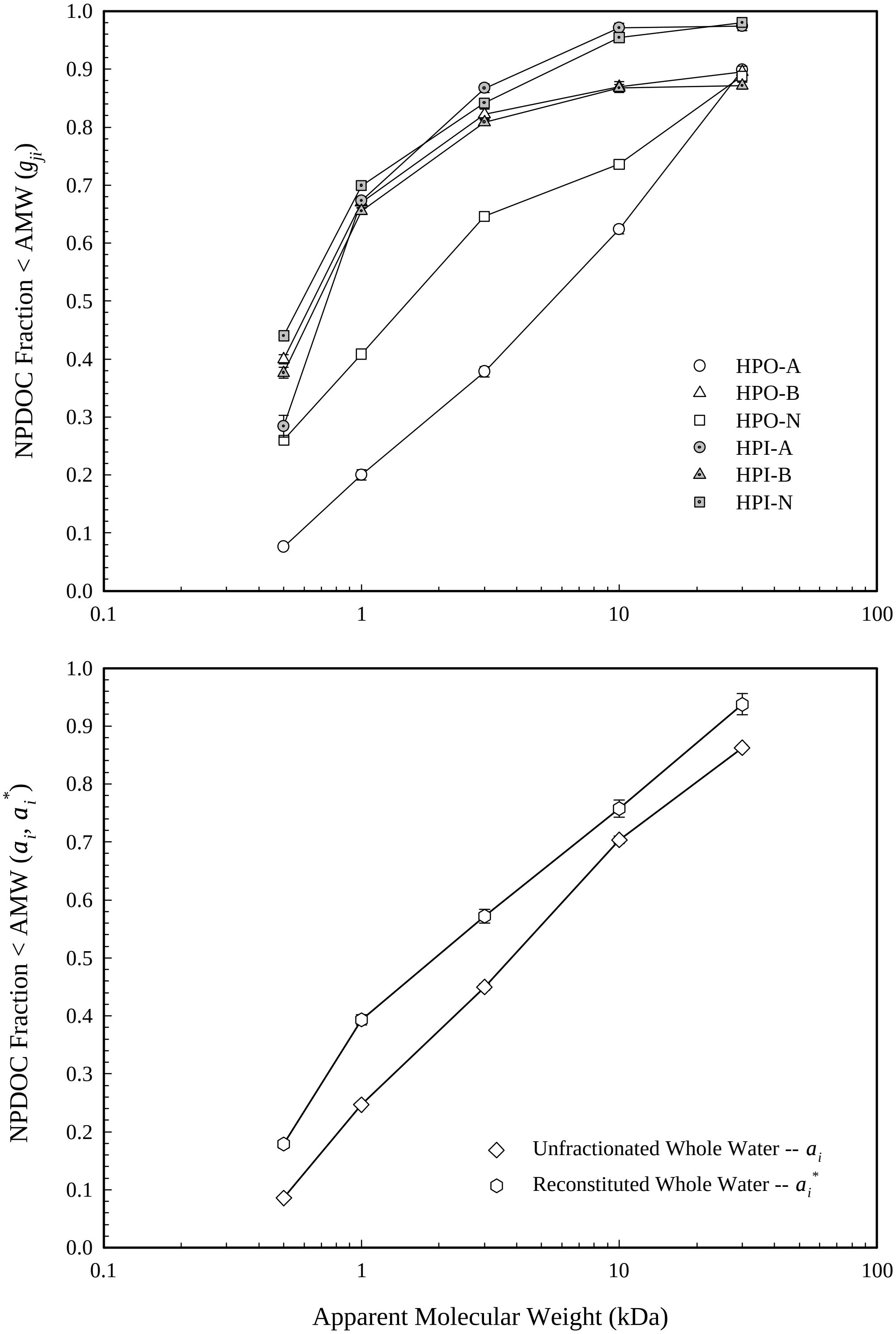

Figure 3.2: Apparent molecular weight distributions based on NPDOC of Lake Drummond DMM fractions, unfractionated whole water, and whole water mathematically reconstituted from DMM fractions.

UV_{254} Absorbing Material

The UV_{254} absorbing material based AMW distributions of DMM fractions recovered from Lake Drummond water, unfractionated Lake Drummond whole water, and whole water mathematically reconstituted from Lake Drummond DMM fractions (Eq. 2) are given in Figure 3.3. As with the NPDOC AMW distributions, considerable variation existed among the UV_{254} absorbing material AMW distributions of the DMM fractions. The UV_{254} based AMW distributions of the DMM fractions displayed trends in relative size similar to those of comparable NPDOC based AMW distributions, with the notable exception of the HPO-B DMM fraction. As seen by comparison of Figure 3.2 and Figure 3.3, the UV_{254} based AMW distribution of the HPO-B DMM fraction was shifted toward higher AMW values.

As with the NPDOC based whole water AMW distributions, comparable UV_{254} absorbing material based unfractionated and mathematically reconstituted whole water AMW distributions were not well correlated, as shown in Figure 3.3. The reconstituted water UV_{254} based AMW distribution was shifted toward lower AMW over the entire size spectrum examined. In contrast with unfractionated and reconstituted NPDOC based whole water AMW distributions, which displayed a maximum fractional difference at 1 kDa AMW, the fractional difference between comparable UV_{254} based AMW distributions continuously increased from 0.042 at an AMW of 0.5 kDa to 0.192 at an AMW of 30 kDa.

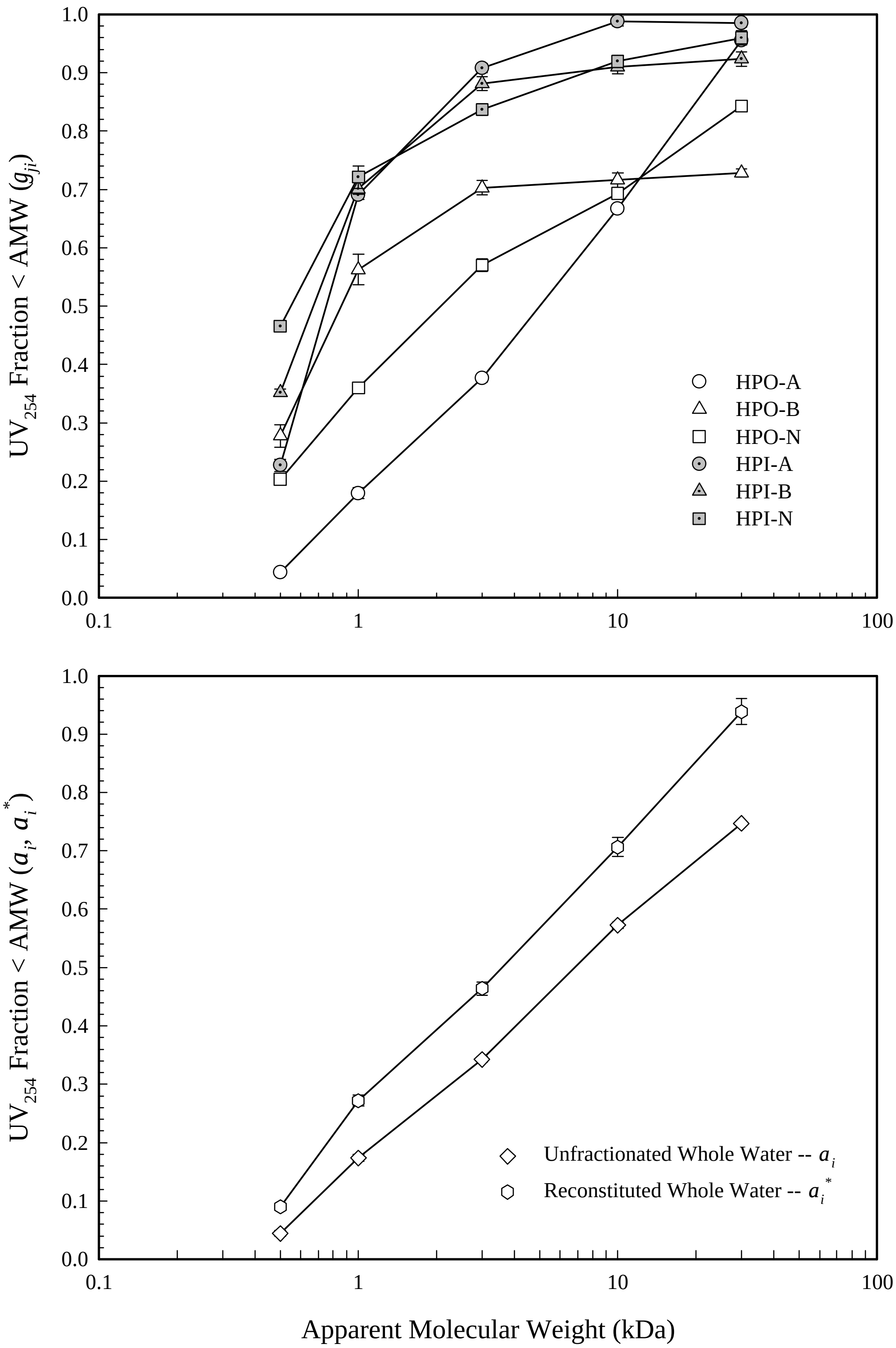

Figure 3.3: Apparent molecular weight distributions based on UV_{254} absorbing material of Lake Drummond DMM fractions, unfractionated whole water, and whole water mathematically reconstituted from DMM fractions.

Iron Content

The distribution of iron with AMW of DMM fractions isolated from Lake Drummond water, unfractionated Lake Drummond whole water, and whole water mathematically reconstituted from DMM fractions (Eq. 2) is given in Figure 3.4. Examination of Figure 3.4 illustrates the wide variation in the distribution of iron as a function of AMW among the Lake Drummond DMM fractions. Two noteworthy trends in the distribution of iron with AMW are apparent in Figure 3.4: the hydrophilic DMM fractions contained a higher proportion of iron which was organically complexed (operationally defined as passing a 30 kDa UF membrane) over the AMW range examined, and within both the hydrophobic and hydrophilic DMM fraction groupings the proportion of iron which was organically complexed varied as neutral > basic > acidic.

The distribution of iron with AMW of unfractionated and mathematically reconstituted Lake Drummond whole waters was not well correlated, as demonstrated in Figure 3.4. The reconstituted whole water iron distribution was shifted toward lower AMW values for the apparent size range examined. As AMW increased from 0.5 kDa to 30 kDa, the fractional difference between unfractionated and reconstituted whole water iron distributions increased from 0.051 to 0.164.

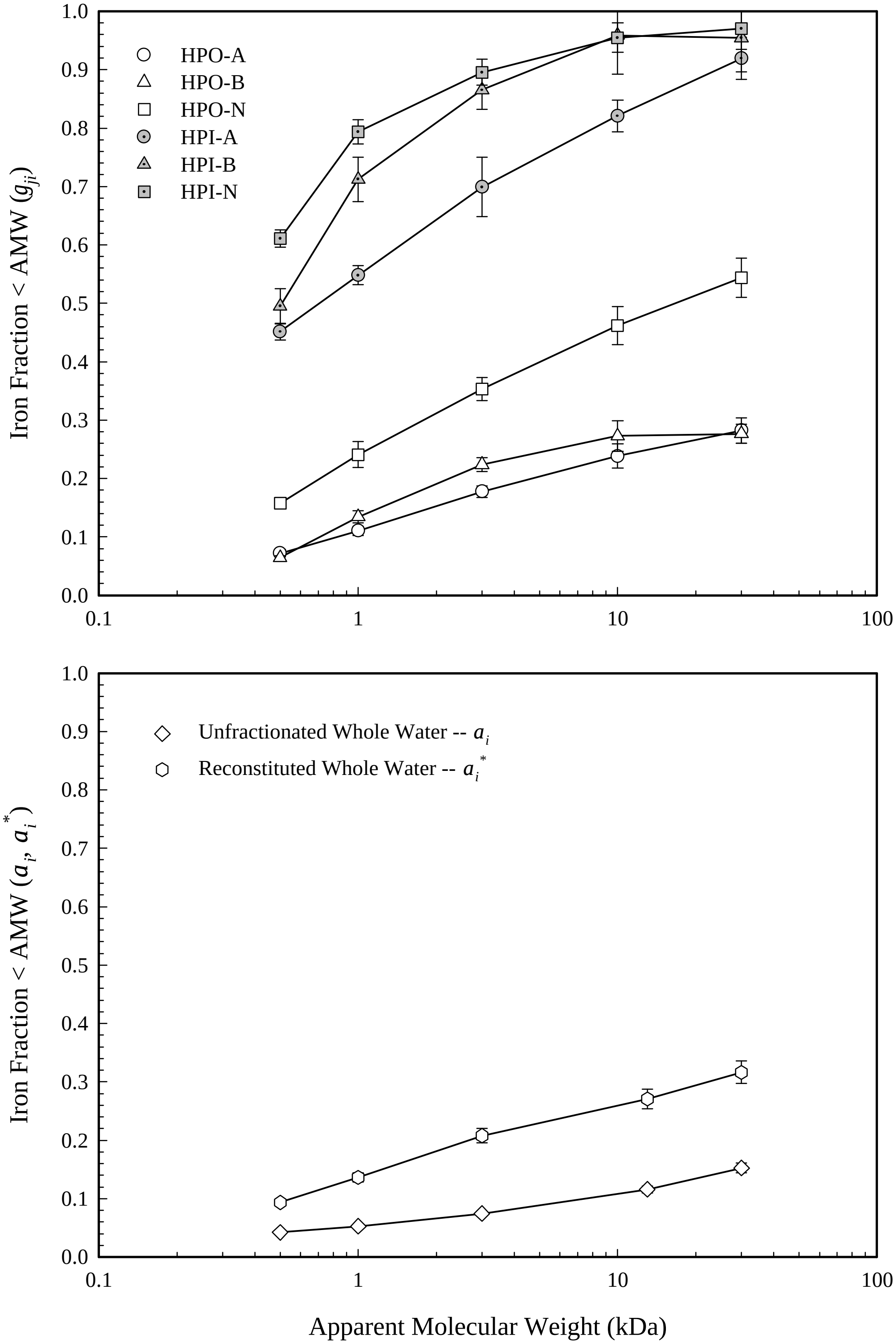

Figure 3.4: Apparent molecular weight distributions based on iron content of Lake Drummond DMM fractions, unfractionated whole water, and whole water mathematically reconstituted from DMM fractions.

Net Specific Charge and Acidic Functional Group Content

The net specific charge associated with DOM (meq_C/mmol DOM) as a function of pH for Lake Drummond DMM fractions, unfractionated Lake Drummond whole water, and whole water mathematically reconstructed from DMM fractions is shown in Figure 3.5. The general trend in net specific organic charge of the DMM fractions was as expected, becoming more negative with increasing pH. In addition, the sign of the net specific charge of each DMM fraction was consistent with its operationally assigned acid-base designation over a wide pH range: the acidic fractions were negatively charged, the basic fractions were positively charged, and the neutral fractions had nearly zero net charge. The HPO-A fraction had a substantially more negative specific charge than the HPI-A fraction at all pH values, while the HPI-B and HPI-N fractions had similar net specific charges as their hydrophobic counterparts for pH values less than approximately 8, but were more negatively charged at higher pH. The net organic charges of the Lake Drummond unfractionated and reconstituted whole waters were nearly identical for acidic pH values below approximately 4, but the reconstituted whole water had a slightly more negative net specific charge at higher pH values.

The specific carboxylic and weakly acidic functional group content of Lake Drummond DMM fractions, unfractionated Lake Drummond whole water, and whole water mathematically reconstructed from DMM fractions were calculated from the net specific DOM charge data presented in Figure 3.5, and are listed in Table 3.3. The influence of silica on weakly acidic functional group content was considered by incorporating [H3SiO4-] in the charge balance given by Eq. 1. Iron, manganese, and aluminum were not included in charge balance calculations since their contribution was minimal due to relatively low concentrations in Lake Drummond derived waters. Error in the charge balance due to pH measurement uncertainty was minimal: for the pH titration range used in this study (3-10) a measurement error of 0.01 pH units would induce at most a 2.6 percent error in the associated charge balance.

Considerable variation existed among both the specific carboxylic and weakly acidic functional group contents of Lake Drummond DMM fractions. Acidic DMM fractions displayed the highest specific carboxyl contents, with values of approximately 28 (meq/mmol DOM) and 5 (meq/mmol DOM), respectively. Specific carboxyl content of the basic and neutral DMM fractions was somewhat lower, ranging between approximately 3 (meq/mmol DOM) and 4 (meq/mmol DOM). Less variation was observed among the weakly acidic functional group contents of the DMM fractions, which were between approximately 3 (meq/mmol DOM) and 7 (meq/mmol DOM). Also, no systematic trend between specific carboxylic and weakly acidic functional group content was apparent.

The specific carboxylic and weakly acidic functional group contents of reconstituted Lake Drummond whole water were higher than the corresponding acidic functional group contents of unfractionated Lake Drummond whole water. The difference between the carboxylic functional group contents of the unfractionated and reconstituted whole waters was 8.2 percent; however, the weakly acidic functional group content of the reconstituted water was approximately 1.8 times that of the unfractionated water. When expressed on a carbon mass basis (μeq/g DOC – data not shown), the magnitude and pH dependence of net specific charge for Lake Drummond DMM fractions and unfractionated water was similar to those previously reported for organic fractions isolated by similar analytical methods from Forge Pond, MA (a eutrophic surface water) (*22*).

Table 3.3: Specific carboxylic and weakly acidic functional group content of Lake Drummond DMM fractions, unfractionated whole water, and whole water mathematically reconstituted from DMM fractions.

DMM Fraction	Carboxylic (meq/mmol DOM)	Weakly Acidic (meq/mmol DOM)
HPO-A	28	4.0
HPO-B	3.6	4.6
HPO-N	4.3	2.5
HPI-A	5.2	2.9
HPI-B	4.1	7.0
HPI-N	2.7	3.6
Unfractionated	16	2.1
Reconstituted	17	3.7

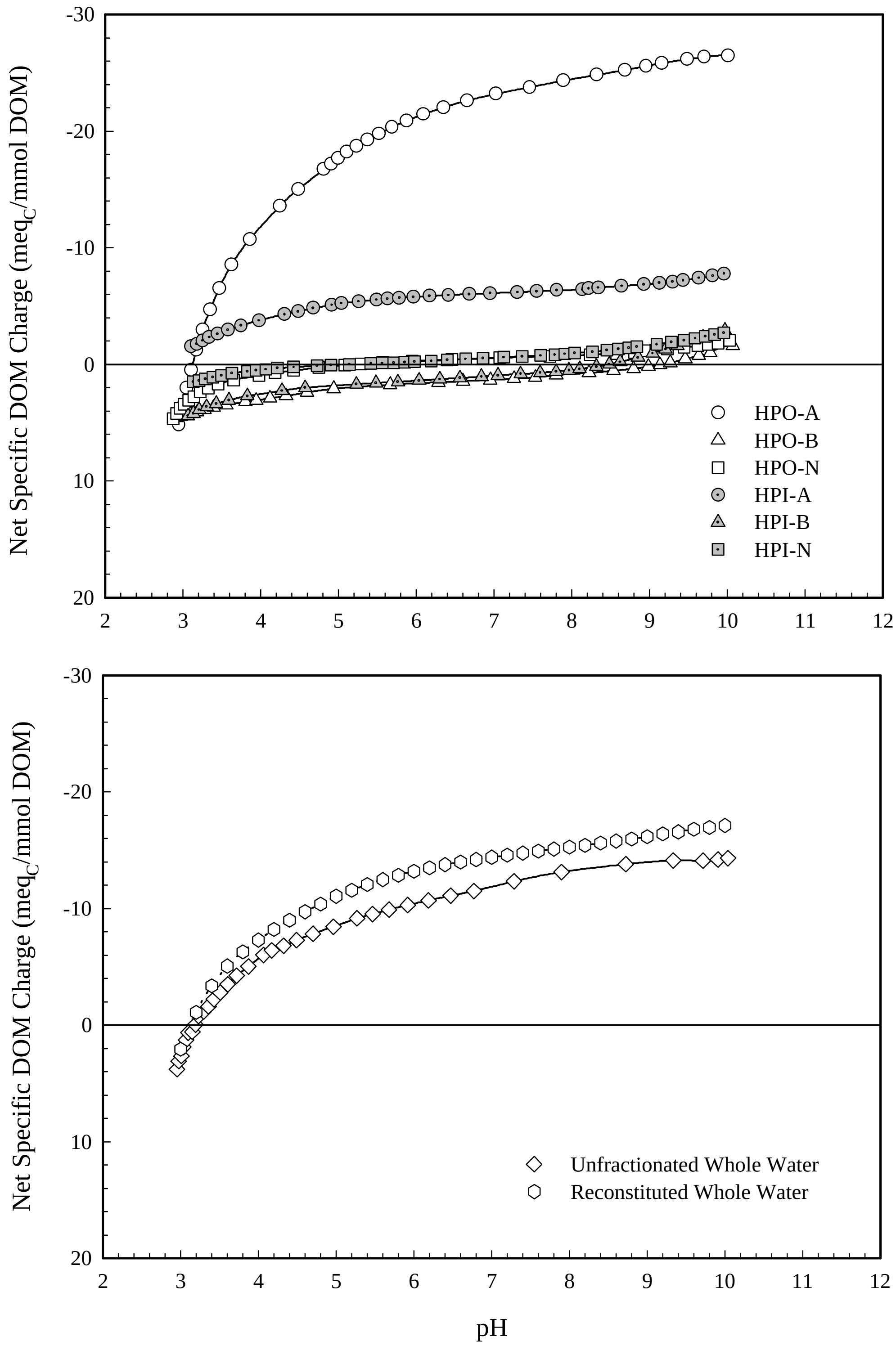

Figure 3.5: Net specific charge associated with DOM in Lake Drummond DMM fractions, unfractionated whole water, and whole water mathematically reconstituted from DMM fractions.

Specific Protein and Carbohydrate Content

The specific protein and carbohydrate contents (w/w) of Lake Drummond DMM fractions, unfractionated Lake Drummond whole water, and whole water mathematically reconstituted from DMM fractions are given in Figure 3.6. Proteinaceous material accounted for a relatively low fraction of the DOM in all Lake Drummond derived samples, with fractional contents of between approximately 0.03 (mg protein C/mg NPDOC) and 0.06 (mg protein C/mg NPDOC). In contrast, substantial variation was observed among the specific carbohydrate contents of Lake Drummond derived samples. Specific carbohydrate content was correlated with acid-base character of the DMM substituent fractions: the basic DMM fractions had the highest fractional carbohydrate content at between approximately 0.18 (mg carbohydrate C/mg NPDOC) and 0.25 (mg carbohydrate C/mg NPDOC), followed by the neutral DMM fractions with a fractional carbohydrate content of approximately 0.12 (mg carbohydrate C/mg NPDOC), and finally the acidic DMM functional groups which had the lowest fractional carbohydrate content of approximately 0.09 (mg carbohydrate C/mg NPDOC).

Limited information on the distribution of proteinaceous and carbohydrate DOM constituents was obtained for unfractionated Lake Drummond whole water. Analysis of DOM size fractionated by ultrafiltration indicated that on a mass basis (w/w) proteinaceous carbon accounted for 4.3 percent of NPDOC with AMW < 30 kDa and 5.6 percent of NPDOC with AMW > 30 kDa. Based on the NPDOC size distribution in Figure 3.2, 81 percent of total proteinaceous NPDOC had AMW < 30 kDa. Carbohydrate analysis on the same size fractionated whole water displayed the opposite trend with NPDOC AMW: carbohydrate contributed 2.3 percent of NPDOC with AMW < 30 kDa and 42 percent with AMW > 30 kDa, or 76 percent of total carbohydrate NPDOC had AMW > 30 kDa.

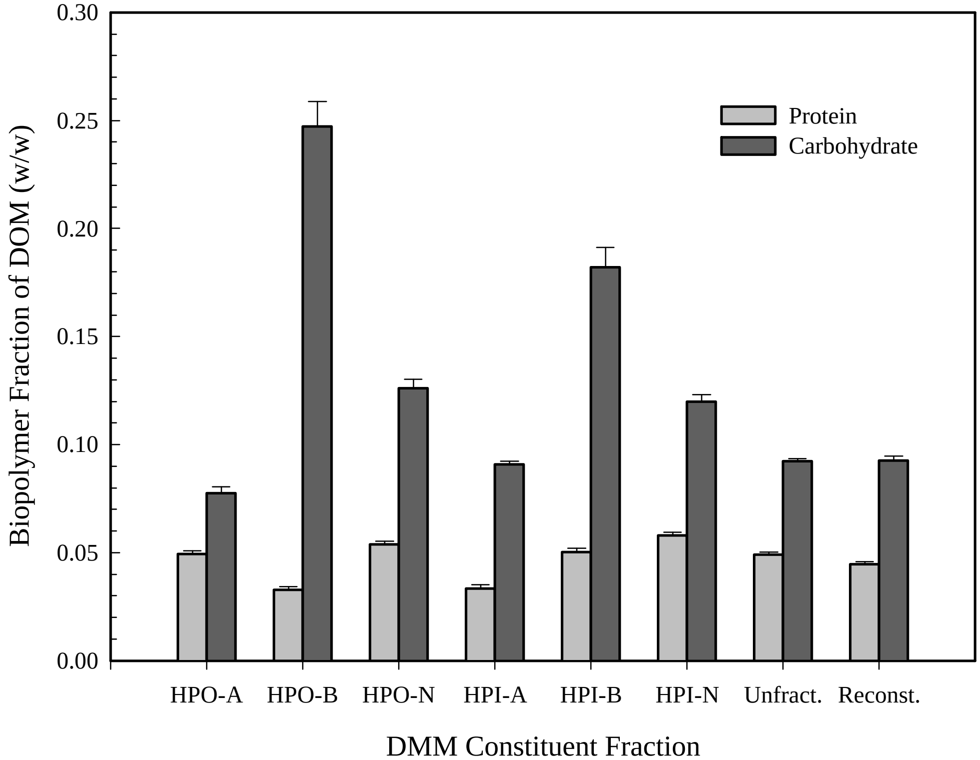

Figure 3.6: Specific protein and carbohydrate content (mg biopolymer C/mg NPDOC) of Lake Drummond DMM fractions, unfractionated whole water, and whole water mathematically reconstituted from DMM fractions.

The protein and carbohydrate contents of Lake Drummond derived samples were consistent with values presented in previous studies of DOM in natural waters. Reported protein and carbohydrate contents of aquatic DOM range from 1 to 15 percent of NPDOC each, with typical values of 4 percent for protein and 10 percent for carbohydrate (*23-28*). Previous studies of DOM physicochemical properties have shown that the size distribution of biopolymers is bimodal: proteinaceous material is usually associated with lower molecular weight DOM fractions (< 10 kDa), while carbohydrates are primarily present as polysaccharides of high molecular weight (> 100 kDa). Several studies have reported between 58 and 76 percent of soluble protein in freshwater lakes was in the apparent molecular weight range less than 10 kDa (*29*,*30*). In contrast, carbohydrates appear to be almost exclusively associated with DOM retained by a 100 kDa AMW ultrafiltration membrane (*27*,*31*,*32*).

Free Ammonia Content

The free ammonia contents (NH_4^+) of Lake Drummond DMM fractions, unfractionated Lake Drummond whole water, and whole water mathematically reconstituted from DMM fractions are listed in Table 3.4. Considerable variation was observed among the NH_4^+ concentrations of the DMM fractions, with the neutral fractions containing approximately 7 times the concentration of the other fractions. The NH_4^+ content of mathematically reconstituted whole water was 40 percent higher than that of unfractionated whole water.

Comparison of the NH_4^+ concentrations listed in Table 3.4 with the DOM fractional protein contents given in Figure 3.6 reveals a general trend of increasing free ammonia with increasing protein for the Lake Drummond DMM fractions. For DMM fractions where direct comparison was possible ammonium ion concentrations measured by ion chromatography and the phenate ion method were relatively consistent: values measured by the phenate ion method were 6 to 9 percent lower than comparable values measure by ion chromatography. Poor correspondence between the NH_4^+ concentrations of reconstituted whole waters was due to incomplete data provided by each measurement technique.

Table 3.4: Free ammonia content [NH_4^+] of Lake Drummond DMM fractions, unfractionated whole water, and whole water mathematically reconstituted from DMM fractions.

DMM Fraction	[NH_4^+] by IC (mmol/L)	[NH_4^+] by PIM (mmol/L)
HPO-A	--*	$1.00 \cdot 10^{-3}$
HPO-B	$9.98 \cdot 10^{-4}$	--**
HPO-N	$7.88 \cdot 10^{-3}$	$7.20 \cdot 10^{-3}$
HPI-A	--*	$3.25 \cdot 10^{-4}$
HPI-B	--*	$1.12 \cdot 10^{-3}$
HPI-N	$7.09 \cdot 10^{-3}$	$6.68 \cdot 10^{-3}$
Unfractionated	--*	$9.54 \cdot 10^{-4}$
Reconstituted	$7.13 \cdot 10^{-4}$	$1.33 \cdot 10^{-3}$

* Na^+ ion interference
** Sample not available

Discussion

Alteration of both physical and chemical DOM properties was observed following application of the DMM Fractionation Protocol. DOM AMW distributions based on NPDOC, UV_{254} absorbing material, and DOM complexed iron were shifted toward smaller AMW. Comparison of the unfractionated and mathematically reconstituted whole water DOM AMW distributions in Figure 3.2, Figure 3.3, and Figure 3.4 illustrates the substantial reduction in DOM size for the AMW range examined. Increases in specific carboxylic and weakly acidic functional group contents and an associated shift of DOM charge to more negative values were observed. An increase in free $[NH_4^+]$ and a decrease in proteinaceous DOM content were also noted. Collectively, these physicochemical alterations may be related to decreased association of low molecular weight DOM with colloidal iron-oxide surfaces or formation of low molecular weight DOM hydrolysis products.

Reduced Association of NOM with Colloidal Iron-Oxides

pH conditions imposed during the DMM Fractionation Protocol are sufficient to produce reduced association between DOM and colloidal surfaces due to dissolution of iron oxides at acidic pH or DOM hydrolysis at basic pH. Each of the DMM fractions is exposed to acidic pH either during application of the aqueous sample to or elution of isolated DOM from the resin columns. The HPO-B and HPO-N DMM fractions isolated during the first sample pass through the XAD-8 resin column are subjected to pH 1-2 (0.1-0.01 N HCl) during elution of the HPO-B fraction. Following initial passage of the aqueous sample through the XAD-8 resin column, the entire sample is acidified to pH 2 for the remainder of the fractionation process (*7*). In the current study subsequent processing of the 189 L sample through XAD-8, MSC-1, and Duolite A-7 resin columns required 3 d. Elution of isolated HPO-A, HPI-A, and HPI-B DMM fractions with NaOH imposes pH values of 12-14 for approximately 30 min (*7*).

Release of surface associated low molecular weight DOM from naturally occurring colloidal iron-oxides present in the Lake Drummond working solution used in this study has been observed previously at both acidic and basic pH (*8*). Colloidal iron oxide surfaces and associated DOM were isolated from Lake Drummond working solution by repeated ultrafiltration against a 30 kDa AMW cut-off membrane at a constant ionic strength of 0.01. The AMW distribution of iron and DOM in isolated colloidal material as a function of pH is given in Table 3.5. When isolated colloidal material was acidified to pH 2 for 1 h dissolution of iron oxide surfaces was substantially complete. In an acidified sample dissolved iron (passing a 30 kDa UF membrane) accounted for 87 percent of total iron, compared with 3 percent in an unacidified aliquot of the same colloidal material. After 1 h at pH 12 the iron content of isolated colloidal material remained predominantly colloidal in character, with 82 percent retained by a 30 kDa UF membrane. Ultrafiltration of pH adjusted aliquots of isolated colloidal material indicated that between 24 and 92 percent of its organic content had AMW < 30 kDa, but was retained by a 30 kDa UF membrane at neutral pH due to association with colloidal iron-oxide surfaces. Anion exchange with phosphate under non-hydrolyzing conditions (0.1 M PO_4^{3-}, pH 7) showed that 47 percent of the organic content of Lake Drummond colloidal material was actually sorbed DOM with AMW < 30 kDa.

Table 3.5: AMW distribution of iron and DOM in colloidal material isolated from unfractionated Lake Drummond whole water by ultrafiltration.

pH	Iron		DOM	
	< 30 kDa	>30 kDa	< 30 kDa	>30 kDa
2	87	13	24	76
7	3	97	11	89
12	18	82	92	8

From reference (*8*)

Indications of pH induced DOM release from colloidal iron-oxide surfaces were also observed in the current study. At 30 kDa AMW the fractional difference between the unfractionated and reconstituted whole water NPDOC based AMW distributions shown in Figure 3.2 was 0.075, or the AMW of DOM amounting to 7.5 percent of the whole water total organic content was shifted to < 30 kDa as the result of fractionation. Since 13.8 percent of unfractionated whole water DOM had AMW > 30 kDa, approximately half of the organic material in this size fraction was affected by the chemical fractionation process. This observation correlates well with the previously cited estimate that 47 percent of DOM associated with colloidal iron-oxide surfaces in unfractionated Lake Drummond water was actually in the < 30 kDa size category.

The shift in UV_{254} absorbing material toward lower AMW following fractionation also supports decreased association of DOM with colloidal iron oxides. Comparison of the un-normalized UV_{254} absorbances of unfractionated and reconstituted whole waters as a function of AMW (not shown) indicated that the 23 percent decrease in whole water UV_{254} absorbance produced by fractionation (Table 3.2) was restricted to organic matter with AMW > 30 kDa: the absolute UV_{254} absorbances of DOM in unfractionated and reconstituted waters differed by less than 2 percent – 0.2830 and 0.2774, respectively. Sorption of DOM on mineral oxide surfaces generally shifts the associated UV absorbance spectrum to longer wavelengths, resulting in increased absorbance at any given wavelength (*33*). The decrease in UV_{254} absorbance of organic material with AMW > 30 kDa induced by fractionation is therefore consistent with decreased association of high AMW DOM with colloidal iron oxide surfaces.

Evidence of colloidal iron-oxide dissolution was also observed based on the shift in DOM complexed iron (iron which passed a 30 kDa UF membrane) toward lower AMW following fractionation. The preparative-scale DMM fractionation conducted in this study resulted in a 54 percent reduction in total iron, as indicated by comparison of the total iron content of unfractionated and mathematically reconstituted whole waters listed in Table 3.2. However, DOM complexed iron was reduced by only 4.8 percent (84 μg/L to 80 μg/L) following fractionation, suggesting that the shift in iron content toward lower AMW seen in Figure 3.4 was primarily due to loss of colloidal iron, and not disruption of DOM-iron complexes. DOM-complexed iron in the unfractionated Lake Drummond working solution has been shown to be unaffected at pH 2 (*8*), which supports the previous statement regarding the impact of colloidal iron loss on the distribution of iron with AMW in the reconstituted whole water.

Formation of Low Molecular Weight DOM Hydrolysis Products

The pH induced release of low molecular weight DOM hydrolysis products has been frequently observed in studies of DOM physicochemical properties. Release of amino acids from DOM under hydrolyzing pH conditions is well documented in the literature (*34-37*), and ammonia nitrogen content of natural water samples containing DOM has been observed to increase with hydrolysis time (*36,38*). In addition, monosaccharides and low molecular weight polysaccharides have been observed in the acid hydrolysis digests of DOM (*20,35,39*). Ester hydrolysis has also been shown to occur for DOM exposed to extremes of pH: low molecular weight ester hydrolysis products have been directly observed by ^{1}H NMR (*39,40*) and by capillary GLC (*13*), and a substantial decrease in the ester stretching band has been noted in the IR spectrum of DOM following exposure to base (*14*). Furthermore, base promoted ester hydrolysis has been shown to occur rapidly at moderately basic pH, being largely complete in a matter of minutes at pH 10 (*14*).

pH conditions imposed by the DMM Fractionation Protocol are mild by comparison to hydrolyzing conditions commonly used in protein and polysaccharide analysis. Complete protein hydrolysis requires extremely acidic or basic pH, elevated temperature, and relatively long hydrolysis times (6 N HCl at ≥100°C for 10-100 h or 4 N NaOH at ≥100°C for 4-8 h) (*11,41*). Chemical hydrolysis of polysaccharides requires extremely acidic conditions (concentrated H_2SO_4 at elevated temperature for 30 min), as glycosidic linkages between carbohydrate monomers are not subject to chemical hydrolysis at mildly acidic, neutral, or basic pH (*11,12,42*). Ester linkages between organic moieties commonly found in DOM are subject to both acid and base catalyzed hydrolysis under pH conditions imposed by the DMM Fractionation Protocol. Base catalyzed hydrolysis of naturally occurring ester linkages is particularly rapid, with reported half-lives ($t_{1/2}$) of minutes to seconds at pH values between 10 and 12 (*43*).

Comparison of reconstituted and unfractionated Lake Drummond whole water proteinaceous DOM contents shown in Figure 3.6 indicates an 8.9 percent decrease (w/w on carbon basis) due to fractionation. This small decrease in proteinaceous DOM content is consistent with partial hydrolysis of amide bonds linking amino acid residues in protein. The modified Lowry method used to determine protein content in this study relies on reduction of Cu^{2+} to Cu^{1+} by amide bonds (Biuret reaction), and subsequent colorimetric quantification of a Cu^{1+}·Folin reagent complex (*16,17,44*). Partial degradation of amino acid side chains at either acidic (Asn, Gln, or Trp) or basic (Cys, Ser, Thr, or Arg) pH would not be expected to decrease measured protein content. Due to low DOM total protein content, small fraction of protein hydrolyzed, and low AMW bias (< 30 kDa), any contribution of amide bond hydrolysis to the fractionation induced decrease in DOM AMW distribution would have been minor.

The increase in $[NH_4^+]$ following fractionation of Lake Drummond water was consistent with partial degradation of specific amino acid residue side chains. Since the hydrolyzing conditions imposed by the DMM extraction procedure (0.01 N HCl or 0.01 N NaOH at room temperature) are mild compared with those used in determination of protein amino acid composition, it is reasonable to assume that release of NH_4^+ due to hydrolysis of proteinaceous DOM constituents was largely restricted to the scissile Asn and Gln side chain amine groups (*12,36,41*). Based on the protein concentration of unfractionated Lake Drummond water, the 40 percent increase in $[NH_4^+]$ following fractionation represented 3.6 percent of the whole water total proteinaceous amine content, or 58 percent of the Asn and Gln residue side chain amino groups (*45*). However, the release of NH_4^+ due to hydrolysis of non-proteinaceous amines has been observed in DOM acid hydrosylates (*34,36,46*).

Direct chemical evidence of pH induced hydrolysis of DOM carbohydrate constituents could not be obtained in this study due to limitations on sub-sample volume imposed by the ultrafiltration protocol used to determine DMM AMW distributions (*47*). However, support for carbohydrate hydrolysis was observed through comparison of the relative changes in NPDOC and UV_{254} absorbing material AMW distributions produced by fractionation. The relative changes in NPDOC and UV_{254} absorbing material with AMW size category are listed in Table 3.6. The disproportionately larger increases in NPDOC observed for the < 0.5 kDa and 0.5-1.0 kDa AMW size categories indicate formation of low molecular weight non-UV_{254} absorbing DOM fragments. These low molecular weight fragments are consistent with DOM hydrolysis products such as oligosaccharides and aliphatic carboxylic acids, which do not absorb UV light due to the absence of conjugated bonds in their structures.

Table 3.6: Relative change in selected DOM properties with AMW size category.

DOM Size Category (kDa)	NPDOC (Percent Change)	UV_{254} Absorbance (Percent Change)
< 0.5	+52.6	+36.2
0.5 – 1.0	+26.4	+7.71
1.0 – 3.0	-11.5	-14.1
3.0 – 10.0	-34.5	-22.9
10.0 – 30.0	+13.2	+2.56
> 30.0	-117	-435

The increased carboxylic and weakly acidic (phenolic) functional group contents of mathematically reconstituted whole water compared with unfractionated whole water is consistent with hydrolysis of ester moieties. Structures proposed for DOM generally consist of a highly aromatic core linked by short aliphatic chains, often with ester linkages to aromatic rings (*48*-*54*). Hydrolysis of these ester linkages would be expected to produce equimolar quantities of carboxylic acid and phenolic functional groups, and increased concentrations of alkylphenols have been observed in the acid hydrosylates of DOM (*55*-*57*). Oligosaccharides of bacterial origin have been observed to be incorporated in NOM structures by ester linkages (*37*).

Literature data relating changes in acidic functional group content following DOM hydrolysis under pH conditions similar to those imposed by the DMM Fractionation Protocol are limited. However, one study found a 6-9 percent increase in DOM equivalent weight (meq COOH/meq DOM) following mild alkaline treatment (pH 13) of soil derived NOM (*13*), which is comparable to the 8.2 percent increase in specific carboxylic functional group content of reconstituted whole water compared to unfractionated whole water observed in this work. Quantitative support for the role of ester and protein hydrolysis in the pH induced fragmentation of DOM was also provided by comparison of observed changes in acidic functional group content. Based on the low concentration of protein and small fraction degraded, the contribution of protein hydrolysis to increased carboxyl content was minor (≈ 1 percent). Furthermore, the increase in weakly acidic (phenolic) content represented 124 percent of the increase in carboxylic acid group content. The greater than equimolar increase in phenolic group content suggests the formation of phenolic functional groups by mechanisms other than ester hydrolysis. Hydrolysis of ether linkages or reduction of quinone groups also may have contributed to phenolic functional group formation.

Conclusions

Significant alteration of DOM physicochemical properties was noted following DMM fractionation of a natural surface water. The observed alterations appeared to be principally related to the pH manipulations required to achieve the desired separation of DOM into discrete chemical fractions based on hydrophobic character and charge. Changes in DOM physicochemical properties reported here are consistent with reduced association of DOM with colloidal mineral oxide surfaces and partial hydrolysis of protein, polysaccharide, and ester moieties.

Indication of decreased association of DOM with colloidal iron oxide surfaces following application of the DMM Fractionation Protocol was seen based on the shift of NPDOC, UV_{254} absorbing material, and DOM complexed iron AMW distributions toward lower AMW. Release of low molecular weight DOM due to dissolution of colloidal iron oxides at acidic pH is thought to be one mechanism related to the reduction of DOM AMW produced by fractionation. Segregation of DOM and solublized colloidal iron among DMM fractions and substantial iron losses caused by incomplete elution from MSC-1 cation exchange resin and DMM fraction desalting operations also may have contributed to the reduced DOM·iron surface association observed in reconstituted Lake Drummond whole water.

pH induced hydrolysis of DOM is also thought to have contributed to the shift of DOM physicochemical property distributions toward lower AMW following fractionation. Observed changes in carboxylic and phenolic acidity indicate that cleavage of ester linkages was the dominant DOM hydrolysis process. The approximately 1.25:1 ratio of phenolic to carboxylic acidity increase produced by fractionation implies that hydrolysis of functional groups other than ester linkages between aliphatic and aromatic (phenolic) components in the core DOM structure occurred. Release of aliphatic and oligosaccharide fragments from DOM molecules due to ester bond hydrolysis also correlates with the observed formation of low molecular weight (< 1 kDa) non-UV_{254} absorbing DOM.

Further work is needed to help differentiate between the influences of pH induced colloidal iron oxide loss and DOM hydrolysis on the formation of low molecular weight DOM fragments and to examine the impact of physicochemical property alteration on the chemical reactivity of DOM. The types of physicochemical property alteration observed in this study can be expected to occur to some degree in most DOM extraction and fractionation procedures, since pH manipulation is generally used in some fashion in common analytical methods. Therefore, caution must be exercised when extrapolating the physicochemical properties or chemical reactivity of DOM in its natural state from studies of extracted material.

Application of the DMM Fractionation Protocol for simultaneous concentration and chemical fractionation of DOM derived from aquatic or terrestrial environmental samples may not be appropriate in situations where the chemical reactivity of isolated DOM is to be evaluated. Increased molar DOM concentration or changes in metal distribution and speciation could influence interpretation of observed experimental results. For example, use of fractionated DOM for evaluation of drinking water treatment processes may result in observed behavior uncharacteristic of the unfractionated source water. Loss of potentially catalytic colloidal iron oxide surfaces and decreased association of DOM with these surfaces could substantially alter coagulation behavior or result in underestimation of halogenated by-product formation following disinfection with aqueous chlorine.

The DMM Fractionation Protocol appears more appropriate for investigating the physicochemical characteristics of environmental samples such as the phase distribution and chemical speciation of naturally occurring and contaminant metals. Separation of colloidal material by ultrafiltration against a 100 kDa AMW cutoff membrane prior to chemical fractionation could be incorporated to define the phase distribution of metals, and the chemical speciation of DOM complexed metals defined by subsequent fractionation of the ultrafilter permeate. Application of this modified DMM fractionation scheme could prove useful for studying the fate and transport of hazardous metals in aquatic and terrestrial environments.

Literature Cited

1. Aiken, G. R. (1985). Isolation and Concentration Techniques for Aquatic Humic Substances. In Humic Substances in Soil, Sediment, and Water: Geochemistry, Isolation, and Characterization. G. R. Aiken, D. M. McKnight, R. L. Wershaw, and P. MacCarthy, editors. John Wiley & Sons, New York. 363-386.

2. Leenheer, J. A. (1985). Fractionation Techniques for Aquatic Humic Substances. In Humic Substances in Soil, Sediment, and Water: Geochemistry, Isolation, and Characterization. G. R. Aiken, D. M. McKnight, R. L. Wershaw, and P. MacCarthy, editors. John Wiley & Sons, New York. 409-420.

3. Thurman, E. M., G. R. Aiken, M. Ewald, W. R. Fischer, U. Förstner, A. H. Hack, R. F. C. Mantoura, J. W. Parsons, R. Pocklington, F. J. Stevenson, R. S. Swift, and B. Szpakowska. (1988). Isolation of Soil and Aquatic Humic Substances: Group Report. In Humic Substances and Their Role in the Environment. F. H. Frimmel and R. F. Christman, editors. Dahlem Workshop Report. John Wiley & Sons, Chichester. 31-43.

4. Leenheer, J. A. and E. W. D. Huffman,Jr. (1976). Classification of Organic Solutes in Water Using Macroreticular Resins. *J. Res. U. S. Geol. Surv.* 4:737-751.

5. Leenheer, J. A. (1981). Comprehensive Approach to Preparative Isolation and Fractionation of Dissolved Organic Carbon from Natural Waters and Wastewaters. *Environ. Sci. Technol.* 15:578-587.

6. Leenheer, J. A. and T. I. Noyes. (1984). A Filtration and Column-Adsorption System for Onsite Concentration and Fractionation of Organic Substances from Large Volumes of Water. In U.S. Geological Survey Water-Supply Paper 2230. United States Government Printing Office, Washington. 1-16.

7. Tadanier, C. J. (1998). Influence of Operational Characterization Methods on DOM Physicochemical Properties and Reactivity with Aqueous Chlorine. Doctoral Dissertation, Chapter 1. Virginia Polytechnic Institute & State University.

8. Tadanier, C. J., D. F. Berry and W. R. Knocke. (1997). Distribution of Iron Between Colloidal and Organically Complexed Forms -- Implications for Drinking Water Treatment. Proceedings of the CSCE-ASCE Joint Environmental Conference. Edmonton, Alberta.

9. Solomons, T. W. G. (1992). Organic Chemistry. John Wiley & Sons, Inc. New York.

10. Bruice, P. Y. (1995). Organic Chemistry. Prentice Hall, Upper Saddle River.

11. Voet, D. and J. G. Voet. (1995). Biochemistry. John Wiley & Sons, Inc. New York.

12. Zubay, G. (1998). Biochemistry. Wm. C. Brown Publishers, Dubuque.

13. Gregor, J. E. and H. J. K. Powell. (1987). Effects of Extraction Procedures on Fulvic Acid Properties. *Sci. Total Environ.* 62:3-12.

14. Antweiler, R. C. (1991). The Hydrolysis of Suwannee River Fulvic Acid. In Organic Substances and Sediments in Soils Vol. 1. R. A. Baker, editor. Lewis Publishers, Chelsea. 163-177.

15. Tadanier, C. J. (1998). Influence of Operational Characterization Methods on DOM Physicochemical Properties and Reactivity with Aqueous Chlorine. Doctoral Dissertation, Chapter 2. Virginia Polytechnic Institute & State University.

16. Lowry, O. H., N. J. Rosebrough, A. L. Farr, and R. J. Randall. (1951). Protein Measurement with the Folin Phenol Reagent. *J. Biol. Chem.* 193:265

17. Hartree, E. F. (1972). Determination of Protein: A Modification of the Lowry Method That Gives Linear Photometric Response. *Anal. Biochem.* 48:422

18. DuBois, M., K. A. Gilles, J. K. Hamilton, P. A. Rebers, and F. Smith. (1956). Colorimetric Method for the Determination of Sugars and Related Substances. *Anal. Chem.* 28:350

19. APHA, AWWA, and WEF. (1995). Ammonia. In Standard Methods for the Examination of Water and Wastewater. A. D. Eaton, L. S. Clesceri, and A. E. Greenberg, editors. American Public Health Association, Washington, D.C. 4-80-4-81.

20. Thurman, E. M. and R. L. Malcolm. (1983). Structural Study of Humic Substances: New Approaches and Methods. In Aquatic and Terrestrial Humic Materials. R. F. Christman and E. T. Gjessing, editors. Ann Arbor Science, Ann Arbor. 1-23.

21. Perdue, E. M. (1985). Acidic Functional Groups of Humic Substances. In Humic Substances in Soil, Sediment, and Water: Geochemistry, Isolation, and Characterization. G. R. Aiken, D. M. McKnight, R. L. Wershaw, and P. MacCarthy, editors. John Wiley & Sons, New York. 493-526.

22. Reckhow, D. A., P. Bose, B. Bezbarua, E. Hesse, and A. MacNeill. (1992). Transformations of Natural Organic Material During Preozonation. Cincinnati, Ohio. United States Environmental Protection Agency. CR-814663-01-0. 1-276.

23. Steinberg, C. and U. Muenster. (1985). Geochemistry and Ecological Role of Humic Substances in Lakewater. In Humic Substances in Soil, Sediment, and Water: Geochemistry, Isolation, and Characterization. G. R. Aiken, D. M. McKnight, R. L. Wershaw, and P. MacCarthy, editors. John Wiley & Sons, New York. 105-145.

24. Thurman, E. M. (1985). Organic Geochemistry of Natural Waters. Martinus Nijhoff/Dr W. Junk Publishers, Dordrect.

25. Malcolm, R. L. (1985). Geochemistry of Stream Fulvic and Humic Substances. In Humic Substances in Soil, Sediment, and Water: Geochemistry, Isolation, and Characterization. G. R. Aiken, D. M. McKnight, R. L. Wershaw, and P. MacCarthy, editors. John Wiley & Sons, New York. 181-209.

26. Fox, L. E. (1983). Geochemistry of Humic Acid During Estuarine Mixing. In Aquatic and Terrestrial Humic Materials. R. F. Christman and E. T. Gjessing, editors. Ann Arbor Science, Ann Arbor. 407-427.

27. Hama, T. and N. Handa. (1980). Molecular Weight Distribution and Characterization of Dissolved Organic Matter from Lake Waters. *Arch. Hydrobiol.* 90:106-120.

28. Ishiwatari, R. (1985). Geochemistry of Humic Substances in Lake Sediments. In Humic Substances in Soil, Sediment, and Water: Geochemistry, Isolation, and Characterization. G. R. Aiken, D. M. McKnight, R. L. Wershaw, and P. MacCarthy, editors. John Wiley & Sons, New York. 147-180.

29. Tuschall, J. R. and P. L. Brezonik. (1980). Characterization of Organic nitrogen in Natural waters: Its molecular Size, Protein Content, and Interactions with Heavy Metals. *Limnol. Oceanog.* 25:495-504.

30. Steinberg, C. (1977). Schwer Abbaubare, Stickstoffhaltige Geloeste Organische Substanzen im Schoehsee und in Algenkulturen. *Arch. Hydrobiol. Suppl.* 53:48-158.

31. Sweet, M. S. and E. M. Perdue. (1982). Concentration and Speciation of Dissolved Sugars in River Water. *Environ. Sci. Technol.* 16:692-698.

32. Stabel, H. H. (1977). Gebundene Kohlenhydrate als Stabile Komponenten im Schoehsee und in Scenedesmus-Kulturen. *Arch. Hydrobiol. Suppl.* 53:159-254.

33. McBride, M. B. (1994). Organic Pollutants in Soils. In Environmental Chemistry of Soils. Oxford University Press, New York. 342-393.

34. Schnitzer, M. (1985). Nature of Nitrogen in Humic Substances. In Humic Substances in Soil, Sediment, and Water: Geochemistry, Isolation, and Characterization. G. R. Aiken, D. M. McKnight, R. L. Wershaw, and P. MacCarthy, editors. John Wiley & Sons, New York. 303-325.

35. Parsons, J. W. (1989). Hydrolytic Degradations of Humic Substances. In Humic Substances II: In Search of Structure. M. H. B. Hayes, P. MacCarthy, R. L. Malcolm, and R. S. Swift, editors. John Wiley & Sons Ltd. Chichester. 99-120.

36. Anderson, H. A., W. Bick, A. Hepburn, and M. Stewart. (1989). Nitrogen in Humic Substances. In Humic Substances II: In Search of Structure. M. H. B. Hayes, P. MacCarthy, R. L. Malcolm, and R. S. Swift, editors. John Wiley & Sons Ltd. Chichester. 223-253.

37. Stevenson, F. J. (1994). Organic Forms of Soil Nitrogen. In Humus Chemistry: Genesis, Composition, Reactions. John Wiley & Sons, Inc, New York. 59-95.

38. Khan, S. U. and F. J. Sowden. (1971). Distribution of Nitrogen in Fulvic Acid Fractions Extracted from the Black Solonetzic and Black Chernozemic Soils of Alberta. *Can. J. Soil Sci.* 52:116-118.

39. Wershaw, R. L. (1985). Application of Nuclear Magnetic Resonance Spectroscopy for Determining Functionality of Humic Substances. In Humic Substances in Soil, Sediment, and Water: Geochemistry, Isolation, and Characterization. G. R. Aiken, D. M. McKnight, R. L. Wershaw, and P. MacCarthy, editors. John Wiley & Sons, New York. 561-584.

40. Wilson, M. A., P. J. Collin, R. L. Malcolm, E. M. Perdue, and P. Cresswell. (1988). Low Molecular Weight Species in Humic and Fulvic Fractions. *Org. Geochem.* 12:7-12.

41. Mathews, C. K. and K. E. Van Holde. (1996). Biochemistry. Benjamin/Cummings Publishing Co. Inc. Menlo Park.

42. Moran, L. A., K. G. Scrimgeour, H. R. Horton, R. S. Ochs, and J. D. Rawn. (1994). Biochemistry. Prentice Hall, Englewood Cliffs.

43. Schwarzenbach, R. P., P. M. Gschwend, and D. M. Imboden. (1993). Chemical Transformation Reactions. In Environmental Organic Chemistry. John Wiley & Sons, Inc, New York. 342-435.

44. Smith, P. K., R. I. Krohn, G. T. Hermanson, A. K. Mallia, F. H. Gartner, M. D. Provenzano, E. K. Fujimoto, N. M. Goeke, B. J. Olson, and D. C. Klenk. (1985). Measurement of Protein using Bicinchoninic Acid. *Anal. Biochem.* 150:76-85.

45. Doolittle, R. F. (1989). Redundancies in Protein Sequences. In Predictions of Protein Structure and the Principles of Protein Conformation. G. D. Fasman, editor. Plenum Press, New York. 599-623.

46. Kickuth, R. and F. Scheffer. (1976). Konstituutive und Nutritive Eigenschaften des Sogenannten Pseudo-Amidstickstoffs aus Huminsauren. *Agrochimica* XX:376-386.

47. Tadanier, C. J. (1998). Influence of Operational Characterization Methods on DOM Physicochemical Properties and Reactivity with Aqueous Chlorine. Doctoral Dissertation, Chapter 2. Virginia Polytechnic Institute & State University.

48. Cheshire, M. V., P. A. Cranwell, C. P. Falshaw, A. J. Floyd, and R. D. Haworth. (1967). Humic Acid -- II. Structure of Humic Acid. *Tetrahedron* 1669-1682.

49. Haworth, R. D. (1971). The Chemical Structure of Humic Acids. *Soil. Sci.* 111:71-79.

50. Christman, R. F., D. L. Norwood, Y. Seo, and F. H. Frimmel. (1989). Oxidative Degradation of Humic Substances from Freshwater Environments. In Humic Substances II: In Search of Structure. M. H. B. Hayes, P. MacCarthy, R. L. Malcolm, and R. S. Swift, editors. John Wiley & Sons Ltd. Chichester. 33-67.

51. Ziechmann, W. (1988). Evolution of Structural Models from Consideration of Physical and Chemical Properties. In Humic Substances and Their Role in the Environment. F. H. Frimmel and R. F. Christman, editors. Dahlem Workshop Report. John Wiley & Sons, Chichester. 113-132.

52. Kleinhempel, D. (1970). Ein Beitrag zur Theorie des Huminstoffzustandes. *Albrecht Thear Archives* 14:3-14.

53. Liao, W., R. F. Christman, J. D. Johnson, D. S. Millington, and J. R. Haas. (1982). Structural Characterization of Aquatic Humic Material. *Environ. Sci. Technol.* 16:403-410.

54. Schulten, H.-R. and M. Schnitzer. (1991). A Chemical Structure for Humic Substances. *Naturwissenschaften* 78:311-312.

55. Martin, J. P. (1976). Effects of Extractants on Analytical Characteristics and Pyrolysis-Gas Chromatography of Podzol Fulvic Acids. *Geoderma* 15:253-265.

56. Haider, K., B. R. Nagar, H. L. C. Meuzelaar, C. Saiz-Jimenez, and J. P. Martin. (1977). Studies on Soil Humic Compounds, Fungal Melanins and Model Polymers by Pyrolysis-Mass Spectrometry. In Soil Organic Matter Studies Vol. II. IAEA-Agrochimica, Vienna. 213-220.

57. Haider, K. and H.-R. Schulten. (1985). Pyrolysis-Field Ionization Mass Spectrometry of Lignins, Soil Humic Compounds, and Whole Soil. *J. Anal. Appl. Pyrol.* 8:317-331.

Chapter 4

Alteration of Dissolved Organic Matter Reactivity with Aqueous Chlorine Produced by Resin Based Fractionation of the Dissolved Material Matrix of Natural Waters

Abstract

Chlorination of aquatic dissolved organic matter (DOM) results in formation of a variety of halogenated organic disinfection by-products, some of which are suspected human carcinogens. DOM is commonly concentrated and chemically fractionated from large volumes of natural water to facilitate the study of DBP formation. This study was conducted to evaluate the alteration of DOM reactivity with aqueous chlorine induced by chemical fractionation. Chemically discrete hydrophobic and hydrophilic acid, base, and neutral DOM fractions isolated in a previous study were chlorinated at a Cl_2/DOC ratio of 3:1 (w/w) and the chlorine demand and formation of trihalomethane species monitored for 7 d. The impact of fractionation on DOM reactivity with chlorine was evaluated by comparing the Cl_2 demand and THM formation of unfractionated whole water with those of the whole water mathematically reconstituted from its substituent DOM fractions. Both specific Cl_2 demand (mmol ΔCl_2/mmol DOM) and specific THM formation (mmol THM/mmol DOM) decreased due to fractionation. Specific THM yield (mmol THM/mmol ΔCl_2) also decreased following fractionation. Incorporation of Br^- in THM species decreased after fractionation, and was linearly related to Br^-/Cl_2 and Br^-/DOM molar ratios. Decreased specific Cl_2 demand and Br^- incorporation were attributed to fractionation induced molar DOM concentration increase. Decreased specific THM formation was not adequately explained by increased molar DOM concentration, and fractionation induced loss of colloidal iron was also implicated.

Introduction

Chlorination has been widely used as an oxidation and disinfection unit operation in drinking water and wastewater treatment practice. Formation of halogenated organic disinfection by-products (DBPs) has been variously reported and has been a source of concern due to potential health related effects of several identified DBPs. Of the chemically identifiable halogenated organic DBPs formed during chlorination of drinking water, trihalomethanes and haloacetic acids are typically formed in highest concentration, with lower concentrations of haloacetonitriles, haloketones, chloropicrin, chloral hydrate, cyanogen chloride, and chlorinated phenols among others (*1*-*3*). However, the majority of chlorine demand results in formation of chemically unidentifiable halogenated organic molecules, collectively termed total organic halogens (TOX) (*2*,*4*).

The reactive components of dissolved organic matter (DOM) and reaction pathways responsible for production of halogenated DBPs are generally not well understood. Numerous treatability studies have been conducted in an effort to evaluate and optimize DBP precursor removal processes such as coagulation and filtration, and to evaluate the use of alternative oxidants. A variety of analytical procedures, utilizing various physical and chemical separation driving forces, have been used to extract and chemically fractionate large quantities of DOM source material from natural waters. Processes which have been used for preparative DOM extraction and fractionation include low temperature vacuum distillation, lyophilization, freeze concentration, coprecipitation with inorganic salts, ultrafiltration, reverse osmosis, solvent extraction, and sorption on various solid surfaces such as alumina, carbon, and a variety of ionic and non-ionic polymeric organic resins. The relative merits of these processes have been presented in several excellent literature reviews (and references therein) (*5*-*7*); however, none has proven completely satisfactory due to incomplete DOM recovery or other practical limitations.

A preparative extraction scheme based on selective sorption of DOM constituents onto, and subsequent pH dependent elution from, non-ionic XAD-8, MSC-1 cation, and Duolite A-7 weakly basic anion exchange resins (*8*-*10*) has been shown capable of virtually complete DOM recovery (*11*). Termed the Dissolved Material Matrix (DMM) Fractionation Protocol (*11*), this scheme simultaneously extracts and fractionates DOM into hydrophobic and hydrophilic acid, base, and neutral fractions. Ionic and colloidal inorganic components are also segregated among the six discrete DMM fractions.

The chemistry of complex mixtures such as natural waters is not adequately described by the sum of its component characteristics due to intermolecular forces among DOM molecules (*12*) and sorptive interactions between DOM molecules and colloidal mineral surfaces. Extraction and fractionation of DOM inevitably leads to some degree of DMM alteration, primarily through disruption of DOM intermolecular forces and sorptive interactions. In a previous study, the DMM Fractionation protocol was shown to result in increased molar DOM concentration, which was attributed to pH induced hydrolysis of DOM ester constituents and loss of colloidal iron oxides due to incomplete resin elution (*13*). The objective of this study was to evaluate the alteration of DOM reactivity with aqueous chlorine resulting from use of the DMM Fractionation Protocol to simultaneously extract and chemically fractionate the dissolved and colloidal components of a natural water.

Materials and Methods

Sample Preparation and Analytical Methods

The natural waters analyzed in this study were derived from a single surface water sample collected from Lake Drummond near Suffolk, Virginia. Aliquots of DMM fractions and unfractionated whole water working solutions (~10 mg/L NPDOC) previously prepared to study fractionation induced DOM property alteration (*13*) were used to evaluate changes in DOM reactivity with aqueous chlorine produced by application of the DMM Fractionation Protocol. Measured DOM chemical reactivity parameters were analyzed on a per mole DOM (specific) basis, since chemical fractionation of Lake Drummond water has been shown to result in an increase in DOM molar concentration due to pH induced DOM hydrolysis reactions and decreased DOM association with colloidal iron oxides (*13*). Molar DOM concentrations were determined from NPDOC mass concentrations by assuming an average fractional DOM carbon content of 0.51 (mg C/mg DOM) (*7,14-16*), and applying the number average apparent molecular weights (AMW_N) previously reported for Lake Drummond whole water and extracted DMM fractions as conversion factors (*17*).

Residual free chlorine was measured by amperometric titration using *Standard Method* 4500-Cl (*18*) for the purpose of determining specific chlorine demand as a function of contact time in chlorinated Lake Drummond whole water and DMM fraction samples. Analytical grade potassium iodide was added to 100 mL of chlorine-demand-free water buffered to pH 7 with phosphate and, depending on residual chlorine concentration, 5 mL to 20 mL of sample added. Iodide reduced to iodine by free chlorine was back-titrated with 0.00564 N phenylarsineoxide. A Fisher Scientific computer-aided titrimeter was used for all free chlorine analyses. Specific chlorine demand (mmol Cl_2/mmol DOM) at any given contact time (*t*) was calculated as,

$$\text{Specific Chlorine Demand}\,(t) \;=\; \frac{\text{Initial chlorine dose} \;-\; \text{chlorine residual}\,(t)}{\text{DOM}}. \qquad (1)$$

Trihalomethane (THM) formation was used to evaluate the chemical reactivity of DOM samples with aqueous chlorine. Samples were chlorinated in accordance with *Standard Method* 5710 B. (*19*) subject to the following exceptions: 1) since preliminary investigation determined that chlorine demand was not accurately predicted by the procedure outlined in the standard method, all samples were chlorinated at a uniform Cl_2:NPOC ratio of 3:1 (mg:mg), 2) a reduced sample volume of 125 mL was used due to limited availability of several DMM fractions, and a minimum residual of 1 mg/L Cl_2 at 7 d was used as the criteria for a valid THM test. Chlorinated samples were stored at 25°C in the dark for 0.25 d to 7 d, after which each sample was divided into three 25 mL aliquots for THM analysis and the remainder used for residual chlorine determination. Residual chlorine in the THM analysis sub-samples was quenched with Na_2SO_3.

Trihalomethane concentrations were measured by purge and trap GC analysis in accordance with EPA Method 501.1 (*20*). The purge and trap GC system consisted of a Tekmar 3000 Purge and Trap Concentrator, a Tremetrics 9001 Gas Chromatograph, a Tracor 1000 Hall Detector, and a Hewlett-Packard 3396 Series II integrator. A 5 mL aliquot of sample was injected into the purge vessel and sparged with helium for 8 min at 30°C and 5 psig back-pressure. Volatile sample analytes were collected from the carrier gas by a Tenax trap (30.5 × 0.32 cm) during the purge cycle. Accumulated volatile analytes were transferred to the GC column (Supelco 2-3068: 2.4 m, 2.0 mm i.d., 60/80 mesh Carbopack B, 1% SP-1000) by passing helium carrier gas through the trap at 180°C for 4 min: the GC temperature program and trap desorption cycle were initiated simultaneously. After analyte desorption, the trap was regenerated at 225°C for 10 min. In order to reduce the analyte separation time, the GC temperature program specified by EPA Method 501.1 was modified: the GC oven temperature was initially maintained at 65°C for 3 min, then raised to 220°C at 15°C/min and held for 2 min Previous experience using these analysis conditions showed no adverse impact on THM separation or method sensitivity (*21*). The Hall detector temperature was continuously maintained at 850°C during THM analysis.

Evaluation of DOM Reactivity with Aqueous Chlorine

The extent to which the DMM Fractionation Protocol altered DOM reactivity with aqueous chlorine was evaluated by comparing whole water chemical reactivity parameters with corresponding chemical reactivity parameters mathematically reconstituted from DMM fraction parameters. Specific chlorine demand (mmol ΔCl_2/mmol DOM) and specific THM species formation (mmol THM/mmol DOM) were used as the chemical reactivity parameters for these comparisons. A mathematical reconstitution procedure similar to one used previously to examine physicochemical property alteration produced by sequential chemical and size fractionation (*13*) was employed to compare unfractionated and reconstituted whole water reactivity parameters.

The chemical fractionation scheme used to evaluate the alteration of DOM reactivity with aqueous chlorine is graphically illustrated in Figure 3.1. For each chemical reactivity parameter Φ evaluated, a set of fractionation coefficients $\langle f_j \rangle$ describes the segregation of that reactivity parameter into DMM fractions resulting from chemical fractionation. Reconstituted whole water chemical reactivity parameters Φ^* were calculated from the associated sets of fractionation coefficients $\langle f_j \rangle$. This process is represented mathematically as,

$$\Phi^* = \sum_{j=1}^{6} f_j \, . \qquad (j = 1, \ldots, 6) \qquad (2)$$

If no alteration of DOM reactivity with aqueous chlorine occurs due to chemical fractionation, then each reconstituted reactivity parameter and its corresponding measured whole water reactivity parameter should be equal, or

$$\Phi^* = \Phi \qquad (3)$$

Thus, the extent to which the equality in Eq. (3) is not satisfied may be used as a measure of the alteration of DOM reactivity with aqueous chlorine resulting from chemical fractionation.

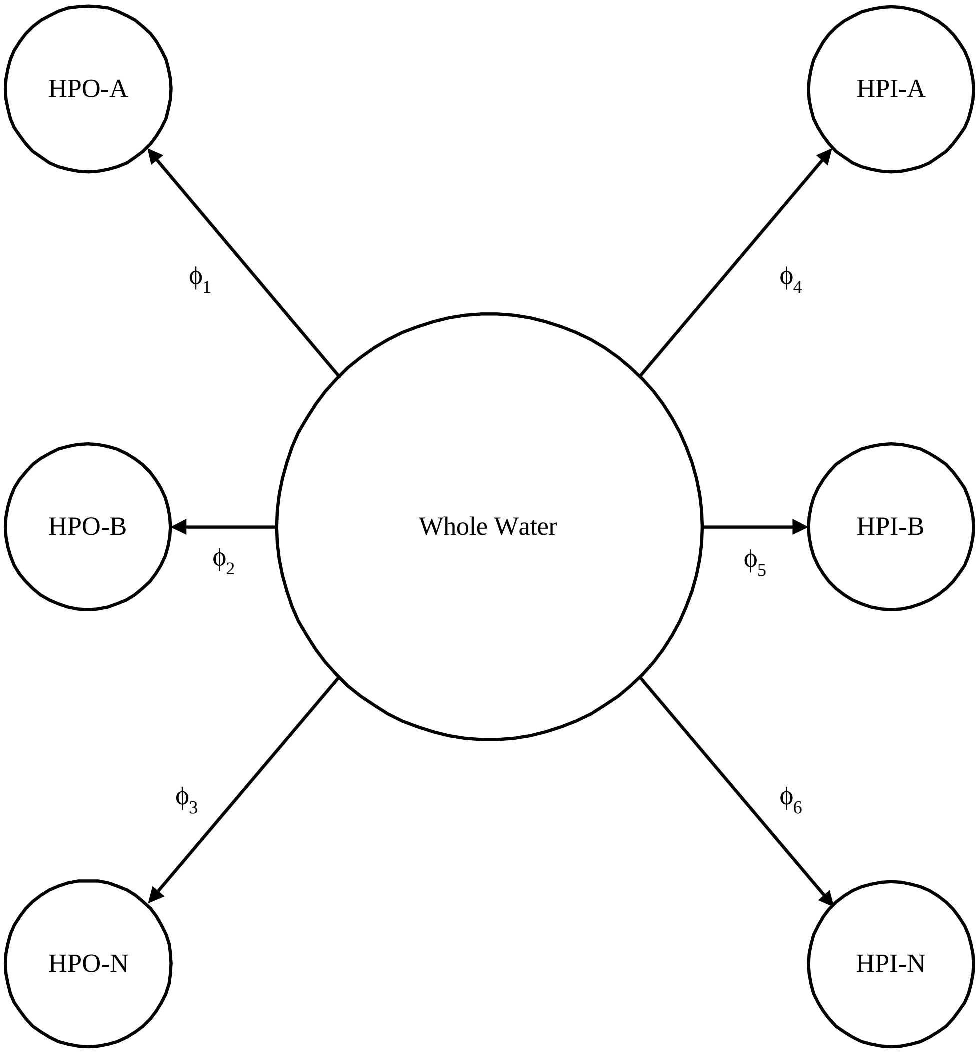

Figure 4.1: Schematic representation of DMM solute chemical fractionation scheme. Coefficients represent the proportion of a DOM property which passed the associated chemical fractionation step.

Results

Specific Chlorine Demand

The specific chlorine demand (mmol Cl_2/mmol DOM) as a function of contact time for DMM fractions recovered from Lake Drummond water, unfractionated Lake Drummond whole water, and whole water mathematically reconstituted from DMM fractions are given in Figure 4.2. The ultimate chlorine demand at a contact time of 7 d varied significantly among the Lake Drummond DMM fractions; with a cluster of low values between 10.3 and 10.7 mmol Cl_2/mmol DOM for the HPO-B, HPI-B, and HPI-N fractions, slightly higher values of 11.7 and 14.8 mmol Cl_2/mmol DOM for the HPI-A and HPO-N fractions, and a maximum value of 67.9 mmol Cl_2/mmol DOM for the HPO-A fraction. Although not easily discernible in Figure 4.2, the ultimate specific chlorine demand of the DMM fractions was related to DOM hydrophobicity, as hydrophobic DMM fractions had higher values than hydrophilic DMM fractions of similar acid base character. However, specific chlorine demand (mmol Cl_2/mmol DOM) was not correlated with absolute chlorine demand (mg Cl_2/L), as residual chlorine after the 7 d contact time was less than 2 mg Cl_2/L for the HPO-B, HPI-B, and HPI-N DMM fractions, but between 4 and 8 mg Cl_2/L for the remaining fractions. The specific chlorine demand curves for unfractionated and reconstituted Lake Drummond whole waters diverged with increasing contact time: the difference between the unfractionated and reconstituted specific chlorine demand curves increased with contact times up to 1 d, after which the reconstituted specific chlorine demand was approximately 8 mmol Cl_2/mmol DOM lower than the unfractionated specific chlorine demand. The kinetics of chlorine consumption, as evaluated by the slope of the specific chlorine demand curves in Figure 4.2, were characteristically high at low contact times and then gradually decreased with increasing contact time. This type of temporal response is typical during chlorination of drinking water, and is related to decreases in both available chlorine and DOM DBP precursor sites with time. The initial specific rate of chlorine demand (mmol Cl_2/mmol DOM·d) for the HPO-A DMM fraction was approximately 5 times higher than the initial specific chlorine demands of the remaining DMM fractions, and remained measurably higher for all contact times. At contact times of greater than 3 d, the rates of chlorine demand for the HPO-B, HPI-B, and HPI-N DMM fractions were lower than for the remaining DMM fractions; probably due to the low residual Cl_2 in these fractions at high contact time. Also, the rate of chlorine consumption observed for unfractionated Lake Drummond whole water was higher than the reconstituted whole water value for contact times less than 1 d, after which these rates were similar.

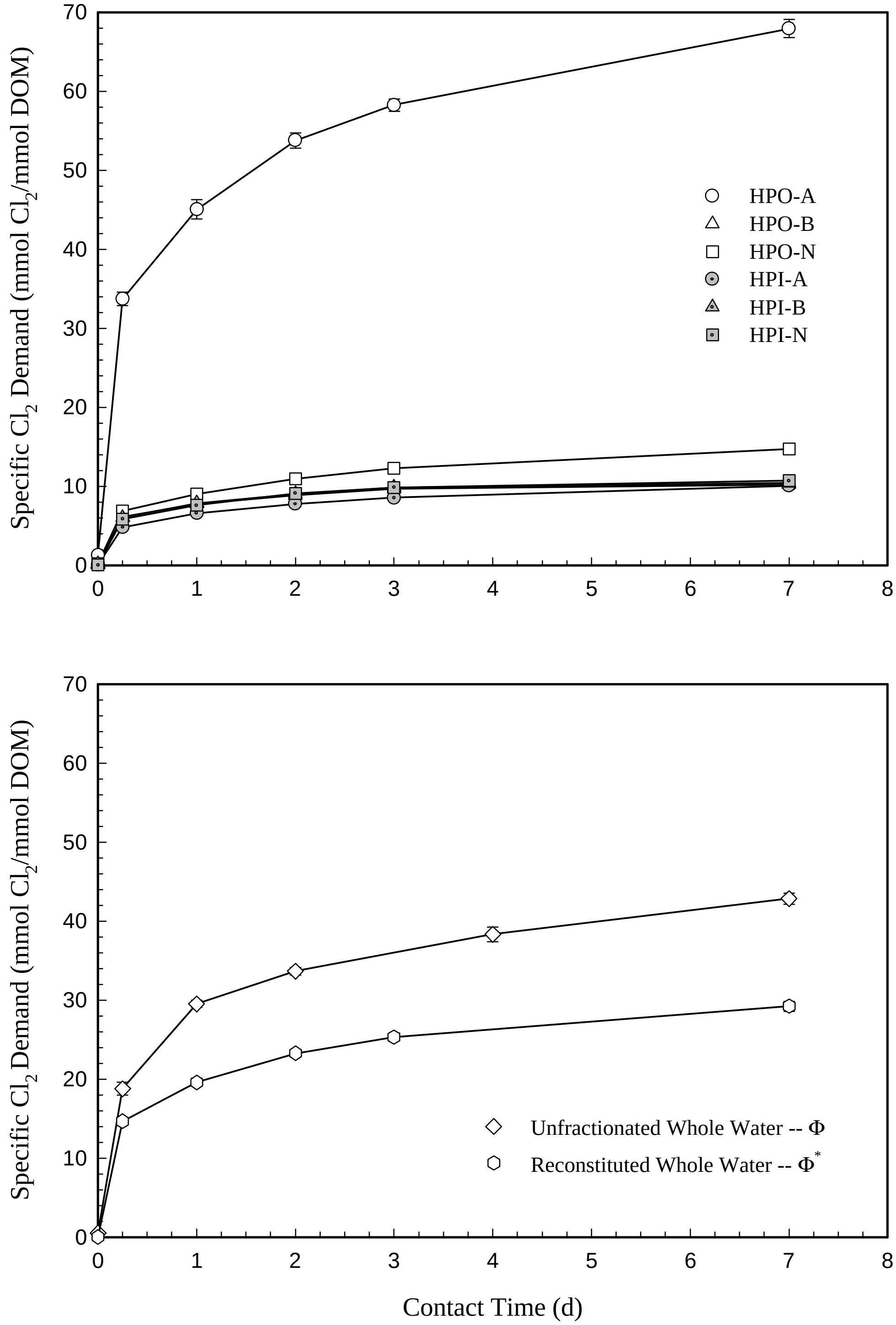

Figure 4.2: Specific chlorine demand of Lake Drummond DMM fractions, unfractionated whole water, and whole water mathematically reconstituted from DMM fractions.

Specific Trihalomethane Formation

The formation of chloroform, bromodichloromethane, and total trihalomethane species as a function of contact time were determined at an applied chlorine to NPDOC ratio of 3:1 (mg Cl_2/mg NPDOC) for Lake Drummond DMM fractions, unfractionated Lake Drummond whole water, and whole water mathematically reconstituted from DMM fractions (Eq. 2) as shown in Figure 4.3 to Figure 4.5. Considerable variation existed among the specific quantities of trihalomethane species formed in the Lake Drummond DMM fractions. The HPO-A fraction exhibited the highest specific $CHCl_3$ formation of the Lake Drummond DMM fractions, 1.6 mmol $CHCl_3$/mmol DOM at a 7 d contact time, while the specific $CHCl_3$ formation of the remaining DMM fractions was less than 0.3 mmol $CHCl_3$/mmol DOM. The relative trend in specific $CHCl_3$ formation of the DMM fractions was similar to that observed for specific chlorine demand. At a contact time of 7 d, the unfractionated whole water specific $CHCl_3$ formation was 1.0 mmol $CHCl_3$/mmol DOM compared with a value of 0.60 mmol $CHCl_3$/mmol DOM for the mathematically reconstituted whole water.

The substantially higher specific $CHCl_3$ formation of the HPO-A fraction was primarily related to its much higher initial $CHCl_3$ formation rate. As evaluated by the slope of the $CHCl_3$ formation curves given in Figure 4.3, the initial $CHCl_3$ formation rate of the HPO-A fraction was 10 to 15 times higher than the initial $CHCl_3$ formation rates of the other DMM fractions. The specific $CHCl_3$ formation rates of the remaining DMM fractions were also lower than that of the HPO-A fraction for contact times greater than 0.25 d. The specific $CHCl_3$ formation rates of the HPO-B, HPI-B and HPI-N fractions were nearly 0 for contact times greater than 3 d. However, caution must be exercised when interpreting the considerably lower $CHCl_3$ specific formation rates of these DMM fractions, since these fractions contained relatively low residual Cl_2 concentrations at contact times greater than 3 d (1.2 to 1.6 mg Cl_2/L). The specific $CHCl_3$ formation rate of the unfractionated Lake Drummond whole water was initially higher than that of the mathematically reconstituted whole water, with the difference increasing for contact times up to 2 d and then remaining relatively constant.

The patterns of specific $CHCl_2Br$ formation exhibited by the Lake Drummond DMM fractions, unfractionated whole water, and mathematically reconstituted whole water were dramatically different than those of $CHCl_3$ formation. As seen by comparison of the specific

THM formation data in Figure 4.3 and Figure 4.4, the specific $CHCl_2Br$ formed in each Lake Drummond DMM fraction was less than 10 percent of the specific $CHCl_3$ formed, and only the HPI-B, HPO-B, and HPI-A DMM fractions exhibited significant $CHCl_2Br$ formation. Specific $CHCl_2Br$ formation in the unfractionated and reconstituted whole waters were also markedly distinct compared to specific $CHCl_3$ formation, as the reconstituted water exhibited 72 percent of the whole water working solution specific $CHCl_2Br$ formation. The kinetics of specific $CHCl_2Br$ formation were faster than for $CHCl_3$ formation, with $CHCl_2Br$ formation largely complete at a contact time of 0.25 d. The low levels of brominated THM species formed in Lake Drummond derived water samples was consistent with the low Br^- concentrations of these waters. Due to the low level of brominated THM species formation, the total specific THM formation for Lake Drummond derived water samples illustrated in Figure 4.5 was quite similar to the specific $CHCl_3$ formation observed in Figure 4.3.

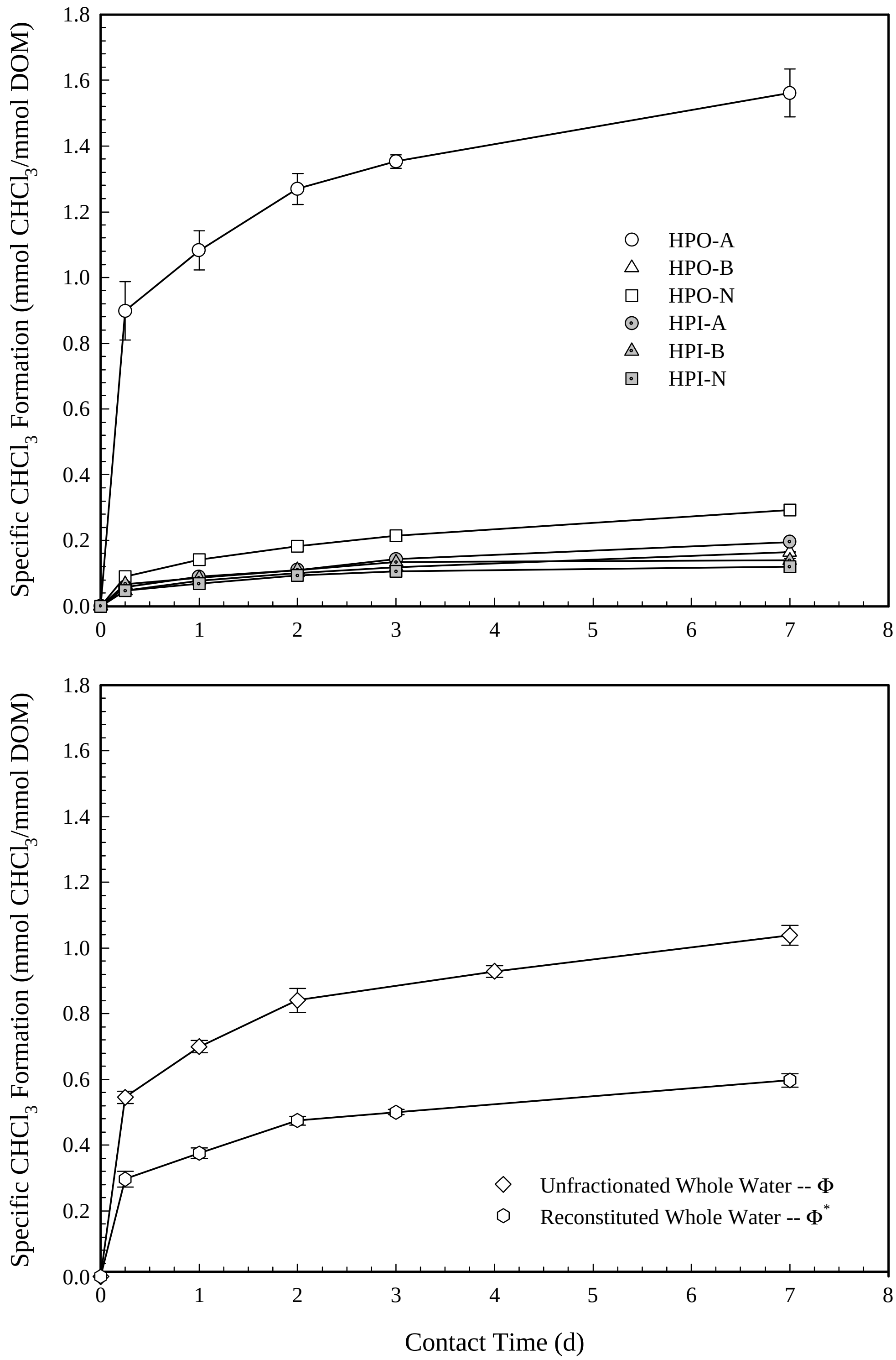

Figure 4.3: Specific chloroform formation of Lake Drummond DMM fractions, unfractionated whole water, and whole water mathematically reconstituted from DMM fractions.

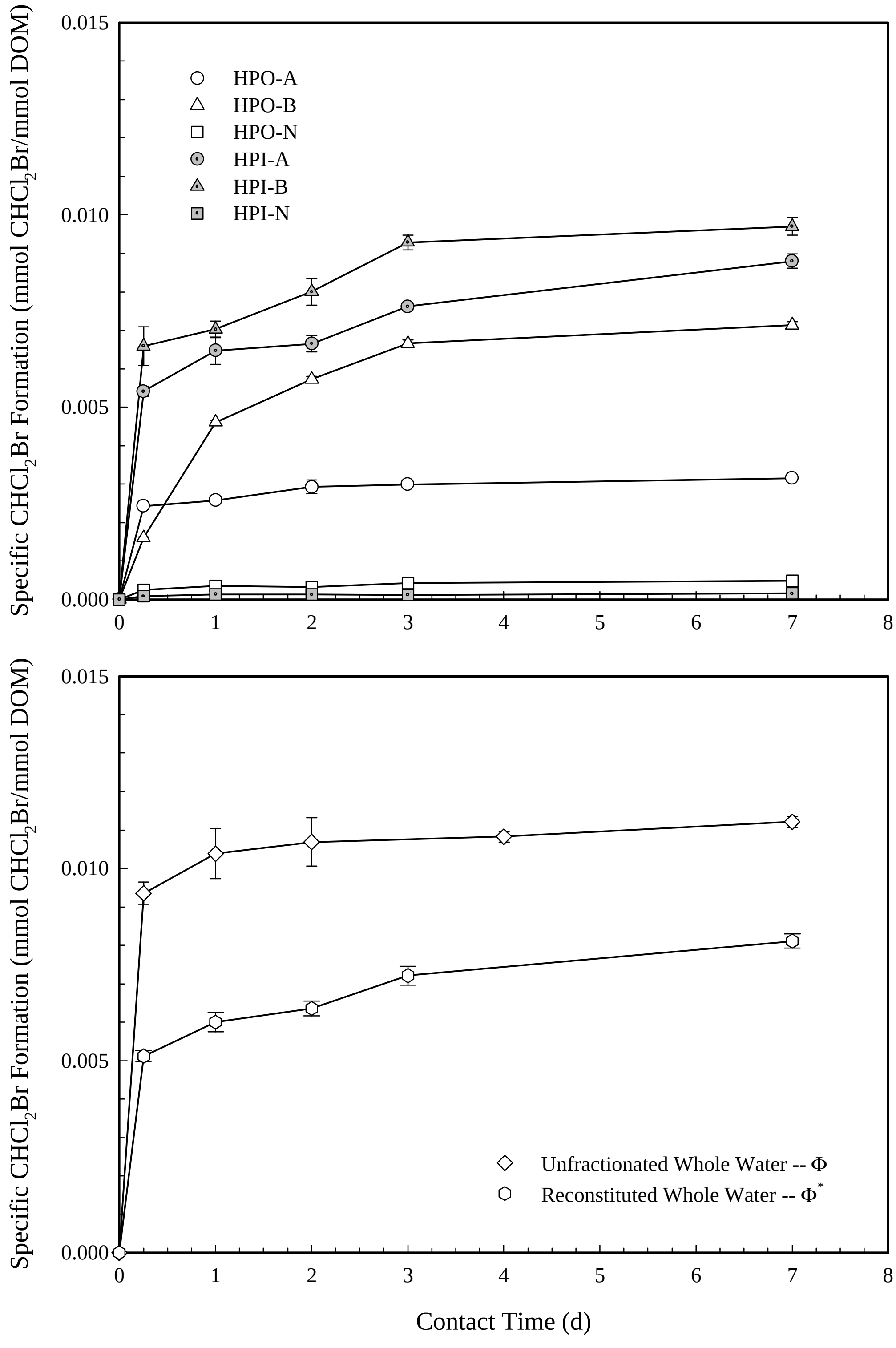

Figure 4.4: Specific bromodichloromethane formation of Lake Drummond DMM fractions, unfractionated whole water, and whole water mathematically reconstituted from DMM fractions.

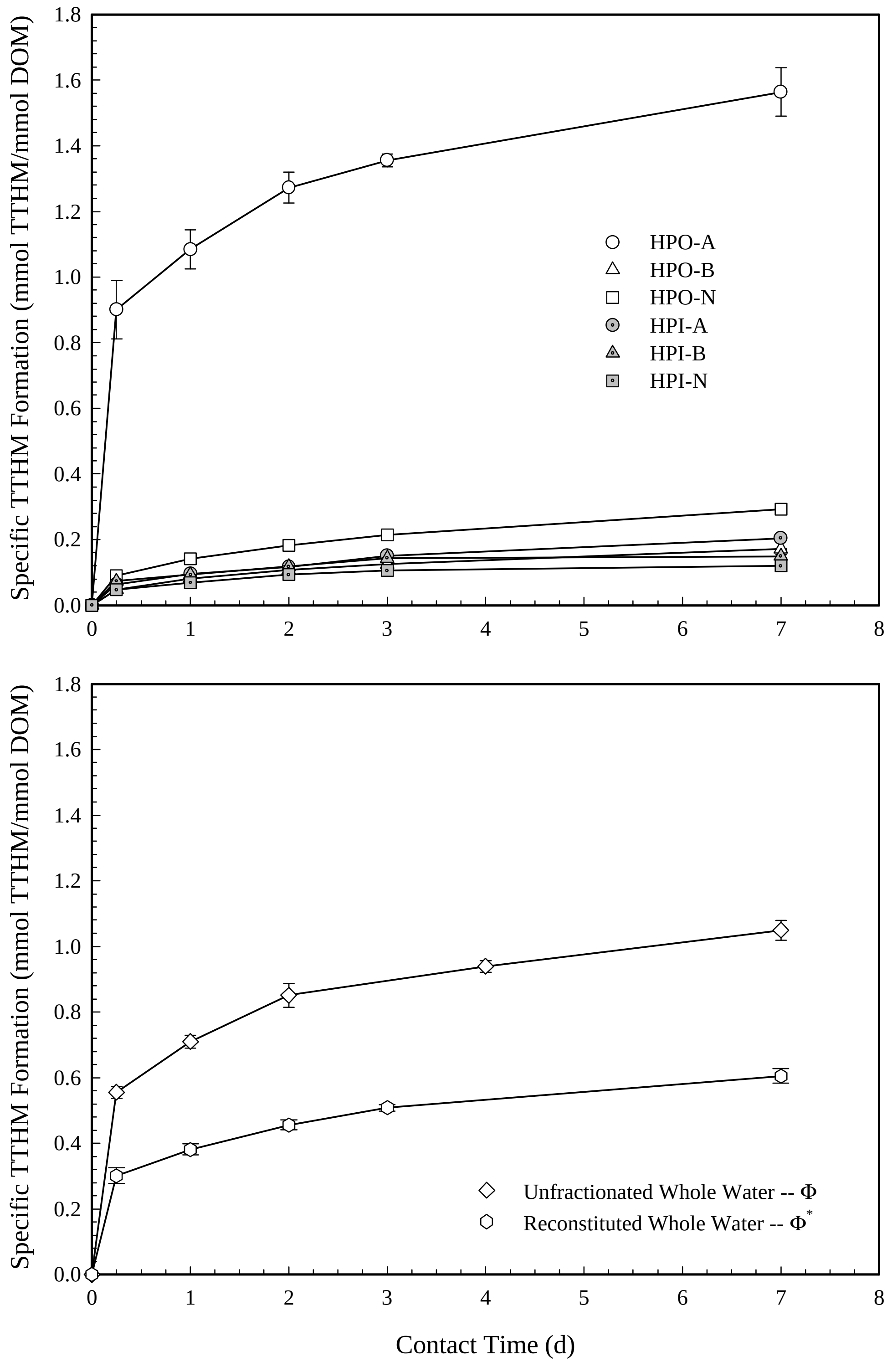

Figure 4.5: Specific total trihalomethane formation of Lake Drummond DMM fractions, unfractionated whole water, and whole water mathematically reconstituted from DMM fractions.

Bromine Incorporation in THM Species

Incorporation of bromine in THM species was strongly correlated with Br^- concentration for Lake Drummond derived water samples. Bromide concentrations of Lake Drummond DMM fractions and unfractionated whole water are listed in Table 4.1. The brominated fraction of THM species (THM·Br/TTHM) appeared linearly related to the initial Br^-/Cl_2 dose ratio for Lake Drummond DMM fractions and unfractionated whole water, as seen in Figure 4.6. The incorporation of bromine in THM species in Lake Drummond derived waters was also observed to be correlated with Br^-/DOM molar ratio, as demonstrated by the general trend of increasing brominated THM species specific yield (THM·Br/DOM) with increasing Br^-/DOM molar ratio shown in Figure 4.7. Brominated THM fractions and specific brominated THM yields of the HPO-N and HPI-N DMM fractions are not shown in Figure 4.6 and Figure 4.7, as the $[Br^-]$ in these fractions was less than the MDL of 0.03 μM (2.4 μg/L). The greater than 100 percent recovery of Br^- may be due to trace contamination of HCl used to acidify the aqueous sample after the first pass through the XAD-8 resin column.

Table 4.1: $[Br^-]^\dagger$ of Lake Drummond DMM fractions, unfractionated whole water, and whole water mathematically reconstituted from DMM fractions.

Fraction	$[Br^-]$ (μM)	THM·Br Incorporated Fraction of Br^-
HPO-A	0.032	0.52
HPO-B	0.34	0.81
HPO-N	ND	ND
HPI-A	0.33	0.72
HPI-B	0.66	0.57
HPI-N	ND	ND
Unfractionated	0.10	0.81
Reconstituted	0.14	0.64

ND – Not determined due to $[Br^-]$ < MDL
†Single replicates

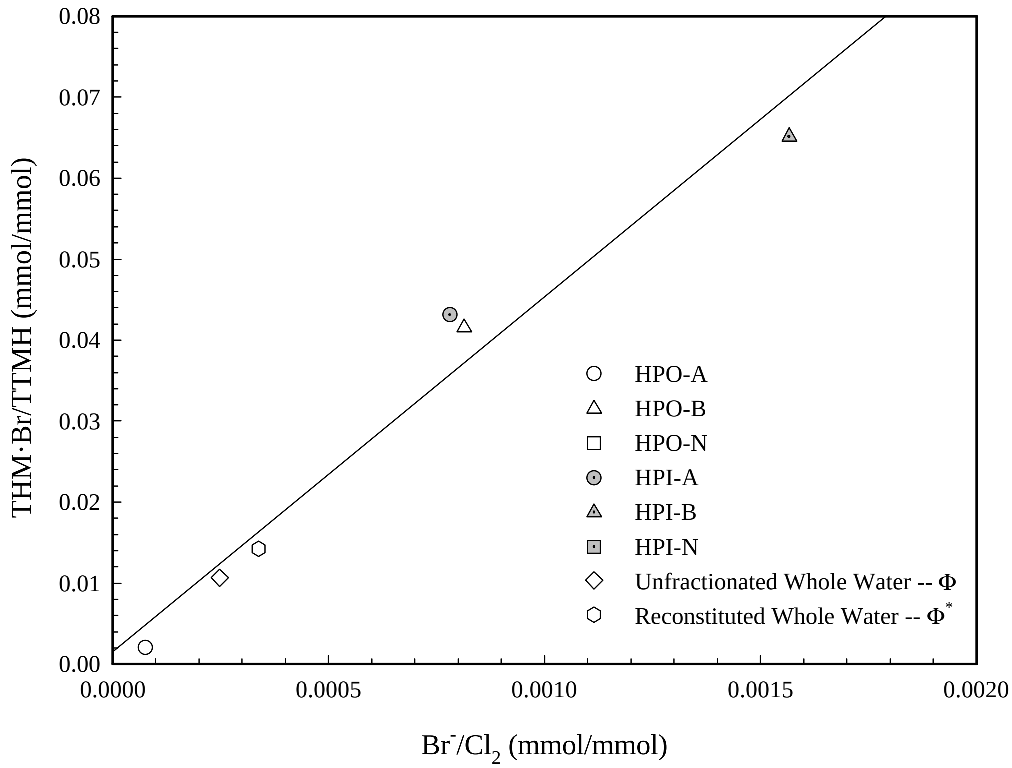

Figure 4.6: Bromine substitution in THM species versus initial Br^-/Cl_2 ratio of Lake Drummond DMM fractions, unfractionated whole water, and whole water mathematically reconstituted from DMM fractions. HPO-N and HPI-N DMM fractions not shown since $[Br^-]$ < MDL. $R^2 = 0.96$.

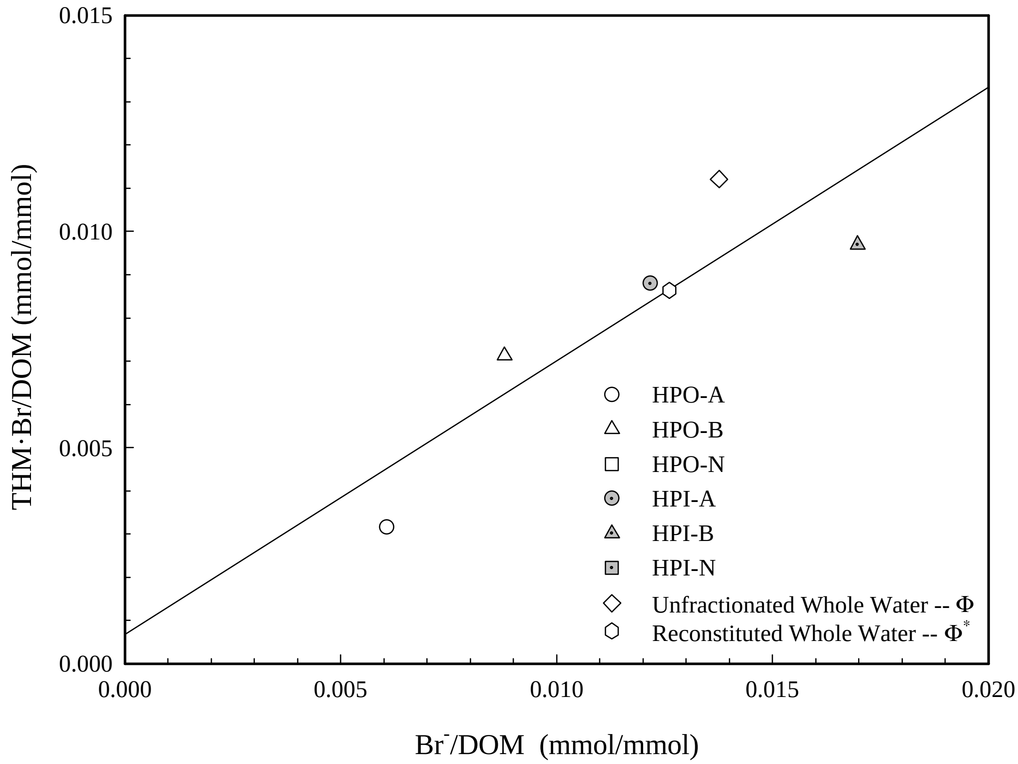

Figure 4.7: Specific bromine substitution versus initial Br^-/DOM ratio of Lake Drummond DMM fractions, unfractionated whole water, and whole water mathematically reconstituted from DMM fractions. HPO-N and HPI-N DMM fractions not determined since [Br^-] < MDL. $R^2 = 0.76$.

Discussion

THM Speciation and Formation Kinetics

The distribution of THM species was dominated by $CHCl_3$, which accounted for 99 percent of TTHM at 7 d contact time. The only brominated THM species detected was $CHCl_2Br$. The low concentrations of THM·Br species measured in this study were likely related to the low [Br^-] (< 1 μM) in all Lake Drummond derived waters. Formation of THM·Br was observed to be dependent on the initial Br^-/Cl_2 and Br^-/DOM molar ratios for all Lake Drummond derived waters, as has been previously reported in the literature (*22,23*). As demonstrated in Figure 4.6 and Figure 4.7, this dependence appeared to be generally linear for waters of differing DOM chemical character (DMM fractions and whole water), suggesting that Br^-/Cl_2 and Br^-/DOM molar ratios may be the controlling factors in THM·Br formation rather than DOM chemistry.

Brominated THM species displayed faster formation kinetics than $CHCl_3$, consistent with previous studies of THM formation rates (*22-24*). Examination of Figure 4.3 and Figure 4.4 indicates that $CHCl_2Br$ formation in Lake Drummond derived waters was largely complete after 1 d, while $CHCl_3$ formation continued throughout the 7 d test period. The faster formation kinetics displayed by THM·Br species has been attributed to the relative effectiveness of HOCl and HOBr as halogenating agents: HOCl acts preferentially as an oxidant, whereas HOBr behaves predominantly as a substituting agent (*25*). During chlorination of natural waters HOBr is rapidly formed due to oxidation of Br^- by HOCl (*26*). In the present study, rapid depletion of the low initial Br^- concentrations in Lake Drummond derived waters also may have contributed to the low specific THM·Br formation rates observed at contact times greater than 1 d.

The preferential segregation of Br^- into certain DMM fractions may influence the observed distribution of brominated DBPs. Based on the resin extraction steps of the DMM Fractionation Protocol, Br^- would be expected to be isolated in the HPI-A fraction eluted from Duolite A-7 anion exchange resin. The HPI-A DMM fraction displayed measurable [Br^-] and $CHCl_2Br$ formation. Unexpectedly, the HPI-B and HPO-B DMM fractions had higher [Br^-] and similar $CHCl_2Br$ formation compared with the HPI-B fraction. Association of Br^- ions with positively charged basic DOM molecules may explain the presence of Br^- in the basic DMM fractions.

Distribution of Chlorine Demand Among DMM Components

The reactivity of Lake Drummond DOM, as evaluated by oxidation with aqueous chlorine, was markedly altered following extraction and chemical fractionation. As illustrated in Figure 4.2 the specific chlorine demand of unfractionated Lake Drummond whole water was substantially higher than that observed for the comparable mathematically reconstituted water. The 27 percent decrease in specific chlorine demand exhibited by the reconstituted water after 7 d contact time may have been due to increased reaction of chlorine with inorganic DMM constituents, diminished production of either THM or non-THM disinfection by-product (DBP) species, increased DOM molar concentration produced by fractionation (*13*), or a combination of these factors.

Aqueous chlorine (as HOCl) may be consumed in oxidation-reduction reactions with inorganic constituents in natural waters. The decrease in specific chlorine demand (mmol ΔCl_2/mmol DOM) observed for the reconstituted whole water may have been related to increased reduction of chlorine by one or more of the reduced inorganic species listed in Table 4.2. The total concentration of these reduced inorganic species present in unfractionated Lake Drummond whole water was previously determined (HPIC and AES) to be 10.8 μM (*13*). When compared to the applied chlorine dose of 840 μM HOCl (30 mg/L Cl_2), reduced inorganic species could account for only about 1 percent of total chlorine demand. Therefore, the substantial decrease in specific chlorine demand attributable to chemical fractionation must be a DOM related phenomenon.

The impact of DMM fractionation on DOM reactivity with aqueous chlorine is more explicitly illustrated by consideration of the specific THM yield (mmol THM/mmol ΔCl_2), or fraction of chlorine demand which is incorporated in THM species. The specific THM yields of $CHCl_3$ and $CHCl_2Br$ in unfractionated and reconstituted Lake Drummond whole waters were calculated by dividing the specific THM data in Figure 4.3 and Figure 4.4 by the specific chlorine demand data in Figure 4.2, respectively. Specific THM yield as a function of chlorination contact time is shown in Figure 4.8. Suprisingly, the specific THM yields of unfractionated and reconstituted whole waters were relatively constant with contact time. Specific THM yield

Table 4.2: Possible oxidation-reduction couples of aqueous chlorine with major inorganic components in natural waters.

Reaction Type	Reaction
Oxidation	$Fe^{2+} \Leftrightarrow Fe^{3+} + e^-$
	$Fe^{2+} + 3H_2O \Leftrightarrow Fe(OH)_{3(am)} + 3H^+ + e^-$
	$Mn^{2+} + 2H_2O \Leftrightarrow MnO_{2(s)} + 4H^+ + 2e^-$
	$Mn^{2+} + 4H_2O \Leftrightarrow MnO_4^- + 8H^+ + 5e^-$
	$NH_4^+ + 2H_2O \Leftrightarrow NO_2^- + 8H^+ + 6e^-$
	$NH_4^+ + 3H_2O \Leftrightarrow NO_3^- + 10H^+ + 8e^-$
	$NO_2^- + H_2O \Leftrightarrow NO_3^- + 2H^+ + 2e^-$
	$H_2S + 4H_2O \Leftrightarrow SO_4^{2-} + 10H^+ + 8e^-$
Reduction	$HOCl + H^+ + 2e^- \Leftrightarrow Cl^- + H_2O$

data indicate that $CHCl_3$ formation accounted for between 1.5 and 2.5 percent of total chlorine demand at 7 d contact time, whereas, $CHCl_2Br$ production contributed less than 0.1 percent of total chlorine demand. The specific THM yields of reconstituted water were substantially lower than those of comparable unfractionated whole water. The relatively minor contribution of inorganic chlorine demand and low specific THM yields of unfractionated and mathematically reconstituted Lake Drummond whole waters indicates that formation of non-THM organic DBPs must have constituted the vast majority of total chlorine demand.

The 27 percent decrease in specific chlorine demand observed in this study may be related to the 33 percent increase in molar DOM concentration produced by application of the DMM Fractionation Protocol to Lake Drummond whole water (*13*). The non-specific chlorine demands (mmol Cl_2/L) of unfractionated and reconstituted whole waters were nearly equal for contact times less than 7 d, as demonstrated in Figure 4.9. Also, the non-zero slope of whole water chlorine demand curves at 7 d contact time shown in Figure 4.2 indicates that the ultimate specific chlorine demand of Lake Drummond whole water was not realized in this study. These observations support the notion that increased molar DOM concentration was largely responsible for decreased specific chlorine demand.

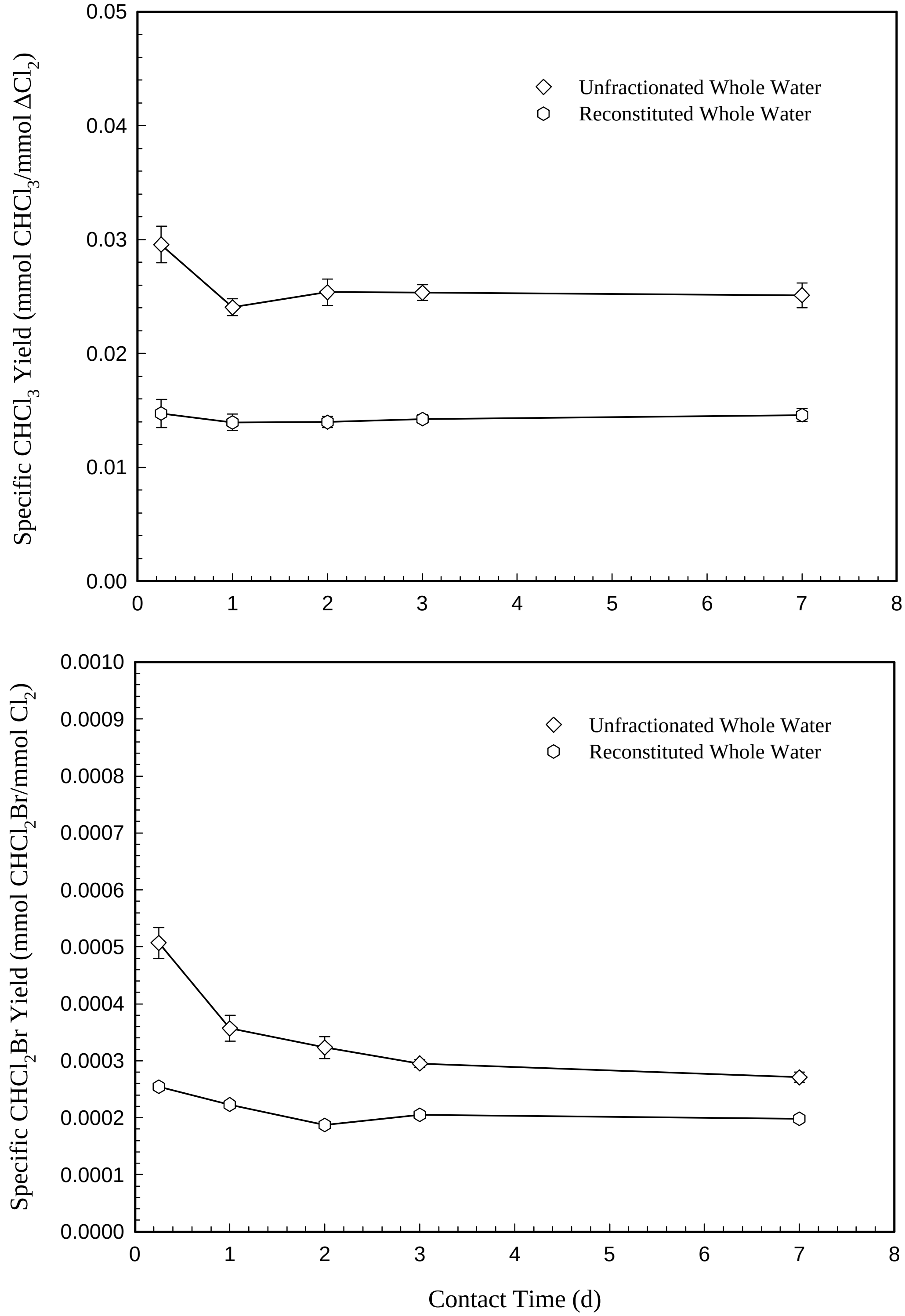

Figure 4.8: Specific THM yields of unfractionated and reconstituted Lake Drummond whole waters.

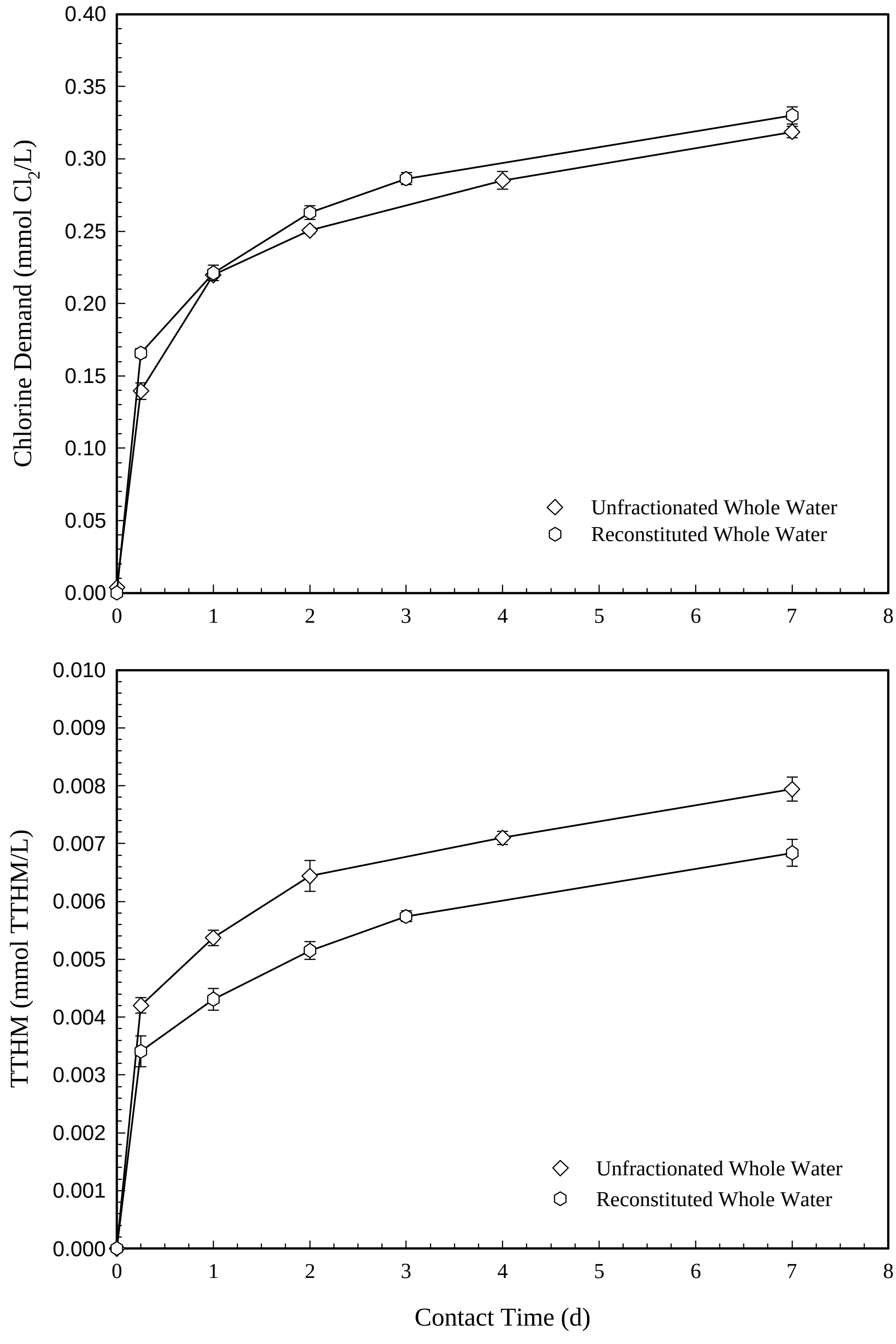

Figure 4.9: Non-specific chlorine demand and trihalomethane formation of Lake Drummond unfractionated whole water and whole water mathematically reconstituted from DMM fractions.

THM Formation

The formation of THM species in chlorinated Lake Drummond whole water was markedly reduced following chemical fractionation. Both specific TTHM formation and specific TTHM yield decreased as shown in Figure 4.5 and Figure 4.8. Possible explanations for the 43 percent decrease in whole-water specific TTHM formation observed include increased inorganic chlorine demand, increased molar DOM concentration, or decreased association of DOM with catalytically active iron oxide surfaces. As previously noted, the maximum possible inorganic chlorine demand was quite small and would not have substantially affected the availability of chlorine for organic DBP formation. Nor does the 33 percent increase in DOM molar concentration produced by fractionation fully explain the observed decrease in specific TTHM formation, as indicated by comparison of Figure 4.5 and Figure 4.9. The influence of iron oxide surfaces on the decrease in specific TTHM formation deserves further consideration, since the other explanations postulated here do not adequately account for the observed results.

Transition metal oxides of iron, manganese, and titanium are known to participate in a variety of oxidation-reduction reactions in both natural and engineered systems due to their ability to participate in charge transfer reactions with sorbed or surface complexed organic and inorganic ligands (*27*). The tendency of transition metal oxides to participate in oxidation-reduction reactions stems from their ability to readily donate or accept electrons from or to their low energy valence shell *3d* orbitals. Iron oxide surfaces are known to catalytically enhance the oxidation of a variety of sorbed organic molecules which are common constituents of DOM (*28*). Examples of environmentally relevant oxidation-reduction reactions involving iron oxide surfaces include reductive dissolution of natural metal oxide and phyllosilicate minerals (*29*), photooxidation of low molecular weight halogenated carboxylic acids (*30*), photochemical degradation of biologically recalcitrant chelating agents such as EDTA (*31*), and the photochemical-oxidation of natural DOM in surface waters (*32,33*). The catalytic activity of mineral oxide coated filter media surfaces has been used during drinking water treatment for removal of nuisance metals by precipitation (*34*).

The decrease in THM species formation observed in this study is consistent with the loss of catalytically active colloidal iron oxide surfaces produced by chemical fractionation of DOM. In a previous study, application of the DMM Fractionation Protocol to a separate aliquot of the

Lake Drummond whole water working solution used in this work resulted in a 54 percent loss in iron, which was primarily associated with colloidal material (*13*). Reaction mechanisms leading to $CHCl_3$ formation generally involve sequential chlorination of aromatic rings, followed by ring opening and hydrolysis. The formation of $CHCl_3$ by this general scheme has been demonstrated in several aromatic model compound chlorination studies (*35-40*) and model compound reaction pathway intermediates have been identified in chlorinated natural waters (*38,41*). It is also well known that the halogenation of aromatic compounds is catalyzed in the presence of iron at ambient temperature and environmental pH (*42,43*).

Although no direct experimental evidence of enhanced halogenated DOM DBP formation in the presence of colloidal transition metal oxide surfaces has been reported in the literature, due to the known catalytic activity of these surfaces for other types of DOM oxidation processes it seems reasonable to assign at least some portion of the reactivity of aquatic DOM with chlorine to their presence. Indirect support for the catalytic role of colloidal iron oxide surfaces in the formation of THM species has been reported by the finding that addition of 10 mg/L of a preformed colloidal hematite surface (α-Fe_2O_3) to Lake Drummond whole water increased TTHM production by approximately 15 percent (*44*).

Conclusions

The distribution of THM DBPs between brominated and non-brominated species formed in chlorinated Lake Drummond derived waters was found to be primarily related to [Br^-]. Formation of brominated THMs ($CHCl_2Br$) was linearly related to the initial Br^-/Cl_2 and Br^-/DOM molar ratios, and relatively independent of DOM chemical character. Segregation of Br^- into certain DOM chemical fractions occurs during application of the DMM Fractionation Protocol, potentially altering the formation of brominated DBPs in chlorinated natural waters.

Alteration of DOM chemical reactivity with aqueous chlorine was observed in this study. Specific chlorine demand and specific TTHM formation both decreased following application of the DMM Fractionation Protocol to Lake Drummond whole water. The 27 percent decrease in 7 d specific chlorine demand was consistent with a 33 percent increase in molar DOM concentration noted in a previous study of fractionation induced DMM physicochemical property alteration. The 43 percent decrease in specific TTHM formation observed was not fully explained by increased molar DOM concentration, or any potential decrease in chlorine availability due to competing inorganic reactions. Based on the substantial fractionation related loss of colloidal iron oxides previously reported and known catalytic activity of iron oxide surfaces in halogenation of aromatic organic compounds, the decreased specific THM formation observed in this work may be related to decreased association of DOM with iron oxide surfaces.

The findings of this study have implications for the use of chlorination as an oxidation or disinfection process in drinking water and wastewater treatment. The formation of halogenated organic DBPs was shifted toward non-THM (non-regulated) species following chemical fractionation of aquatic DOM, ostensibly due to the loss of catalytically active colloidal iron oxide surfaces. A similar change in iron speciation is produced by coagulation, which effectively removes colloidal material during conventional drinking water treatment and in some chemical wastewater treatment systems. Further work is needed to elucidate the role of iron in organic DBP formation in chlorinated waters and to assess the impact drinking water and wastewater treatment practices may have on interactions between iron speciation and subsequent DBP formation potential.

Literature Cited

1. Christman, R. F., D. L. Norwood, D. S. Millington, and J. D. Johnson. (1983). Identity and Yield of Major Halogenated Products of Aquatic Fulvic Acid Chlorination. *Environ. Sci. Technol.* 17:625-628.

2. Krasner, S. W., M. J. McGuire, J. G. Jacangelo, N. L. Patania, K. M. Reagan, and E. M. Aieto. (1989). The Occurrence of Disinfection By-products in US Drinking Water. *Jour. AWWA* 81:41-53.

3. Stevens, A. A., L. A. Moore, and R. J. Miltner. (1989). Formation and Control of Non-Trihalomethane Disinfection By-products. *Jour. AWWA* 81:54-60.

4. Reckhow, D. A. and P. C. Singer. (1985). Mechanisms of Organic Halide Formation During Fulvic Acid Chlorination and Implications with Respect to Preozonation. In Water Chlorination: Chemistry, Environmental Impact and Health Effects. R. L. Jolley, R. J. Bull, W. P. Davis, S. Katz, M. H. J. Roberts, and V. A. Jacods, editors. Lewis Publishers, Inc. Chelsea. 1229-1257.

5. Aiken, G. R. (1985). Isolation and Concentration Techniques for Aquatic Humic Substances. In Humic Substances in Soil, Sediment, and Water: Geochemistry, Isolation, and Characterization. G. R. Aiken, D. M. McKnight, R. L. Wershaw, and P. MacCarthy, editors. John Wiley & Sons, New York. 363-386.

6. Leenheer, J. A. (1985). Fractionation Techniques for Aquatic Humic Substances. In Humic Substances in Soil, Sediment, and Water: Geochemistry, Isolation, and Characterization. G. R. Aiken, D. M. McKnight, R. L. Wershaw, and P. MacCarthy, editors. John Wiley & Sons, New York. 409-420.

7. Thurman, E. M. (1985). Organic Geochemistry of Natural Waters. Martinus Nijhoff/Dr W. Junk Publishers, Dordrect.

8. Leenheer, J. A. and E. W. D. Huffman,Jr. (1976). Classification of Organic Solutes in Water Using Macroreticular Resins. *J. Res. U. S. Geol. Surv.* 4:737-751.

9. Leenheer, J. A. (1981). Comprehensive Approach to Preparative Isolation and Fractionation of Dissolved Organic Carbon from Natural Waters and Wastewaters. *Environ. Sci. Technol.* 15:578-587.

10. Leenheer, J. A. and T. I. Noyes. (1984). A Filtration and Column-Adsorption System for Onsite Concentration and Fractionation of Organic Substances from Large Volumes of Water. In U.S. Geological Survey Water-Supply Paper 2230. United States Government Printing Office, Washington. 1-16.

11. Tadanier, C. J. (1998). Influence of Operational Characterization Methods on DOM Physicochemical Properties and Reactivity with Aqueous Chlorine. Doctoral Dissertation, Chapter 1. Virginia Polytechnic Institute & State University.

12. Leenheer, J. A., P. A. Brown, and T. I. Noyes. (1989). Implications of Mixture Characteristics on Humic-Substance Chemistry. In Aquatic Humic Substances: Influence on Fate and Treatment of Pollutants. I. H. Suffet and P. MacCarthy, editors. Advances in Chemistry. American Chemical Society, Washington, D.C. 25-39.

13. Tadanier, C. J. (1998). Influence of Operational Characterization Methods on DOM Physicochemical Properties and Reactivity with Aqueous Chlorine. Doctoral Dissertation, Chapter 3. Virginia Polytechnic Institute & State University.

14. Thurman, E. M. and R. L. Malcolm. (1983). Structural Study of Humic Substances: New Approaches and Methods. In Aquatic and Terrestrial Humic Materials. R. F. Christman and E. T. Gjessing, editors. Ann Arbor Science, Ann Arbor. 1-23.

15. Steelink, C. (1985). Implications of Elemental Characteristics of Humic Substances. In Humic Substances in Soil, Sediment, and Water: Geochemistry, Isolation, and Characterization. G. R. Aiken, D. M. McKnight, R. L. Wershaw, and P. MacCarthy, editors. John Wiley & Sons, New York. 457-476.

16. Frimmel, F. H. and G. Abbt-Braun. (1991). Comparison of Aquatic Humic Substances of Different Origin. In Humic Substances in the Aquatic and Terrestrial Environment. B. Allard, H. Borén, and A. Grimval, editors. Lecture Notes in Earth Sciences. Springer-Verlag, Berlin. 37-46.

17. Tadanier, C. J. (1998). Influence of Operational Characterization Methods on DOM Physicochemical Properties and Reactivity with Aqueous Chlorine. Doctoral Dissertation, Chapter 2. Virginia Polytechnic Institute & State University.

18. APHA, AWWA, and WEF. (1995). Chlorine (Residual)*. In Standard Methods for the Examination of Water and Wastewater. A. D. Eaton, L. S. Clesceri, and A. E. Greenberg, editors. American Public Health Association, Washington, D.C. 4-36-4-38.

19. APHA, AWWA, and WEF. (1995). Formation of Trihalomethanes and Other Disinfection By-Products. In Standard Methods for the Examination of Water and Wastewater. A. D. Eaton, L. S. Clesceri, and A. E. Greenberg, editors. American Public Health Association, Washington, D.C. 5-50-5-59.

20. U.S. Environmental Protection Agency. (1979). Analysis of Trihalomethanes in Drinking Water. In Federal Register. Washington, D.C. 68672-68682.

21. Via, S. (1995). Impact of Bromide Ion Concentration, Time, Dissolved Organic Carbon and Molecular Weight Cutoff on Haloacetonitrile, Haloketone, Chloropicrin and Trihalomethane Formation Potentials. Masters Thesis. Virginia Polytechnic Institute and State University.

22. Symons, J. M., S. W. Krasner, L. A. Simms, and M. Sclimenti. (1993). Measurement of THM and Precursor Concentrations Revisited: The Effect of Bromide Ion. *Jour. AWWA* 85:51-62.

23. Summers, R. S., M. A. Benz, H. M. Shukairy, and L. Cummings. (1993). Effect of Separation Processes on the Formation of Brominated THMs. *Jour. AWWA* 85:88-95.

24. Minear, R. A. and J. C. Bird. (1980). Trihalomethanes: Impact of Bromide Ion Concentration on Yield, Species Distribution, Rate of Formation, and Influence of Other Variables. In Water Chlorination: Environmental Impact and Health Effects. Ann Arbor Science Publishers, Inc. Ann Arbor. 151-160.

25. Luong, T. V., C. J. Peter, and R. Perry. (1982). Influence of Bromide and Ammonia Upon Formation of Trihalomethanes Under Water Treatment Conditions. *Environ. Sci. Technol.* 16:473

26. Rook, J. J. and et al. (1978). Bromide Oxidation and Organic Substitution in Water Treatment. *Jour. Envir. Sci. Health* A13:91

27. Stumm, W. and J. J. Morgan. (1996). Photochemical Processes. In Aquatic Chemistry. Environmental Science and Technology. John Wiley & Sons, Inc. New York. 726-759.

28. McBride, M. B. (1994). Organic Pollutants in Soils. In Environmental Chemistry of Soils. Oxford University Press, New York. 342-393.

29. Stone, A. T. and J. J. Morgan. (1987). Reductive Dissolution of Metal Oxides. In Aquatic Surface Chemistry. W. Stumm, editor. Environmental Science and Technology. John Wiley & Sons, Inc. New York. 221-254.

30. Pehkonen, S. O., R. L. Siefert, and M. R. Hoffmann. (1995). Photoreduction of Iron Oxyhydroxides and the Photooxidation of Halogenated Acetic Acids. *Environ Sci. Technol.* 29:1215-1222.

31. Kari, F. G., S. Hilger, and S. Canonica. (1995). Determination of the Reaction Quantum Yield for the Photochemical Degradation of Fe(III)--EDTA: Implications for the Environmental Fate of EDTA in Surface Waters. *Environ. Sci. Technol.* 29:1008-1017.

32. Voelker, B. M. and B. Sulzberger. (1996). Effects of Fulvic Acid on Fe(II) Oxidation by Hydrogen Peroxide. *Environ Sci. Technol.* 30:1106-1114.

33. Voelker, B. M., F. M. M. Morel, and B. Sulzberger. (1997). Iron Redox Cycling in Surface Waters: Effects of Humic Substances and Light. *Environ. Sci. Technol.* 31:1004-1011.

34. Merkl, P. B., W. R. Knocke, D. Gallagher, J. Junta-Rosso, and T. Solberg. (1996). Characterizing Filter Media Mineral Coatings. *Jour. AWWA* 88:62-73.

35. Rook, J. J. (1977). Chlorination Reactions of Fulvic Acids in Natural Waters. *Environ. Sci. Technol.* 11:478-482.

36. Boyce, S. D. and J. F. Hornig. (1983). Reaction Pathways of Trihalomethane Formation from the Halogenation of Dihydroxyaromatic Model Compounds for Humic Acid. *Environ. Sci. Technol.* 17:202-211.

37. de Leer, E. W., J. S. Sinnighe Damsté, C. Elkins, and L. de Galan. (1985). Identification of Intermediates Leading to Chloroform and C-4 Diacids in the Chlorination of Humic Acid. *Environ. Sci. Technol.* 19:512-522.

38. Trehy, M. L., R. A. Yost, and C. J. Miles. (1986). Chlorination Byproducts of Amino Acids in Natural Waters. *Environ. Sci. Technol.* 20:1117-1122.

39. Heasley, V. L., M. D. Burns, N. A. Kemalyan, T. C. McKee, H. Schroeter, B. R. Teegarden, S. E. Whitney, and R. L. Wershaw. (1989). Aqueous Chlorination of Resorcinol. *Environmental Toxicology and Chemistry* 8:1159-1163.

40. Tretyakova, N. , Y., A. T. Lebedev, and V. S. Petrosyan. (1994). Degradative Pathways for Aqueous Chlorination of Orcinol. *Environ. Sci. Technol.* 28:606-613.

41. de Leer, E. W. and C. Elkins. (1985). Chloroform Production from Model Compounds of Aquatic Humic Material: The Role of Pentachlororesorcinol as an Intermediate. *Sci. Total Environ.* 47:211-216.

42. Solomons, T. W. G. (1992). Organic Chemistry. John Wiley & Sons, Inc. New York.

43. Bruice, P. Y. (1995). Organic Chemistry. Prentice Hall, Upper Saddle River.

44. Tadanier, C. J., W. R. Knocke and D. F. Berry. (1997). The Influence of Dissolved Organic Matter-Colloidal Material Associations on the Application of Coagulation and Disinfection Processes to Drinking Waters. AWWA Annual Conference Proceedings, Vol. C Water Research. Atlanta, GA. 157-169.

Vita

Christopher J. Tadanier attended the University of Illinois Urbana-Champaign where he was awarded Bachelor of Science and Master of Science degrees in Mechanical Engineering. He then served as an officer in the Submarine Force of the United States Navy for a period of six years. While in the Navy Lt. Tadanier held billets as an instructor at the Naval Nuclear Propulsion School, Orlando, FL and as a nuclear trained submarine warfare qualified officer onboard USS Newport News (SSN-750). As an instructor, Lt. Tadanier taught courses in thermodynamics, fluid mechanics, heat transfer, and themromechanical design. Onboard USS Newport News Lt. Tadanier participated in numerous deployments vital to national security, including a six month emergent deployment to the Mediterranean Sea in support of Operation Desert Storm. He was decorated three times as the result of his sea service, receiving Navy Achievement Medals for sustained superior performance and demonstrated excellence in propulsion plant operation and submarine warfare. After leaving active duty, Mr. Tadanier attended Virginia Polytechnic Institute and State University where he studied Environmental Engineering. He received a Ph.D. degree in June, 1998. Upon completion of doctoral research, Mr. Tadanier became a Post-Doctoral Research Associate, also at VPI&SU, and participated in an interdisciplinary program studying interactions between microorganisms and mineral surfaces.